

EVALUATION OF MULTI-LAYER POLYMER CONCRETE OVERLAYS

By
Bijay Tiwari
David Darwin
Matthew O'Reilly

A Report on Research Sponsored by the
KANSAS DEPARTMENT OF TRANSPORTATION (KDOT)
under K-TRAN Award No. KU-23-3

Structural Engineering and Engineering Materials
SM Report 25-1
January 2025



THE UNIVERSITY OF KANSAS CENTER FOR RESEARCH, INC.
2385 Irving Hill Road, Lawrence, Kansas 66045-7563

EVALUATION OF MULTI-LAYER POLYMER CONCRETE OVERLAYS

By

Bijay Tiwari

David Darwin

Matthew O'Reilly

A Report Sponsored by the

KANSAS DEPARTMENT OF TRANSPORTATION (KDOT)

under K-TRAN Award No. KU-23-3

Structural Engineering and Engineering Materials

SL Report 25-1

THE UNIVERSITY OF KANSAS CENTER FOR RESEARCH, INC.

LAWRENCE, KANSAS

January 2025

ABSTRACT

Multilayer polymer overlays were evaluated using cracked beam and Southern Exposure specimens to investigate their ability to limit corrosion of reinforcing steel in bridge decks. Corrosion rates, corrosion potentials, and total corrosion rates based on linear polarization resistance results were used for the evaluation. Two polymers, the epoxies Sikadur and Flexolith, were used for preparing the polymer overlays. Test specimens were prepared using three systems: one layer of epoxy polymer, one layer of epoxy polymer and aggregate, and two layers of epoxy polymer and aggregate (the manufacturers' recommended application). Specimens without polymer overlays were also tested. Some cracked beam specimens were contaminated with chloride and then coated with polymer overlay to evaluate the ability of polymer overlays to limit corrosion in chloride-contaminated concrete. The design, fabrication, and testing procedures for post-crack specimens, used to evaluate the ability of the overlays to remain intact when cracks form in the concrete after the overlay has been applied, are described, but no test results are yet available. The results of the study show that specimens without the polymer overlay exhibited the highest corrosion rate. One cracked beam specimen with two layers of Sikadur polymer and aggregate, one cracked beam specimen with one layer of Flexolith polymer and aggregate, and one cracked beam specimen with two layers of Flexolith polymer and aggregate exhibited higher corrosion activity than the other specimens with polymer overlays. Other than these three specimens, little corrosion activity was observed, and overall, the results show that multilayer polymer overlays limit corrosion. In addition, a measurable reduction in corrosion rate occurred when chloride-contaminated concrete was coated with a polymer overlay.

Keywords: chlorides, concrete, corrosion, Flexolith, multi-layer polymer overlays, Sikadur,

ACKNOWLEDGEMENTS

This report is based on research performed by Bijay Tawari in partial fulfillment of the requirements for the degree of Master of Science. This research was funded by the Kansas Department of Transportation (KDOT) under K-TRAN Award No. KU-23-3. Materials were provided by Midwest Concrete Materials. Sikadur Lo Mod epoxy polymer was provided by Sika Corporation. Flexolith polymer was provided by Euclid Chemical. PCiRoads provided the aggregate and Sikadur polymer and accommodated a site visit of a bridge to which a multi-layer polymer overlay was being applied.

TABLE OF CONTENTS

ABSTRACT	i
ACKNOWLEDGEMENTS	ii
LIST OF TABLES	v
LIST OF FIGURES	vi
1 INTRODUCTION	1
1.1 GENERAL	1
1.2 CORROSION MECHANISM.....	2
1.3 POLYMER OVERLAYS	3
1.4 OBJECTIVE AND SCOPE	4
2 EXPERIMENTAL WORK	6
2.1 REINFORCEMENT	6
2.2 CONCRETE MIXTURE PROPORTIONS AND AGGREGATE PROPERTIES	6
2.3 EPOXY POLYMERS.....	7
2.3.1 Application Procedure	7
2.4 SOUTHERN EXPOSURE (SE) AND CRACKED BEAM (CB) TESTS	10
2.4.1 Description	10
2.4.2 Materials and Equipment	11
2.4.3 Fabrication	13
2.4.4 Test Procedure	15

2.4.5	Corrosion Monitoring and Measurements	15
2.5	POST-CRACK SPECIMENS.....	17
2.5.1	Description and Fabrication.....	17
2.5.2	Test Procedure	19
2.6	Test Program.....	20
3	RESULTS- CRACKED BEAM AND SOUTHERN EXPOSURE.....	22
3.1	CORROSION RATE AND CORROSION POTENTIALS	22
3.2	CORROSION LOSS.....	50
3.3	LINEAR POLARIZATION RESISTANCE (LPR) RESULTS	52
4	SUMMARY AND CONCLUSIONS	55
	REFERENCES.....	56
	APPENDIX A	57
	APPENDIX B	68

LIST OF TABLES

Table 1: Chemical composition of reinforcement bar	6
Table 2: Mixture proportion for cracked beam and Southern Exposure specimens based on SSD aggregate per yd ³ (per m ³)	7
Table 3: Application Rate of Polymer and Aggregate.....	8
Table 4: Result of tensile rupture strength of bond of Sikadur polymer overlay with concrete.....	9
Table 5: Result of tensile rupture strength of bond of Flexolith polymer overlay with concrete...	9
Table 6: Corrosion test specimens with Sikadur and Flexolith polymers	21
Table 7: Chloride-Contaminated and Control Specimens	21
Table 8: Average macrocell and total corrosion rates for Southern Exposure and cracked beam specimens at week 24.....	53
Table 9: Average macrocell and total corrosion rates for chloride exposed cracked beam specimens at weeks 8 and 24.....	54

LIST OF FIGURES

Figure 1: Southern Exposure (SE) specimen	10
Figure 2: Cracked Beam (CB) specimen	11
Figure 3: Heat Tent Dimensions	13
Figure 4: Post-crack specimen	17
Figure 5: Formwork orientation after casting first half of post-crack specimen	18
Figure 6: Formwork orientation to cast second half of post-crack specimen	19
Figure 7: Post-crack specimen prototype.....	20
Figure 8: Macrocell corrosion rate versus time for cracked beam specimens with one layer of Sikadur®-22 Lo-Mod epoxy.....	23
Figure 9: Corrosion potential of top mat of steel versus time for cracked beam specimens with one layer of Sikadur®-22 Lo-Mod epoxy	23
Figure 10: Macrocell corrosion rate versus time for cracked beam specimens with one layer of Sikadur®-22 Lo-Mod epoxy and aggregate	24
Figure 11: Corrosion potential of top mat of steel versus time for cracked beam specimens with one layer of Sikadur®-22 Lo-Mod epoxy and aggregate	25
Figure 12: Macrocell corrosion rate versus time for cracked beam specimens with two layers of Sikadur®-22 Lo-Mod epoxy and aggregate	26
Figure 13: Corrosion potential of top mat of steel versus time for cracked beam specimens with two layers of Sikadur®-22 Lo-Mod epoxy and aggregate	26
Figure 14: Macrocell corrosion rate versus time for Southern Exposure specimens with one layer of Sikadur®-22 Lo-Mod epoxy	27

Figure 15: Corrosion potential of top mat of steel versus time for Southern Exposure specimens with one layer of Sikadur®-22 Lo-Mod epoxy	28
Figure 16: Macrocell corrosion rate versus time for Southern Exposure specimens with one layer of Sikadur®-22 Lo-Mod epoxy and aggregate	29
Figure 17: Corrosion potential of top mat of steel versus time for Southern Exposure specimens with one layer of Sikadur®-22 Lo-Mod epoxy and aggregate	29
Figure 18: Macrocell corrosion rate versus time for Southern Exposure specimens with two layers of Sikadur®-22 Lo-Mod epoxy and aggregate	30
Figure 19: Corrosion potential of top mat of steel versus time for Southern Exposure specimens with two layers of Sikadur®-22 Lo-Mod epoxy and aggregate	31
Figure 20: Macrocell corrosion rate versus time for cracked beam specimens with one layer of Flexolith epoxy	32
Figure 21: Corrosion potential of top mat of steel versus time for cracked beam specimens with one layer of Flexolith epoxy	32
Figure 22: Macrocell corrosion rate versus time for cracked beam specimens with one layer of Flexolith epoxy and aggregate	33
Figure 23: Corrosion potential of top mat of steel versus time for cracked-beam specimens with one layer of Flexolith epoxy and aggregate	34
Figure 24: Macrocell corrosion rate versus time for cracked beam specimens with two layers of Flexolith epoxy and aggregate	35
Figure 25: Corrosion potential of top mat of steel versus time for cracked beam specimens with two layers of Flexolith epoxy and aggregate	35

Figure 26: Macrocell corrosion rate versus time for Southern Exposure specimens with one layer of Flexolith epoxy	36
Figure 27: Corrosion potential of top mat of steel versus time for Southern Exposure specimens with one layer of Flexolith epoxy	36
Figure 28: Macrocell corrosion rate versus time for Southern Exposure specimens with one layer of Flexolith epoxy and aggregate.....	37
Figure 29: Corrosion potential of top mat of steel versus time for Southern Exposure specimens with one layer of Flexolith epoxy and aggregate.....	38
Figure 30: Macrocell corrosion rate versus time for Southern Exposure specimens with two layers of Flexolith epoxy and aggregate.....	39
Figure 31: Corrosion potential of top mat of steel versus time for Southern Exposure specimens with two layers of Flexolith epoxy and aggregate	39
Figure 32: Average macrocell corrosion rate versus time of cracked beam specimens coated with Sikadur along with control specimens	40
Figure 33: Average corrosion potential of top mat versus time of cracked beam specimens coated with Sikadur along with control specimens	41
Figure 34: Average macrocell corrosion rate versus time of Southern Exposure specimens coated with Sikadur along with control specimens	42
Figure 35: Average corrosion potential of top mat versus time of Southern Exposure specimens coated with Sikadur along with control specimens.....	42
Figure 36: Average macrocell corrosion rate versus time of cracked beam specimens coated with Flexolith along with control specimens	44

Figure 37: Average macrocell corrosion rate versus time of cracked beam specimens coated with Flexolith along with control specimens	44
Figure 38: Average macrocell corrosion rate versus time of Southern Exposure specimens coated with Flexolith along with control specimens	45
Figure 39: Average corrosion potential of top mat versus time of Southern Exposure specimens coated with Flexolith along with control specimens.....	46
Figure 40: Macrocell corrosion rate versus time for chloride exposed cracked-beam specimens coated with Sikadur epoxy.....	48
Figure 41: Corrosion potential of top mat of steel versus time for chloride exposed cracked beam specimens coated with two layers of Sikadur epoxy and aggregate.....	48
Figure 42: Macrocell corrosion rate versus time for chloride exposed cracked-beam specimens coated with Flexolith epoxy.....	49
Figure 43: Corrosion potential of top mat of steel versus time for chloride exposed cracked-beam specimens coated with Flexolith epoxy	49
Figure 44: Average corrosion loss (μm) based on total area for cracked beam specimens with Sikadur polymer along with control specimens.....	51
Figure 45: Average corrosion loss (μm) based on total area for Southern Exposure specimens with Sikadur polymer along with control specimens.....	51
Figure 46: Average corrosion loss (μm) based on total area for cracked beam specimens with Flexolith polymer along with control specimens.....	51
Figure 47: Average corrosion loss (μm) based on total area for Southern Exposure specimens with Flexolith polymer along with control specimens.....	52

Figure A.48: Corrosion potential of bottom mat of steel versus time for cracked beam specimens with one layer of Sikadur®-22 Lo-Mod epoxy	57
Figure A.49: Corrosion potential of bottom mat of steel versus time for cracked beam specimens with one layer of Sikadur®-22 Lo-Mod epoxy and aggregate	58
Figure A.50: Corrosion potential of bottom mat of steel versus time for cracked beam specimens with two layers of Sikadur®-22 Lo-Mod epoxy and aggregate	58
Figure A.51: Corrosion potential of bottom mat of steel versus time for Southern Exposure specimens with one layer of Sikadur®-22 Lo-Mod epoxy.....	59
Figure A.52: Corrosion potential of bottom mat of steel versus time for Southern Exposure specimens with one layer of Sikadur®-22 Lo-Mod epoxy and aggregate	59
Figure A.53: Corrosion potential of bottom mat of steel versus time for Southern Exposure specimens with two layers of Sikadur®-22 Lo-Mod epoxy and aggregate.....	60
Figure A.54: Corrosion potential of bottom mat of steel versus time for cracked beam specimens with one layer of Flexolith epoxy	60
Figure A.55: Corrosion potential of bottom mat of steel versus time for cracked-beam specimens with one layer of Flexolith epoxy and aggregate.....	61
Figure A.56: Corrosion potential of bottom mat of steel versus time for cracked beam specimens with two layers of Flexolith epoxy and aggregate	61
Figure A.57: Corrosion potential of bottom mat of steel versus time for Southern Exposure specimens with one layer of Flexolith epoxy	62
Figure A.58: Corrosion potential of bottom mat of steel versus time for Southern Exposure specimens with one layer of Flexolith epoxy and aggregate	62

Figure A.59: Corrosion potential of bottom mat of steel versus time for Southern Exposure specimens with two layers of Flexolith epoxy and aggregate	63
Figure A.60: Corrosion potential of bottom mat of steel versus time for chloride exposed cracked beam specimens coated with two layers of Sikadur epoxy and aggregate	63
Figure A.61: Corrosion potential of bottom mat of steel versus time for chloride exposed cracked-beam specimens coated with Flexolith epoxy	64
Figure A.62: Macrocell corrosion rate versus time for control cracked beam specimens.....	64
Figure A.63: Corrosion potential for top mat of steel versus time for control cracked beam specimens.....	65
Figure A.64: Corrosion potential for bottom mat of steel versus time for control cracked beam specimens.....	65
Figure A.65: Macrocell corrosion rate versus time for control Southern Exposure specimens ...	66
Figure A.66: Corrosion potential for top mat of steel versus time for control Southern Exposure specimens.....	66
Figure A.67: Corrosion potential for bottom mat of steel versus time for control Southern Exposure specimens.....	67
Figure B.68: Corrosion Loss for cracked beam specimens with one layer of Sikadur®-22 Lo-Mod epoxy.....	68
Figure B.69: Corrosion Loss for cracked beam specimens with one layer of Sikadur®-22 Lo-Mod epoxy and aggregate	69
Figure B.70: Corrosion Loss for cracked beam specimens with two layers of Sikadur®-22 Lo-Mod epoxy and aggregate	69

Figure B.71: Corrosion Loss for Southern Exposure specimens with one layer of Sikadur®-22 Lo-Mod epoxy	70
Figure B.72: Corrosion Loss for Southern Exposure specimens with one layer of Sikadur®-22 Lo-Mod epoxy and aggregate.....	70
Figure B.73: Corrosion Loss for Southern Exposure specimens with two layers of Sikadur®-22 Lo-Mod epoxy and aggregate	71
Figure B.74: Corrosion Loss for cracked beam specimens with one layer of Flexolith epoxy	71
Figure B.75: Corrosion Loss for cracked-beam specimens with one layer of Flexolith epoxy and aggregate.....	72
Figure B.76: Corrosion Loss for cracked beam specimens with two layers of Flexolith epoxy and aggregate.....	72
Figure B.77: Corrosion Loss for Southern Exposure specimens with one layer of Flexolith epoxy	73
Figure B.78: Corrosion Loss for Southern Exposure specimens with one layer of Flexolith epoxy and aggregate	73
Figure B.79: Corrosion Loss for Southern Exposure specimens with two layers of Flexolith epoxy and aggregate	74
Figure B.80: Corrosion Loss for chloride exposed cracked beam specimens coated with two layers of Sikadur epoxy and aggregate.....	74
Figure B.81: Corrosion Loss for chloride exposed cracked-beam specimens coated with Flexolith epoxy.....	75
Figure B.82: Corrosion Loss for control cracked beam specimens	75
Figure B.83: Corrosion Loss for control Southern Exposure specimens.....	76

1 INTRODUCTION

1.1 GENERAL

Corrosion damages reinforced concrete structures primarily because the corrosion products, commonly known as rust, are greater in volume than the original steel, creating tensile stresses that lead to cracking and delamination of concrete. Corrosion is of particular importance in bridges, where the estimated annual direct cost of corrosion over 20 years ago was \$8.3 billion (Koch 2002). Additionally, the total indirect costs, primarily caused by traffic delays and lost productivity, are estimated to be ten times the direct costs (Koch 2002).

Corrosion of reinforcing steel in concrete occurs when CO_2 or Cl^- penetrates to the level of steel (Broomfield 1996). These aggressive agents cause the breakdown of the passive layer of steel. In the absence of a passive layer, the formation of electrochemical cells inside the reinforced concrete structure results in corrosion. The electrochemical process involves the anodic oxidation of iron and the cathodic reduction of oxygen, with the pore solution in the concrete serving as the electrolyte.

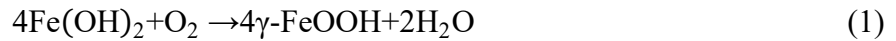
Corrosion protection systems limit corrosion, adding to the longevity of the reinforced concrete structures and reducing the costs associated with corrosion. Corrosion resistant reinforcement, epoxy-coated reinforcement, corrosion inhibitors, and using a lower water to cement ratio are some methods that will limit corrosion.

Polymer overlays, specifically on bridge decks, represent another system with the potential to protect both newly constructed and existing structures. In concept, the overlays form a waterproof membrane on the bridge deck that limit the penetration of water and chlorides into the concrete. Polymer overlays, which consist of consist of multiple layers of polymer and aggregate

applied in succession to the surface on a bridge deck, have been in use across the United States since the 1980s (Krauss and Hawkins 2023). The application of multilayer polymer overlays by Kansas Department of Transportation (KDOT) began in 1999 (Meggers 2016). The primary purpose of this study is to determine how effectively multilayer polymer overlays work as a corrosion protection system for steel reinforcement in bridge decks.

1.2 CORROSION MECHANISM

Concrete pore solution has a high pH, which causes steel to form a γ -ferric oxyhydroxide layer that prevents corrosion. To sustain this passive layer, a pH of 11.5 to 13.8 in concrete is required.



The breakdown of passive layer in reinforcing steel occurs due to chloride ingress from the use of deicing salts, carbonation of concrete and other environmental factors. Carbonation lowers the pH of concrete pore solution and Cl^- ion reacts with the passive layer, both of which causes the breakdown of the passive layer. When the passive layer of steel breaks down, oxygen reacts with the steel causing corrosion. The anodic oxidation of reinforcing steel releases electrons which move to a different location on the reinforcement serving as a cathode. The movement of electrons occurs through the reinforcing steel or through form ties. In the presence of oxygen and moisture at the cathode, reduction of oxygen produces hydroxyl ions which move to the anode through the concrete pore solution.

The chemical reactions occurring during corrosion in concrete are presented below.



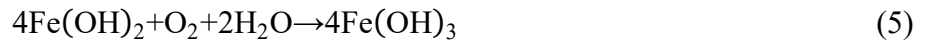
Equation 2 is an anodic reaction where iron oxidizes to a ferrous ion and releases two electrons.



Equation (3) is a cathodic reaction, which involves the reduction of oxygen into hydroxyl ions. The ferrous ions produced at anode react with the hydroxyl ions formed at the cathode to produce ferrous hydroxide as shown in Eq, (4).



Further oxidation of ferrous hydroxide occurs forming ferric hydroxide, when moisture and oxygen is present, as shown in Eq. (5). The resulting rust has a greater volume than the original steel, causing tensile stress and cracking in the concrete.



1.3 POLYMER OVERLAYS

Polymer overlays are a combination of epoxy resin and aggregate that is applied on an existing surface, serving as a repair material and, at times, applied before the structure has been placed in service. The overlays reduce the penetration of water and chlorides into the concrete as the epoxy resin forms a waterproof membrane on the surface. Polymer overlays can be divided into three categories: multi-layer, pre-mixed and slurry (Sprinkel et al. 1993). Among these, multi-layer polymer overlays are the most widely used (Sprinkel et al. 1993). The application of multi-layer polymer overlays involves coating the prepared concrete surface with one or two layers of polymer followed by spreading aggregate on top of each layer of polymer (Roper and Henley 1991). Pre-mixed and slurry overlays involve mixing polymer and aggregate together before their application. In either case, the surface of reinforced concrete bridge decks should be adequately prepared by removing delaminated concrete, oils, dirt, paint, and other contaminants before the application of the overlay. This ensures proper bonding of polymer overlays and concrete.

Sprinkel et. al (1993) analyzed the chloride permeability of bridge decks coated with a polymer overlay and compared it to the permeability of uncoated reinforced concrete bridge decks. This was done by taking cores from the bridge decks coated with a polymer overlay and those without any treatment. The top 2 in. of the core and 2 to 4 in. depth of the core were evaluated, with the latter described as the base concrete. The permeability of top 2 in. of the core from an untreated bridge deck had 50 % of the permeability of base concrete, which was due to the surface finishing, carbonation, and traffic contamination. However, the permeability of the top 2 in. of the core coated with polymer overlays was significantly below 50 % of the permeability of base concrete.

Krauss and Hawkins (2023) concluded that polymer overlays applied to bridge decks that are not contaminated with chloride will have longer life compared to polymer overlays applied to bridge decks with chloride contamination and active corrosion. The latter can exhibit delamination starting 4 to 7 years after the application of overlay despite the excellent reduction in chloride penetration up to 5 years.

1.4 OBJECTIVE AND SCOPE

The purpose of this study is to evaluate the effectiveness of multi-layer polymer concrete overlays when used for repair and in new construction to protect the reinforcing steel in bridge decks. The study involves the use of two different types of polymers: Sikadur Lo Mod Fs and Flexolith by Euclid. Only conventional, uncoated reinforcement is used for the study. Cracked beam specimens, Southern Exposure specimens, and field test specimens are used to evaluate the effectiveness of the multilayer polymer overlays in limiting corrosion of reinforcing steel. “Post-crack specimens” are used to evaluate the ability of the overlays to remain intact when cracks form in the concrete after the overly has been applied. This report describes the experiment methods

used for both the corrosion and post-crack specimens. Because the tests of the post-crack tests were just beginning as of this writing, however, only the results for cracked beam and Southern Exposure specimens are presented.

2 EXPERIMENTAL WORK

2.1 REINFORCEMENT

The reinforcement used for this study is No. 5 (No. 16) ASTM 615 Grade 60 steel reinforcement produced by Commercial Metals Company (CMC). The Heat No. for this steel is 1069035. The reinforcement is termed “conventional” and has the chemical composition shown in Table 1.

Table 1: Chemical composition of reinforcement bar

Material	C	Mn	P	S	Si	Cu	Cr	Ni	Mo	V	Cb	Sn
Conventional	0.36	0.73	0.01	0.024	0.24	0.28	0.14	0.13	0.036	0.003	0.001	0.011

2.2 CONCRETE MIXTURE PROPORTIONS AND AGGREGATE PROPERTIES

The following materials were used in the concrete mix:

Water: Municipal tap water from the City of Lawrence.

Cement: Type IL portland cement.

Coarse Aggregate: Crushed Limestone from Eudora Quarry. Nominal maximum size= 0.75 in. (19 mm), bulk specific gravity (SSD) = 2.63, absorption = 2.64%, unit weight = 96.12 lb/ft³ (1540 kg/m³).

Fine Aggregate: Kansas River sand. Bulk specific gravity (SSD) = 2.63, absorption = 0.5%, fineness modulus = 2.84.

Air Entraining Agent: Daravair 1400

The mixture proportions are shown in Table 2:

Table 2: Mixture proportion for cracked beam and Southern Exposure specimens based on SSD aggregate per yd³ (per m³)

Type IL Cement	Water	Fine Aggregate	Coarse Aggregate	Air- Entraining Agent
lb/yd ³ (kg/m ³)	lb/yd ³ (kg/m ³)	lb/yd ³ (kg/m ³)	lb/yd ³ (kg/m ³)	oz/yd ³ (mL/m ³)
598 (355)	270 (160)	1436 (852)	1473 (874)	10.3 (400)

2.3 EPOXY POLYMERS

The polymers used in this study are Sikadur Lo-Mod Fs and Flexolith by Euclid.

2.3.1 Application Procedure

Surface Preparation: The concrete surface was prepared using a needle scaler to produce a surface relief matching International Concrete Repair Institute (ICRI) Surface Preparation Level 6.

Placing the multi-layer polymer concrete overlays: The polymers used in this study were two-part epoxies. The two parts were combined with a paddle mixer in equal proportions until a uniform color was achieved; the polymer was then applied to the concrete surface with the application rate given in Table 3. A notched squeegee was used to spread the polymer uniformly over the surface. Each layer of polymer was covered uniformly with aggregate particles within 10 minutes of polymer application. Excess aggregate particles were vacuumed after the curing period of each layer. The specimens were tested with three different coating configurations. In the first configuration, the concrete surface was coated with a single layer of epoxy polymer. The second configuration involved coating the surface with a layer of epoxy polymer, followed by broadcasting a layer of aggregate on top. The third configuration is built upon the second by adding

an additional layer of epoxy polymer and aggregate, resulting in a total of two layers of polymer and aggregate, in line with the manufacturers' recommendations. This approach allowed for a thorough assessment of the effectiveness of these coating techniques.

Application Rate: The application rates for the multi-layer polymer concrete overlays are as mentioned in Table 3.

Table 3: Application Rate of Polymer and Aggregate

Course (Layer)	Polymer Rate	Aggregate Rate
	oz/in. ²	lb/in. ²
1	>0.022	0.008
2	>0.044	0.011

Regardless of the aggregate rate mentioned in the table; additional aggregate is broadcast to cover the exposed polymer.

Curing: When more than a single layer of polymer was used, the first layer was cured for a day before applying the second layer of polymer and aggregate. The second layer of polymer and aggregate was cured for a minimum of one day before the initiation of ponding.

Testing: The tensile rupture strength of the bond of the polymer overlay to the concrete was tested following the procedure outlined in Kansas Test Method KT-70.. This test was done 1 week after the application of the polymer overlay on the concrete surface. A PosiTest adhesion tester was used to perform the tensile rupture test, which involves the use of a 2-in. diameter test dolly. The test was performed for both polymer overlays. The loading rate was 8 psi per second. The results are shown in Tables 4 and 5.

Table 4: Result of tensile rupture strength of bond of Sikadur polymer overlay with concrete

Test Dolly	Cored Depth in.	Tensile rupture Strength psi	Depth at failure of concrete	Failure Type
1	1.25	308	> ¼ in. over more than 50% of area	1
2		261		
3		316		

Table 5: Result of tensile rupture strength of bond of Flexolith polymer overlay with concrete

Test Dolly	Cored Depth in.	Tensile rupture Strength psi	Depth at failure of concrete	Failure Type
1	1.25	354	> ¼ in. over in more than 50% of area	1
2		279		

The average tensile rupture strengths of the bond of polymer overlays made using Sikadur and Flexolith polymer with concrete were 295 psi and 317 psi, respectively. According to Kansas Test Method KT-70, when the failure of concrete occurs at depth greater than or equal to ¼ in. over more than 50% of the test area, it is considered Type 1, indicating proper bonding of polymer overlay with the concrete. Type 2 failure refers to the failure of concrete at a depth of less than ¼ in. across more than 50% of the test area. Type 3, Type 4, and Type 5 failures correspond to the following: debonding between the polymer overlay and the concrete surface, failure of the polymer overlay itself, and failure of the test adhesive used to bond the test dolly to the surface of the polymer overlay, respectively. In this study, the polymer overlays were applied correctly as evidenced by the Type 1 failure achieved for both polymer overlays.

2.4 SOUTHERN EXPOSURE (SE) AND CRACKED BEAM (CB) TESTS

2.4.1 Description

Southern Exposure (SE) and Cracked Beam (CB) specimens were used in this study, collectively referred to as bench scale specimens. The SE specimen, shown in Figure 1, measures $12 \times 12 \times 7$ in. ($305 \times 305 \times 178$ mm) and has two mats of reinforcing bars: the top mat contains two No. 5 (No. 16) bars, while the bottom mat includes four bars. These 12-in. (305-mm) long bars are placed with a 1-in. (25-mm) clear cover on both the top and bottom and are spaced 2.5 in. (64 mm) apart, centered within the prism. To determine the macrocell corrosion rate, the top and bottom mats are electrically connected by a wire that passes through a terminal box across a 10-ohm resistor. A 0.75-in. (19-mm) deep concrete dam is cast integrally with the sample to hold on the ponded salt solution.

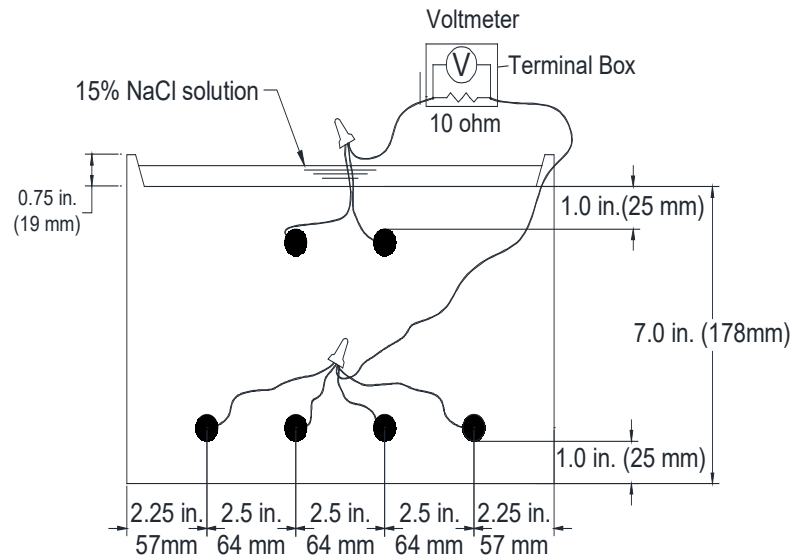


Figure 1: Southern Exposure (SE) specimen

The CB specimens, shown in Figure 2, are half the width of the SE specimens, with dimensions of $12 \times 6 \times 7$ in. ($305 \times 152 \times 178$ mm). These specimens also contain two layers of

reinforcement, with the top mat consisting of a single No. 5 (No. 16) bar and the bottom mat containing two No. 5 (No. 16) bars. To create a simulated crack, a 12-mil (0.3-mm) thick stainless-steel shim, 6 in. (152 mm) long, is placed in contact with the top bar inside the mold. The shim is removed 18 to 24 hours after casting, creating a crack in the specimen.

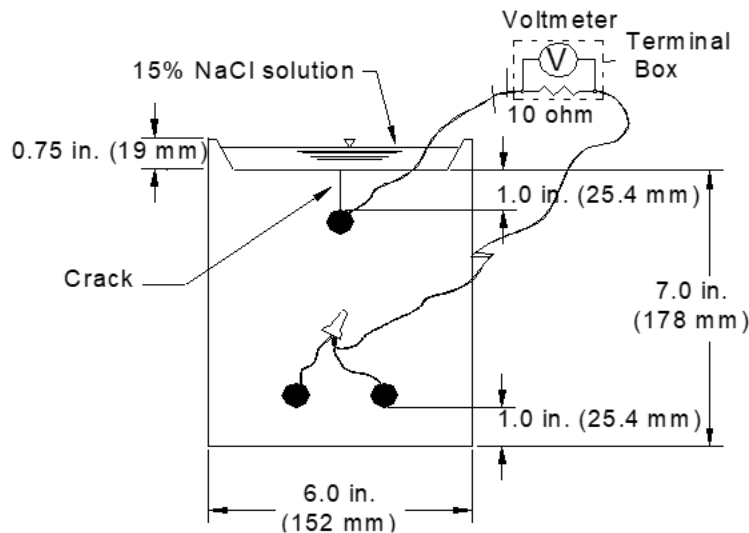


Figure 2: Cracked Beam (CB) specimen

Chloride-exposed cracked beams have same dimensions as the cracked beam specimens. In contrast to cracked beam specimens, which are used as either control specimens or coated with the polymer overlays before the initiation of ponding, these specimens are ponded with salt solution for 8 weeks and then coated with the polymer overlays to evaluate the effectiveness of polymer overlays in resisting corrosion in chloride contaminated bridge decks.

2.4.2 Materials and Equipment

Bench scale specimens comprised the following materials and equipment.

Wire: 16-gauge multi-strand copper wire is used to make an external connection between the top and bottom mats of steel through a terminal box.

Terminal Box: A terminal box accommodates several stations for each Cracked Beam and Southern Exposure specimen. A station comprises of a red post connected to an anodic wire and a

black post is connected to a cathodic wire both coming through top and bottom mat of the specimens respectively, where, a switch is placed, connected in series with a 10-ohm resistor to measure voltage drop, to interrupt the connection to measure corrosion potential and LPR data.

Multimeter: A Fluke 8808A 5.5-digit multimeter is used to take voltage drop and corrosion potential reading.

Reference Electrode: Corrosion potential measurements are taken using silver-silver chloride electrode.

Epoxy: Sikagard 62 epoxy, manufactured by Sika, is used to prevent the electric connections from corroding. This epoxy is applied on the four sides of the specimens to prevent contamination of specimen with spilled salt solution and to prevent salt within the specimens from leaching out through the sides.

Stainless Steel Screws/Washers are used to secure the reinforcement within the formwork and to connect the wires to the specimens during testing.

Wet/Dry Vacuum: Salt solution is removed from the specimens using a wet/dry vacuum.

Heat Tent: Heating tents are used to maintain high temperatures throughout the tests. The tents are made of 0.75-in. (19 mm) plywood and are supported by six 2 x 4-stud supports. They are 8 ft (2.44 m) long, 4 ft (1.22 m) wide, and 3.5 ft (1.07 m) high. Three 250-watt heat lamps are installed on the roof, 1.5 ft (0.45 meters) above the specimens, and plastic sheeting is positioned between the studs for insulation. The tent's temperature is controlled by a thermostat at $100 \pm 3^\circ \text{F}$ ($38 \pm 2^\circ \text{C}$).

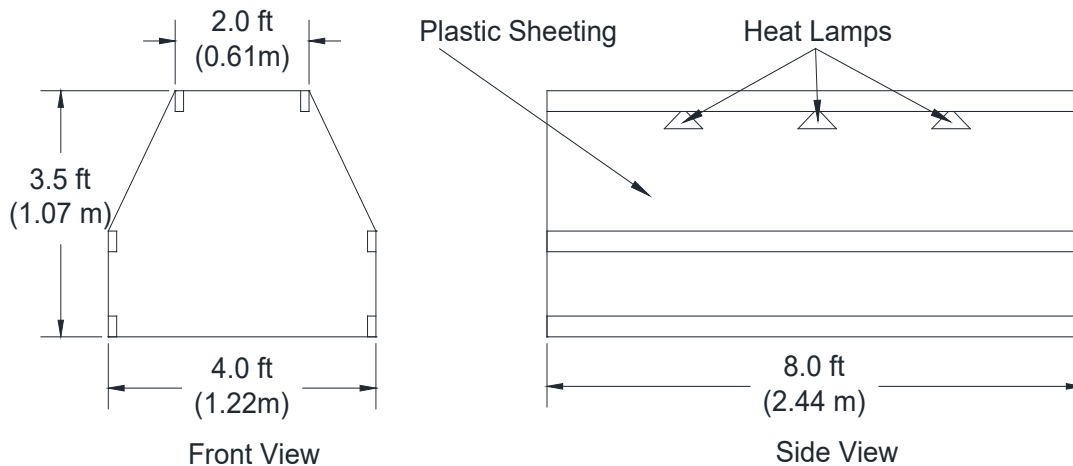


Figure 3: Heat Tent Dimensions

Formwork: The formwork for the Southern Exposure (SE) and Cracked Beam (CB) specimens is constructed from 0.75-in. (19 mm) plywood treated with polyurethane. Each form consists of four side panels and a base, with the specimens cast upside-down. For the SE specimens, the base includes a $10.5 \times 10.5 \times 0.75$ -in. ($267 \times 267 \times 19$ mm) plywood insert that forms a concrete dam to hold the ponding solution. To accommodate a 12-mil (0.3-mm) stainless steel shim, the CB formwork has a $4.5 \times 10.5 \times 0.75$ -in. ($114 \times 267 \times 19$ mm) insert with a centered slot. The reinforcing bars are secured by drilling holes into two opposing panels, and 1.25-in. (32 mm) 10-24 stainless steel machine screws are used to construct the formwork components by fastening them into threaded inserts. The shim is precisely positioned for the CB specimens, and baby oil is used to all inside surfaces prior to casting.

2.4.3 Fabrication

1. The reinforcing bars are cut to a length of 12 in. (305 mm) using a band saw. The ends of the bars are then drilled and tapped to a depth of 0.75 in. (19 mm) with a 10-24 thread.
2. The bars are positioned within the formwork and secured using 1.25 in. (32 mm) stainless steel machine screws.

3. The concrete is cast using a mix with proportions given in Table 2. The specimens are filled in two layers, with each layer consolidated using a 60-Hz, 0.15-mm (6-mil) amplitude vibrating table for 30 seconds. The exposed surface of the concrete (the bottom of the specimen) is then finished with a float.
4. The specimens are allowed to cure in forms for 24 hours at room temperature. To prevent evaporation, they are covered with a plastic sheet. The shims used in the CB specimens are removed 18 to 24 hours after casting, once the concrete has adequately set.
5. After 24 hours, the formwork is removed. The specimens are then placed in a plastic bag containing deionized water for an additional two days of curing, followed by a 25-day air curing period.
6. According to the KDOT Standard Specifications for State Roads and Bridges, Construction Section 729, surface preparation is done so that a surface relief equal to the International Concrete Repair Institute (ICRI) level 6 is attained by using a needle scaler. After that, on days 27 and 28, respectively, the first and, if used, second layers of the polymer overlay are placed. For chloride-exposed cracked beams, surface preparation and application of polymer overlay is done at 8th week of ponding those specimens.
7. Prior to the initiation of testing, wire leads are connected to the reinforcing bars using 10-24 × 0.5-in. (13 mm) stainless steel screws along with a No. 10 stainless steel washer. Sikagard epoxy is applied to the vertical sides of the specimens, ensuring that the top and bottom remain uncoated.
8. The top and bottom mats of reinforcing steel are connected to a terminal box across a 10-ohm resistor, enabling measurements of macrocell corrosion rates. The specimens are

placed on 2 × 2 in. studs to facilitate airflow underneath, and testing begins 30 days after casting.

2.4.4 Test Procedure

The test is completed in 96 weeks altering between cycles of ponding-drying and continuous ponding, each with a duration of 12 weeks. Tests start with a ponding-drying cycle in which the specimens are ponded with 15% NaCl solution and covered with plastic to reduce evaporation. The CB and SE specimens, respectively, receive 300 and 600 ml of solution. Corrosion measurements are taken on the fourth day of ponding. After the completion of the corrosion measurements, the salt solution is vacuumed off the specimens and covered with a heat tent maintained at 100 ± 3 °F (38 ± 2 °C) for 3 days. The specimens are again ponded after removing the heat tent. This cycle continues for 12 weeks after which the continuous ponding cycle begins, and the specimens are left with 15% NaCl solution for the next 12 weeks at room temperature. Deionized water is added to replace any solution lost due to evaporation. The reading is taken each week for 96 weeks.

2.4.5 Corrosion Monitoring and Measurements

Macrocell Corrosion Rate

Macrocell corrosion rate is obtained by measuring the voltage drop across a 10-ohm resistor connected to the wire which is connected to the anode and cathode bar of a test specimen. Ohm's law gives the current density:

$$i_{\text{corr}} = 10^{-6} * \frac{V}{RA} \quad (7)$$

where,

i_{corr} = current density ($\mu\text{A}/\text{cm}^2$)

V = measured voltage drop across resistor (volts)

R = resistance of resistor (ohms)

A = surface area of anode (cm²)

Faraday's law is utilized to convert the current density into corrosion rate and expressed in terms of material loss per year:

$$r = k \frac{ia}{nF\rho} \quad (8)$$

where,

r = corrosion rate (μm/year)

I = current density (μA/cm²)

n = number of electrons lost per atom of metal oxidized; for iron, $n = 2$

F = Faraday's constant (96485 coulombs/equivalent)

ρ = density of metal (g/cm³); for iron, $\rho = 7.87$ g/cm³

a = atomic weight of corroding metal (g/mol); for iron, $a = 55.85$ g/mol

Corrosion Potential

Voltage drop readings are followed by corrosion potential readings, which are started after the switch in a terminal box is turned off, breaking the connection between anode and cathode, for at least 1.5 hours allowing potential stabilization. A silver-silver chloride electrode is used to measure the corrosion potential of top and bottom mat in bench-scale tests, and the potential is presented with respect to copper -copper sulfate electrode (CSE) in graphs.

Linear Polarization Resistance

Since the readings based on voltage drop account for macrocell corrosion measurement only, Linear Polarization Resistance (LPR) is measured at four-week intervals to provide a measure of the total corrosion rate, which includes both macrocell corrosion (anode and cathode are on separate bars) and microcell corrosion (anode and cathode are on the same bar).

2.5 POST-CRACK SPECIMENS

2.5.1 Description and Fabrication

The post-crack specimen, shown in Figure 4, is $12 \times 12 \times 7$ in. ($305 \times 305 \times 178$ mm) and is cast in two steps.

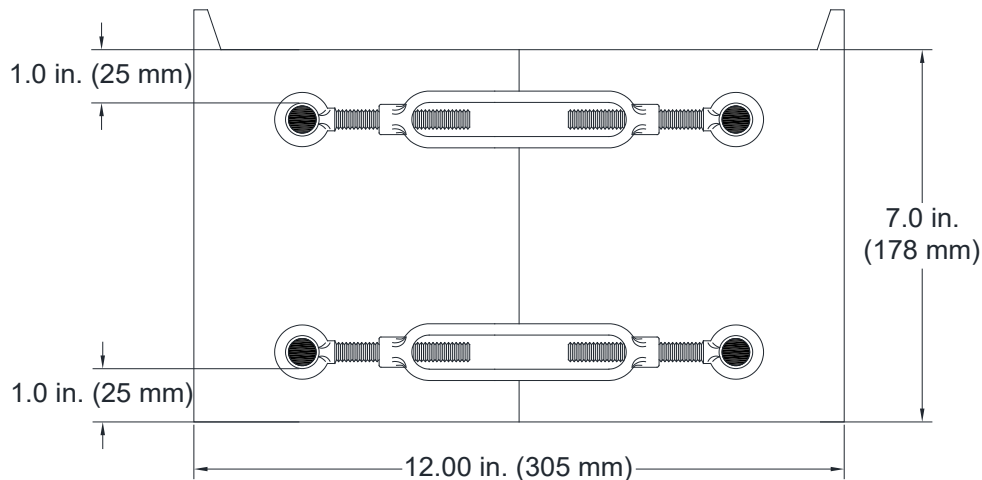


Figure 4: Post-crack specimen

First a $12 \times 6 \times 7$ in. ($305 \times 152 \times 178$ mm) specimen is cast. A second $12 \times 6 \times 7$ in. ($305 \times 152 \times 178$ mm) specimen is then match-cast adjacent to the first, leaving a potential crack plane at the interface. To accomplish this, the first specimen is cast to fill half the depth of the formwork used for an SE specimen (Figure 5). One day after casting the first half, the empty top portion of the formwork, as shown in Figure 5, is closed with a piece of plywood, while one of the side pieces (labelled 1 in Figure 5) is removed. The resulting formwork, shown in Figure 6, is used to cast the second half. The second half of the specimens, also $12 \times 6 \times 7$ in. ($305 \times 152 \times 178$ mm), is then match-cast next to the first beam forming a post-crack specimen.

The specimen contains four 20 in. (508 mm) long reinforcing bars with a clear cover of 1 in. (25 mm) on both top and the bottom placed 8 in. (203 mm) apart. Turnbuckles are welded to the bars to allow the two halves of the specimen to be separated to simulate a crack opening after

the overlay has been installed (Figure 4). Welding prevents a gap from forming between the reinforcing bar and the eye of the turnbuckle.

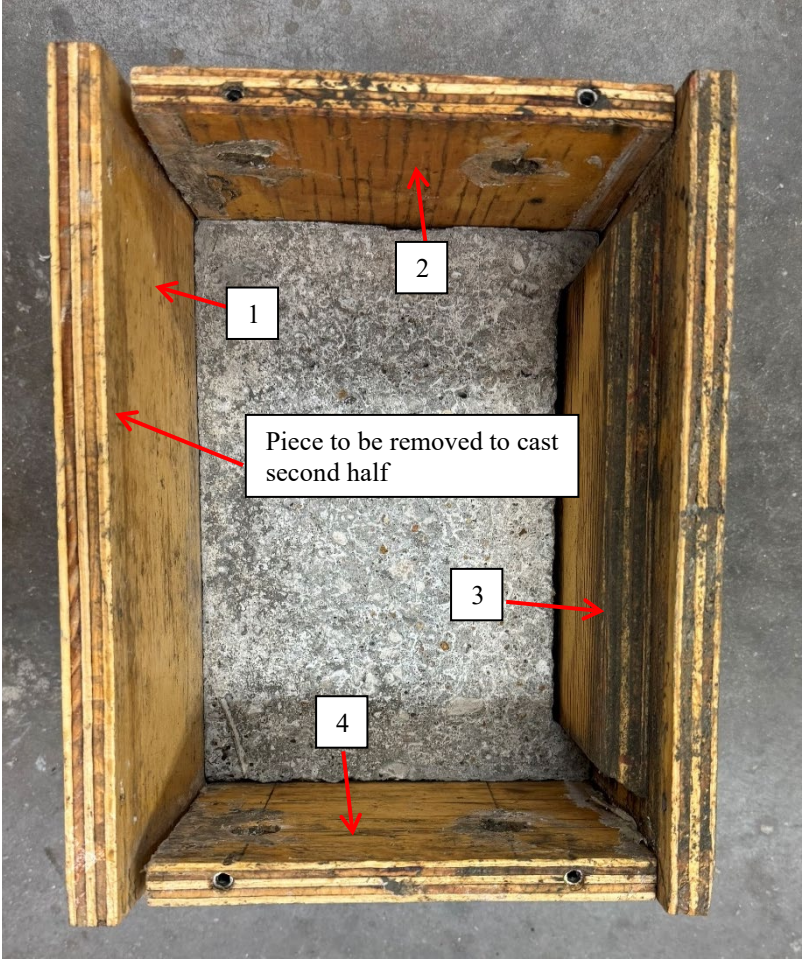


Figure 5: Formwork orientation after casting first half of post-crack specimen



Figure 6: Formwork orientation to cast second half of post-crack specimen

2.5.2 Test Procedure

Two bars on each of the layers accommodate a turnbuckle. To obtain the desired crack width using the turnbuckles, the circumference of the turnbuckle screws is marked with divisions spaced 8 degrees apart. To measure the crack width with a caliper during separation, two posts are attached, one on each side of the crack. The setup of caliper with posts can be seen in Figure 7. The rotation of the turnbuckle needed to obtain a crack width between 12 and 16 mils (0.012 and 0.016 in.),

typical of widths observed on bridge decks, is measured on each specimen prior to application of the polymer. First, the turnbuckle on the upper bars on one side is rotated 1 division, followed by the rotation of 1 division of the turnbuckle on the lower bars on the same side; the turnbuckles on the other side are rotated in a similar manner. This process continues until a crack width between 12 and 16 mils is obtained on both sides. The crack is then closed, and the process is repeated for a total of five trials to obtain the average rotation needed to attain the desired crack width. The specimen is then coated with polymer and aggregate. After curing the polymer for one month, the turnbuckle is rotated to obtain the desired crack width.

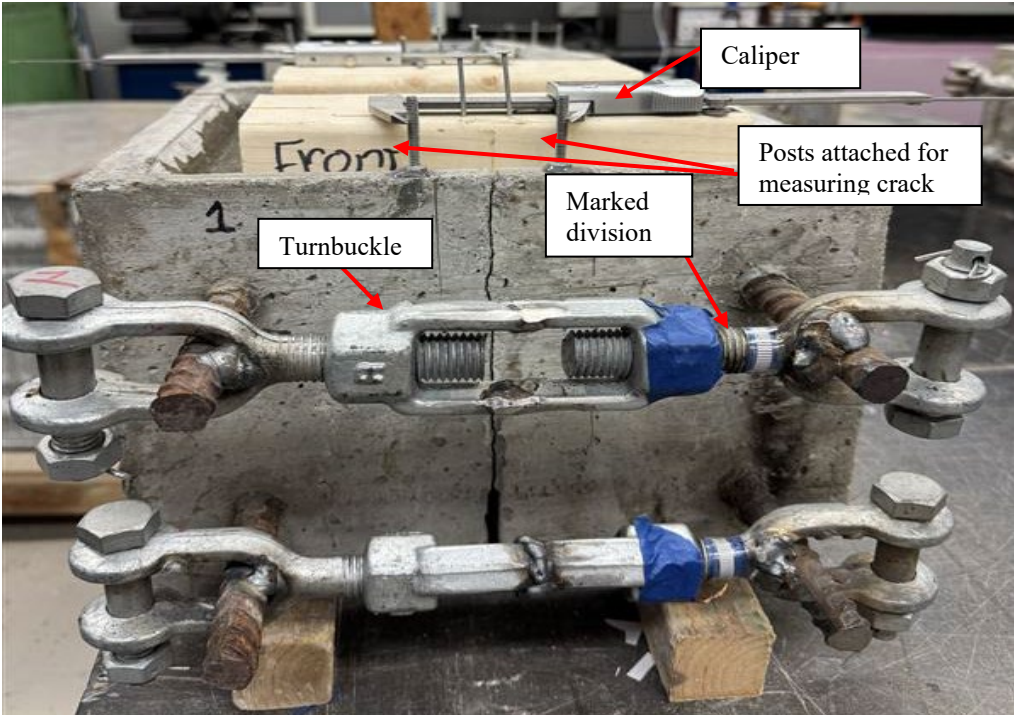


Figure 7: Post-crack specimen prototype

2.6 Test Program

Bench scale tests consist of cracked beam and Southern Exposure specimens coated with different layers of Sikadur and Flexolith polymers and aggregate. All the specimens have conventional reinforcement. The test also includes cracked beam specimens initially ponded with

chloride for 8 weeks to put chloride into the concrete prior to application of the multilayer polymer overlay to evaluate the effectiveness of the overlay to resist corrosion in chloride contaminated bridge structures. The number of specimens is presented in Tables 5 and 6.

Table 6: Corrosion test specimens with Sikadur and Flexolith polymers

Layers of Coating	No of Specimens			
	CB Sikadur	SE Sikadur	CB Flexolith	SE Flexolith
1 layer of Epoxy	4	4	4	4
1 layer of Epoxy and Agg	4	4	4	4
2 layers of Epoxy and Agg	4	4	4	4

Table 7: Chloride-Contaminated and Control Specimens

Specimen	CB Sikadur	CB Flexolith	SE
Chloride-Contaminated	4	4	-
Control Specimen	4		4

3 RESULTS- CRACKED BEAM AND SOUTHERN EXPOSURE

3.1 CORROSION RATE AND CORROSION POTENTIALS

The results include the macrocell corrosion rate and corrosion potentials of anode (top mat) for the cracked beam and Southern Exposure specimens under test. The results shown are through October 2024. Figures 8 through 19 show the results for specimens with the Sikadur®-22 Lo-Mod epoxy, and Figures 20 through 31 show the results for specimens with the Flexolith epoxy. The even numbered figures show the macrocell corrosion rate (between the top and bottom mats of steel) as a function of time and the odd numbered figures show the corrosion potential of the top mat of steel relative to a copper/copper sulfate electrode as a function of time. At the end of October 2024, the oldest Sikadur specimens had been under test for 43 weeks and the oldest Flexolith specimens had been under test for 36 weeks. For some specimens, the corrosion rate may appear to be negative. This negative corrosion rate does not indicate negative corrosion; rather it is caused by minor differences in the oxidation rate between the anode bar (or bars) and the cathode bars.

Figures 8 and 9, respectively, show the macrocell corrosion rates and corrosion potentials of the top mat for individual CB specimens with 1 layer of Sikadur epoxy and no aggregate. The corrosion rates for this group of specimens, as shown in Figure 8, reached as high as 0.06 $\mu\text{m}/\text{yr}$ and the corrosion potential of the top mat was never more negative than -0.15 V, as shown in Figure 9, indicating that no corrosion was occurring.

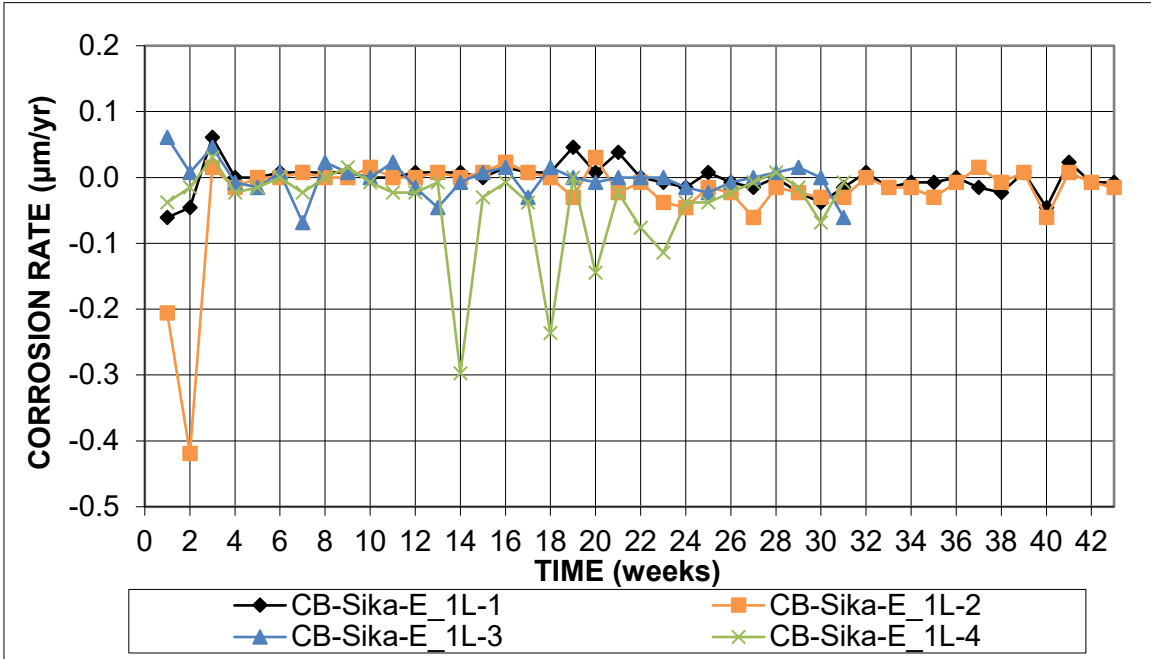


Figure 8: Macrocell corrosion rate versus time for cracked beam specimens with one layer of Sikadur®-22 Lo-Mod epoxy

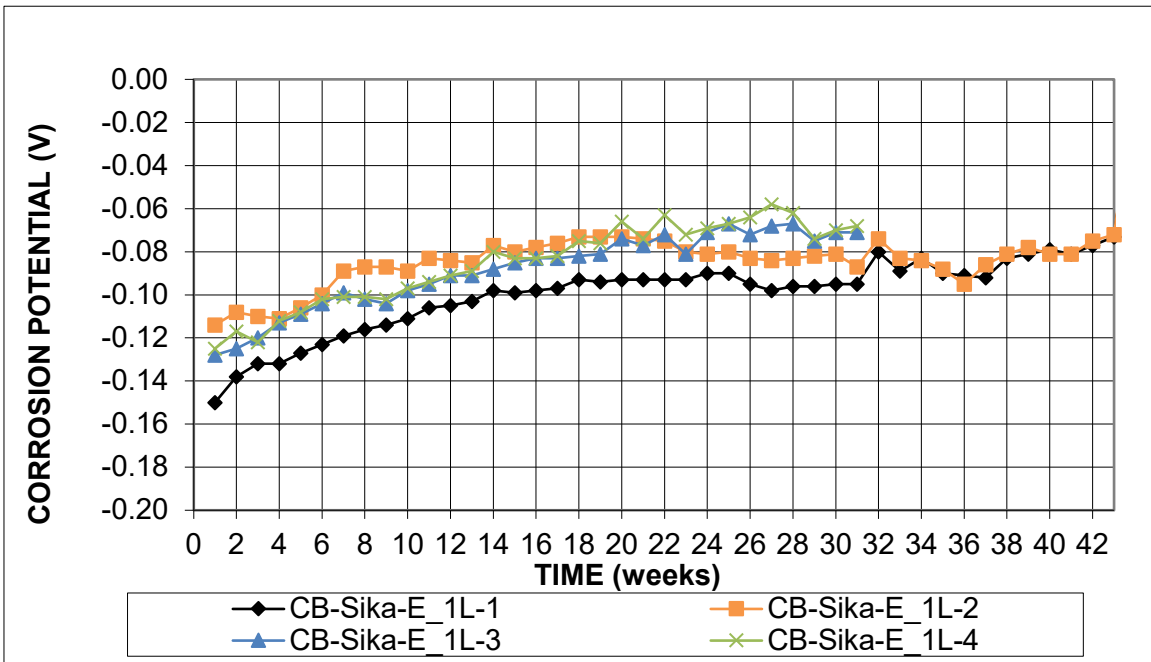


Figure 9: Corrosion potential of top mat of steel versus time for cracked beam specimens with one layer of Sikadur®-22 Lo-Mod epoxy

Figures 10 and 11, respectively, show the macrocell corrosion rates and corrosion potentials of top mat for individual CB specimens with 1 layer of Sikadur epoxy and 1 layer of aggregate. The corrosion rate for one specimen in this group, CB-Sika-E_1L_A-1, as shown in

Figure 10, reached 0.91 $\mu\text{m}/\text{yr}$ on week 3 and dropped to almost 0 $\mu\text{m}/\text{yr}$ afterwards and the corrosion potential of the top mat was never more negative than -0.153 V, as shown in Figure 11. The higher corrosion rate in week 3 can be associated with the disturbance in the connection and not because of the corrosion activity. The corrosion rate for other specimens in this group reached as high as 0.14 $\mu\text{m}/\text{yr}$ and the corrosion potential never more negative than -0.14 V, indicating that no corrosion was occurring.

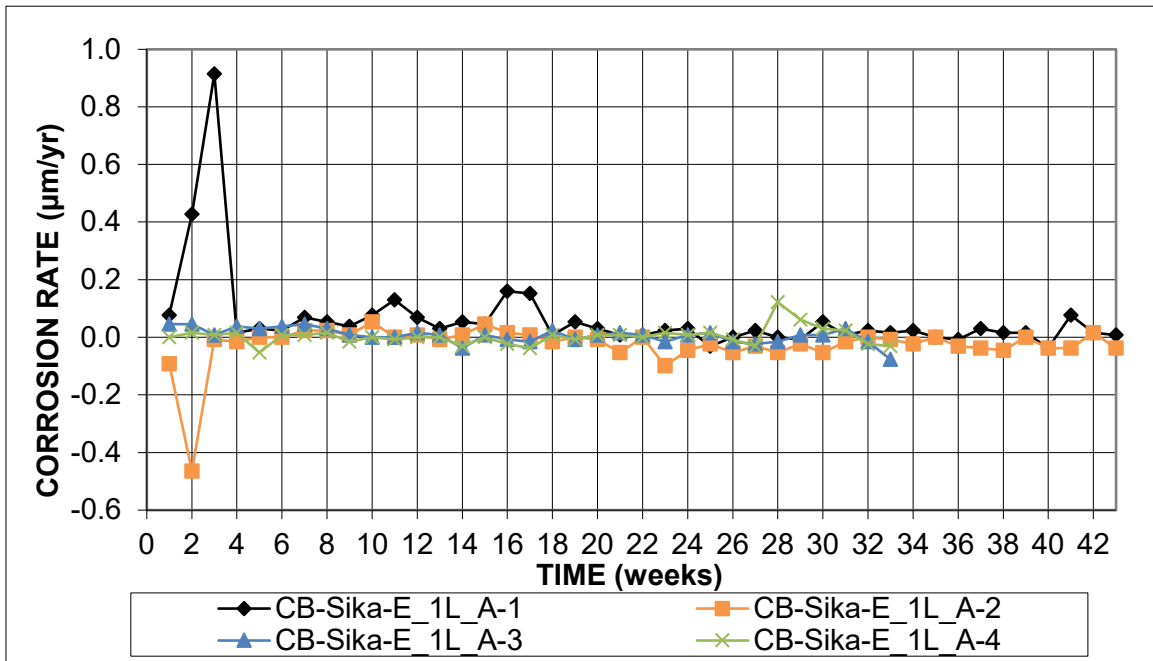


Figure 10: Macrocell corrosion rate versus time for cracked beam specimens with one layer of Sikadur®-22 Lo-Mod epoxy and aggregate

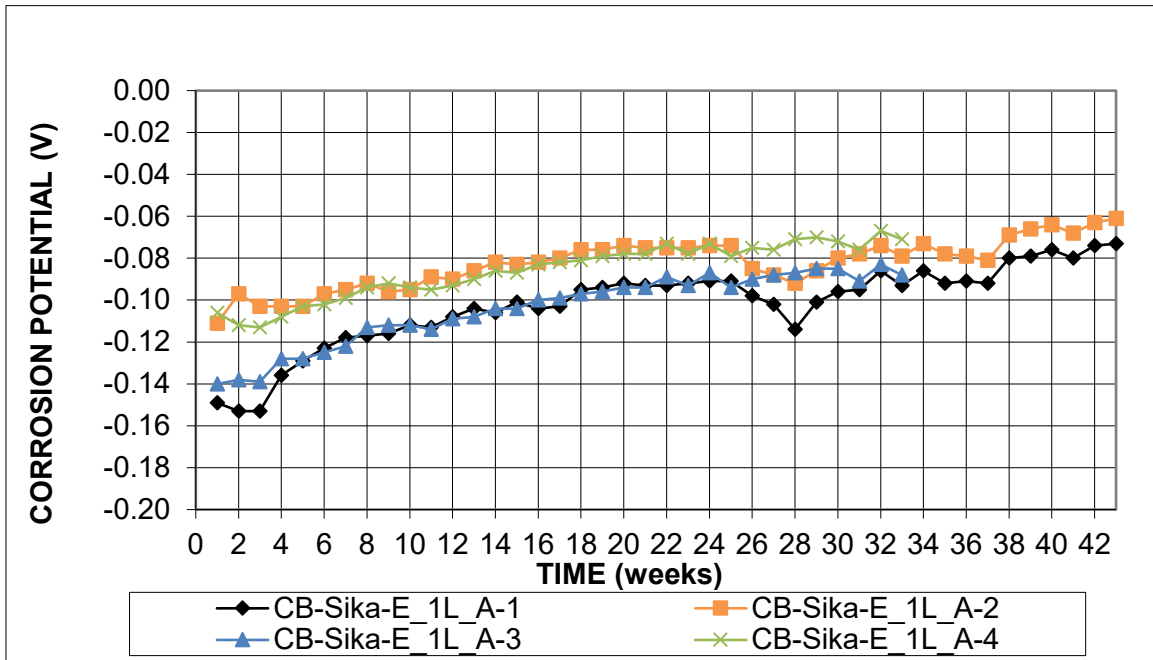


Figure 11: Corrosion potential of top mat of steel versus time for cracked beam specimens with one layer of Sikadur®-22 Lo-Mod epoxy and aggregate

Figures 12 and 13, respectively, show the macrocell corrosion rates and corrosion potentials of top mat for individual CB specimens with 2 layers of Sikadur epoxy and 2 layers of aggregate. The corrosion rate for one specimen in this group, CB-Sika-E_2L_A-1, as shown in Figure 12, reached as high as $3.6 \mu\text{m}/\text{yr}$ and the corrosion potential of the top mat was as low as -0.39 V , as shown in Figure 13, indicating that corrosion was occurring. The corrosion rate for CB-Sika-E_2L_A-4 reached $1.22 \mu\text{m}/\text{yr}$ on week 3 and dropped to almost $0 \mu\text{m}/\text{yr}$ after week 6, and the corrosion potential of the top mat was never more negative than -0.071 V . The higher corrosion rate from week 2 to 5 can be associated with the disturbance in the connection and not because of the corrosion activity. The corrosion rate for other specimens in this group reached as high as $0.28 \mu\text{m}/\text{yr}$, and the corrosion potential of the top mat was never more negative than -0.175 , indicating that no corrosion was occurring.

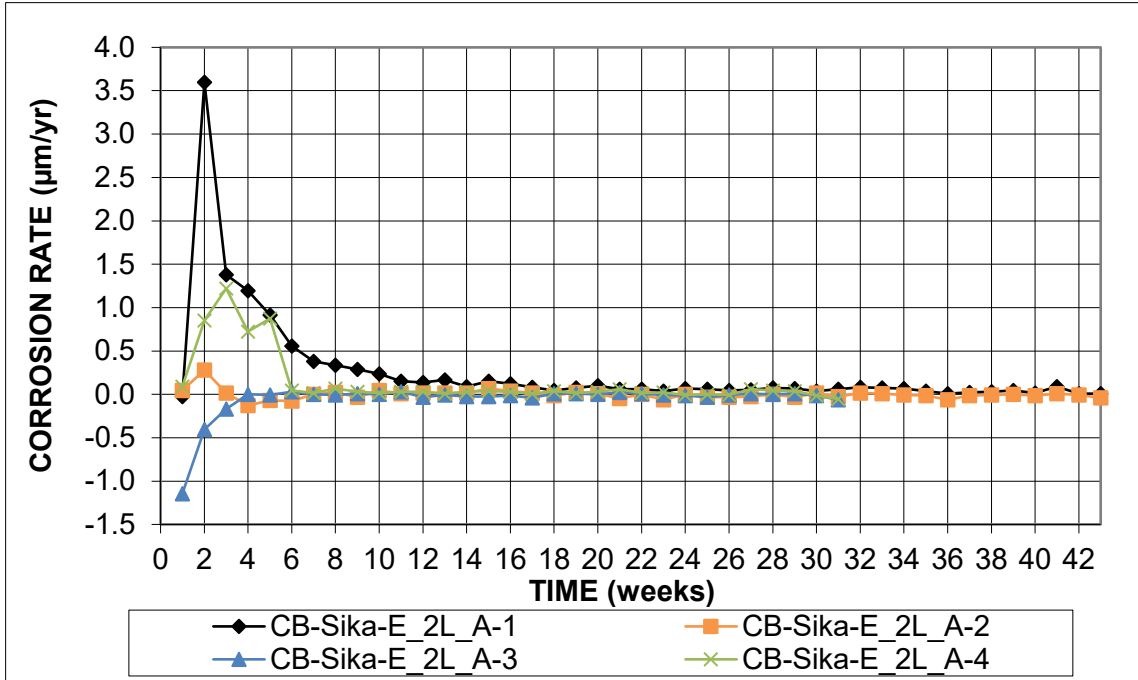


Figure 12: Macrocell corrosion rate versus time for cracked beam specimens with two layers of Sikadur®-22 Lo-Mod epoxy and aggregate

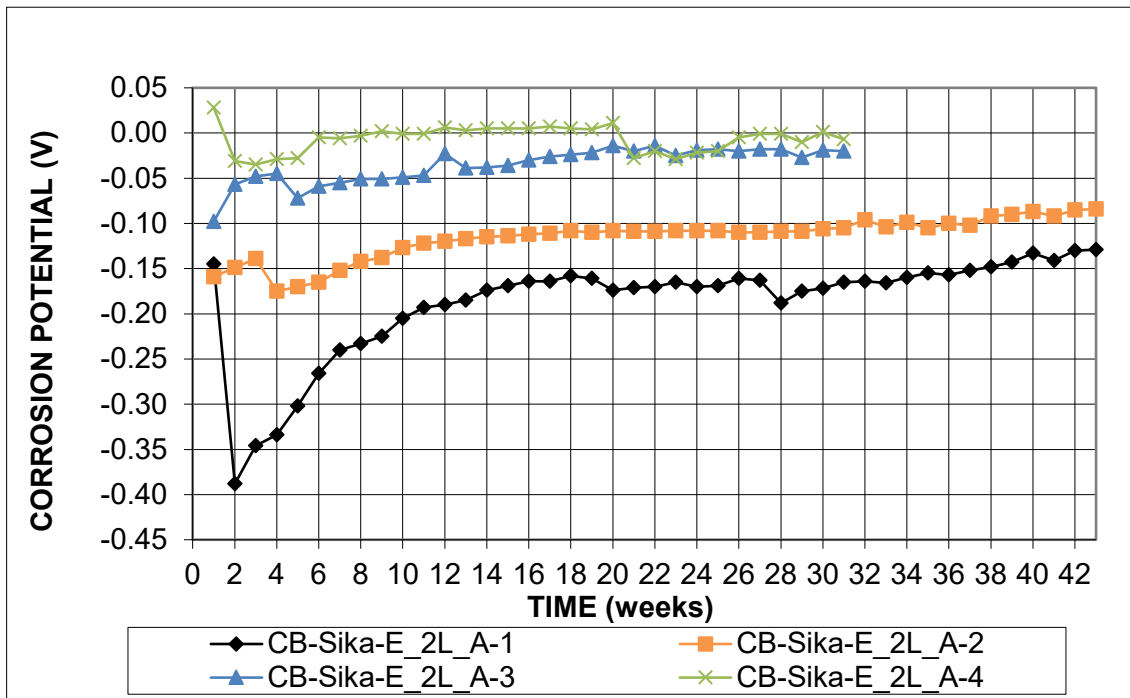


Figure 13: Corrosion potential of top mat of steel versus time for cracked beam specimens with two layers of Sikadur®-22 Lo-Mod epoxy and aggregate

Figures 14 and 15, respectively, show the macrocell corrosion rates and corrosion potentials of top mat for individual SE specimens with 1 layer of Sikadur epoxy. The corrosion

rates for this group of specimens, as shown in Figure 14, reached as high as 0.3 $\mu\text{m}/\text{yr}$ and the corrosion potential of the top mat was never more negative than -0.152 V, as shown in Figure 15, indicating that no corrosion was occurring.

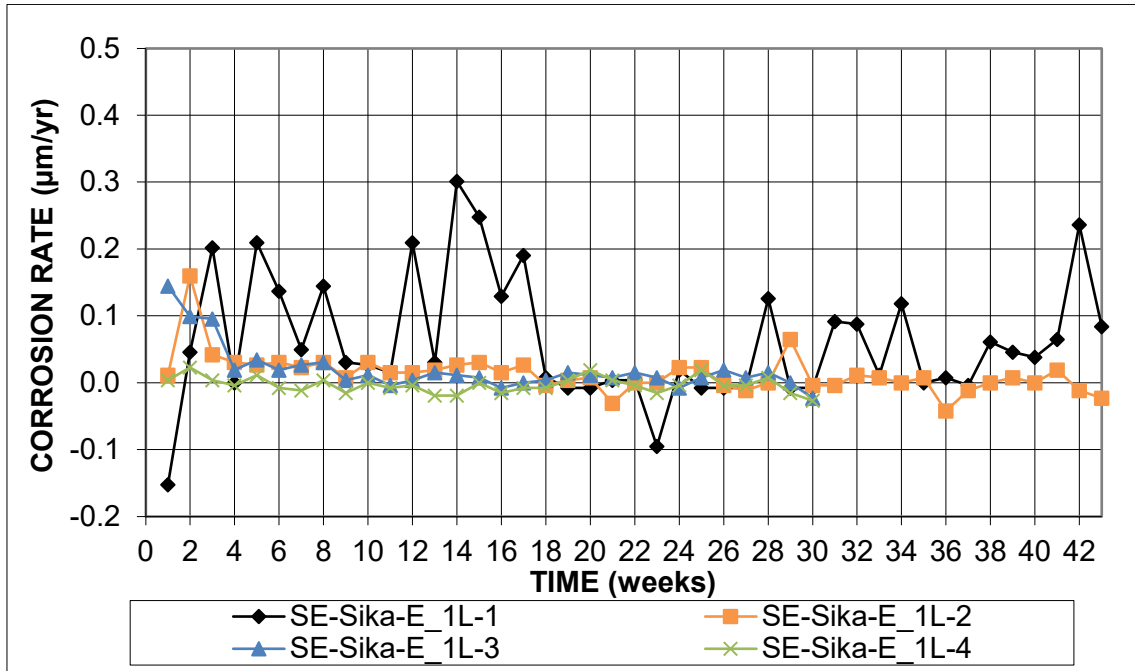


Figure 14: Macrocell corrosion rate versus time for Southern Exposure specimens with one layer of Sikadur®-22 Lo-Mod epoxy

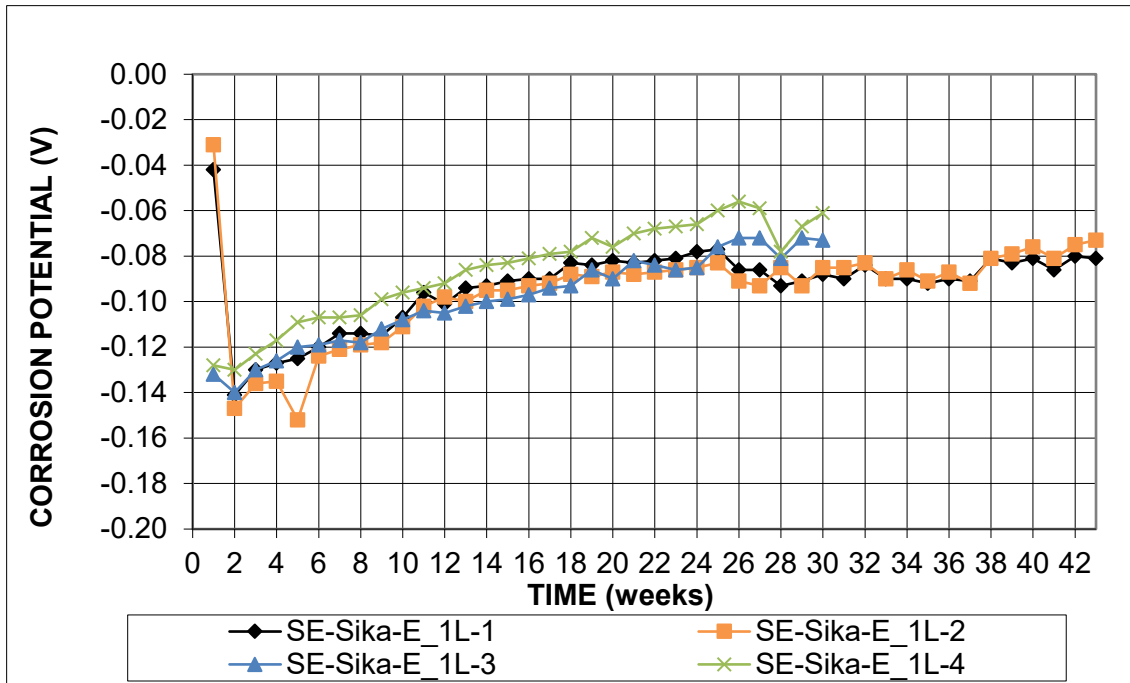


Figure 15: Corrosion potential of top mat of steel versus time for Southern Exposure specimens with one layer of Sikadur®-22 Lo-Mod epoxy

Figures 16 and 17, respectively, show the macrocell corrosion rates and corrosion potentials of top mat for individual SE specimens with 1 layer of Sikadur epoxy and 1 layer of aggregate. The corrosion rates for one specimen in this group, SE-Sika-E_1L_A-3, as shown in Figure 16, reached as high as $0.98 \mu\text{m}/\text{yr}$ and the corrosion potential of the top mat was never more negative than -0.263 V , as shown in Figure 17. The corrosion rate for other specimens in this group reached as high as $0.24 \mu\text{m}/\text{yr}$ and the corrosion potential of the top mat was never more negative than -0.191 V , indicating that no corrosion was occurring.

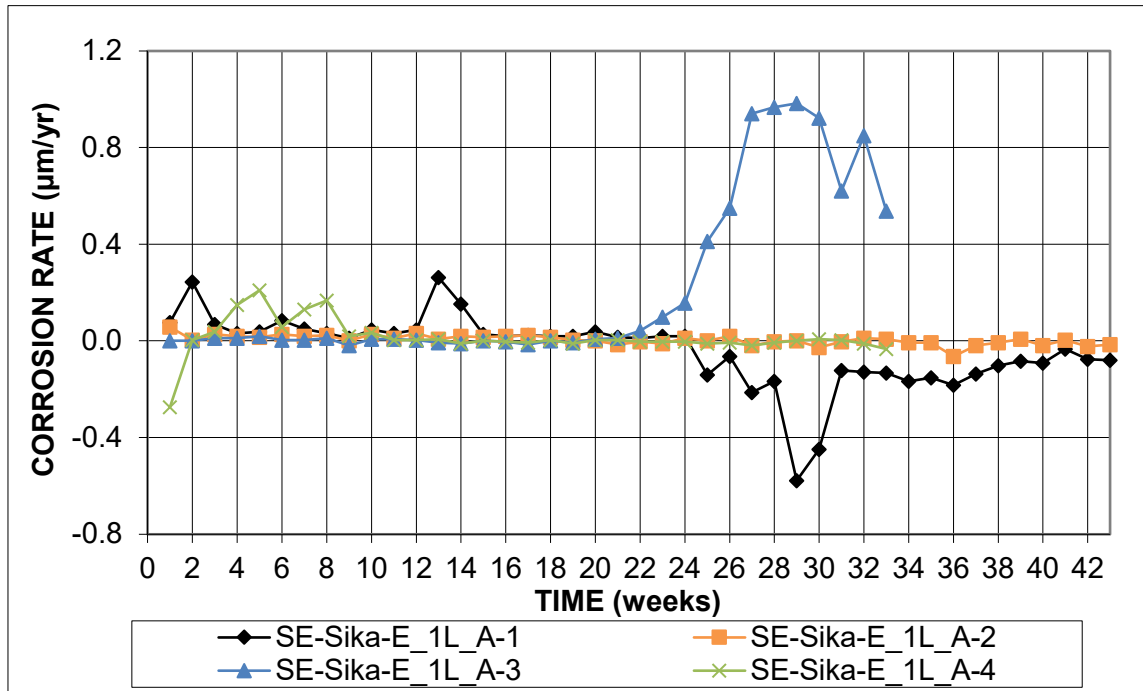


Figure 16: Macrocell corrosion rate versus time for Southern Exposure specimens with one layer of Sikadur®-22 Lo-Mod epoxy and aggregate

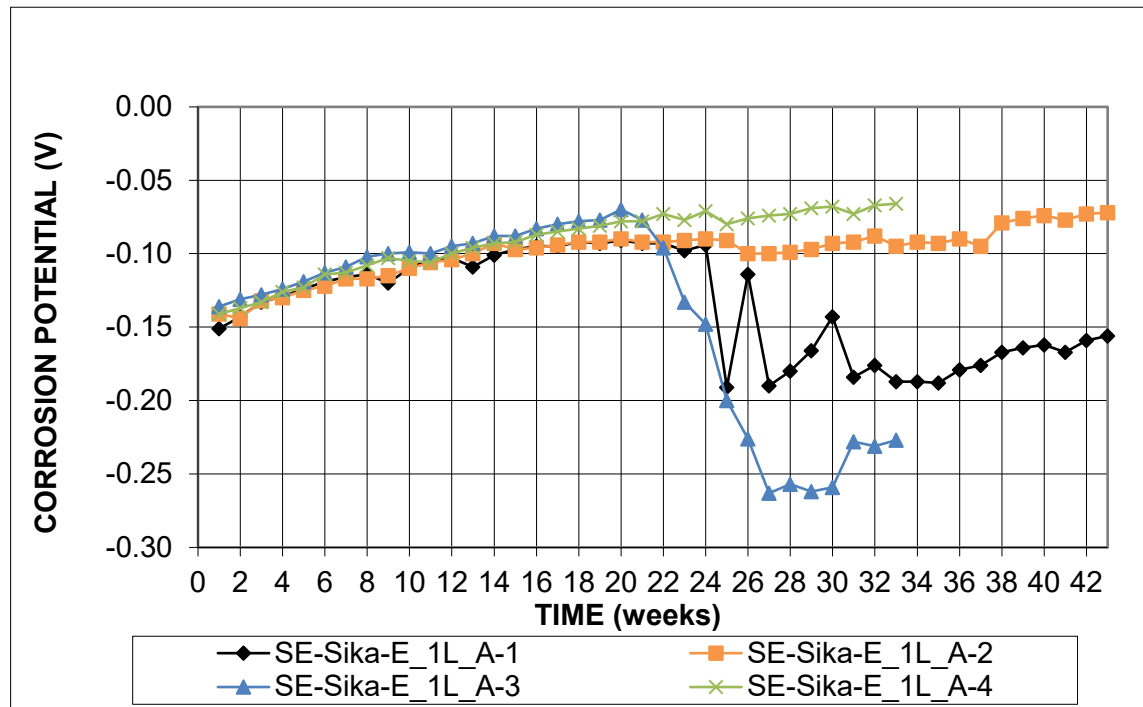


Figure 17: Corrosion potential of top mat of steel versus time for Southern Exposure specimens with one layer of Sikadur®-22 Lo-Mod epoxy and aggregate

Figures 18 and 19, respectively, show the macrocell corrosion rates and corrosion potentials of top mat for individual SE specimens with 2 layers of Sikadur epoxy and 2 layers of

aggregate. The corrosion rates for this group of specimens, as shown in Figure 16, reached as high as 0.32 $\mu\text{m}/\text{yr}$ and the corrosion potential of the top mat was never more negative than -0.243 V, as shown in Figure 17, indicating that no corrosion was occurring.

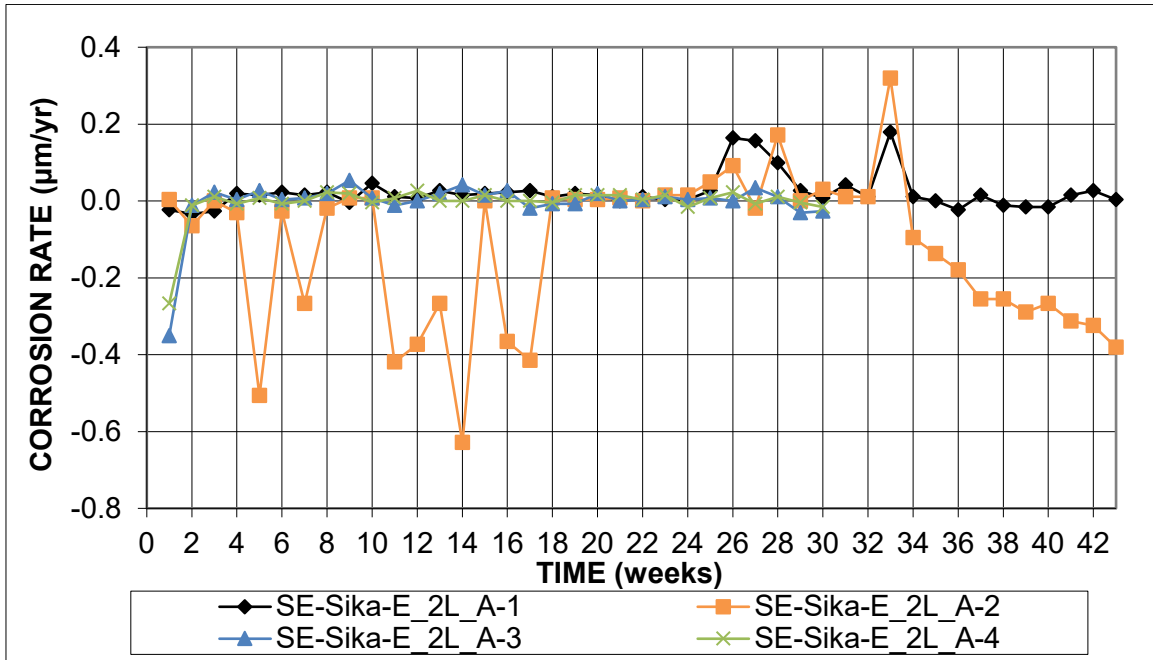


Figure 18: Macrocell corrosion rate versus time for Southern Exposure specimens with two layers of Sikadur®-22 Lo-Mod epoxy and aggregate

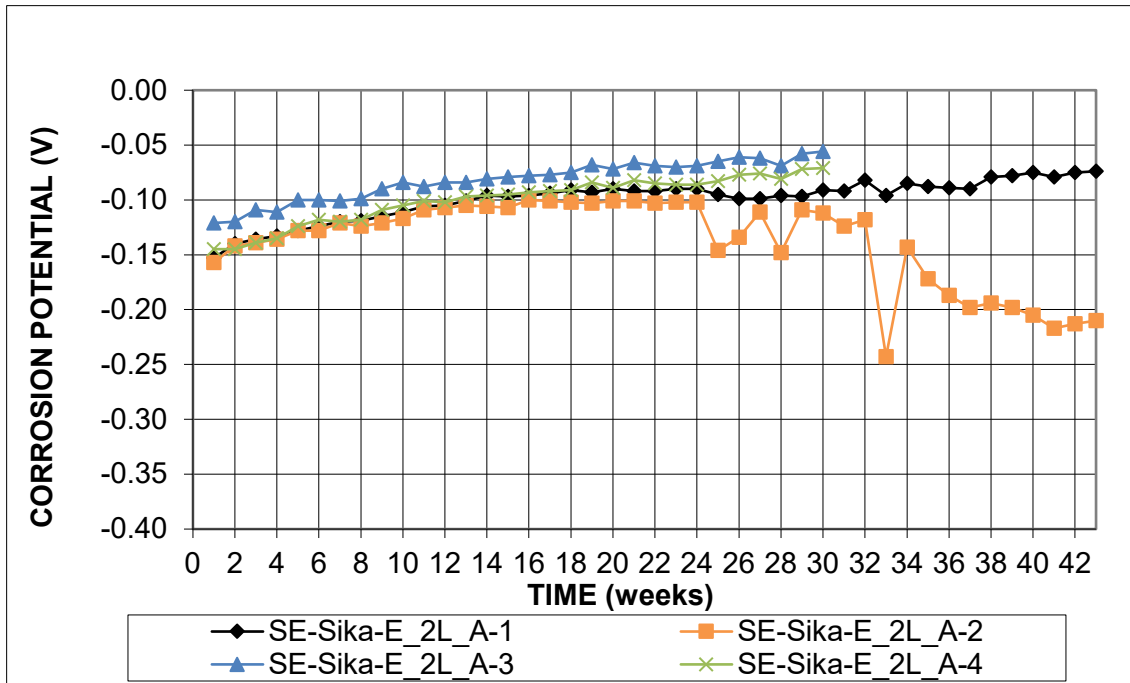


Figure 19: Corrosion potential of top mat of steel versus time for Southern Exposure specimens with two layers of Sikadur®-22 Lo-Mod epoxy and aggregate

Figures 20 and 21, respectively, show the macrocell corrosion rates and corrosion potentials of top mat for individual CB specimens with 1 layer of Flexolith epoxy. The corrosion rates for this group of specimens, as shown in Figure 20, reached as high as 0.41 $\mu\text{m}/\text{yr}$ and the corrosion potential of the top mat was never more negative than -0.134 V, as shown in Figure 21, indicating that no corrosion was occurring.

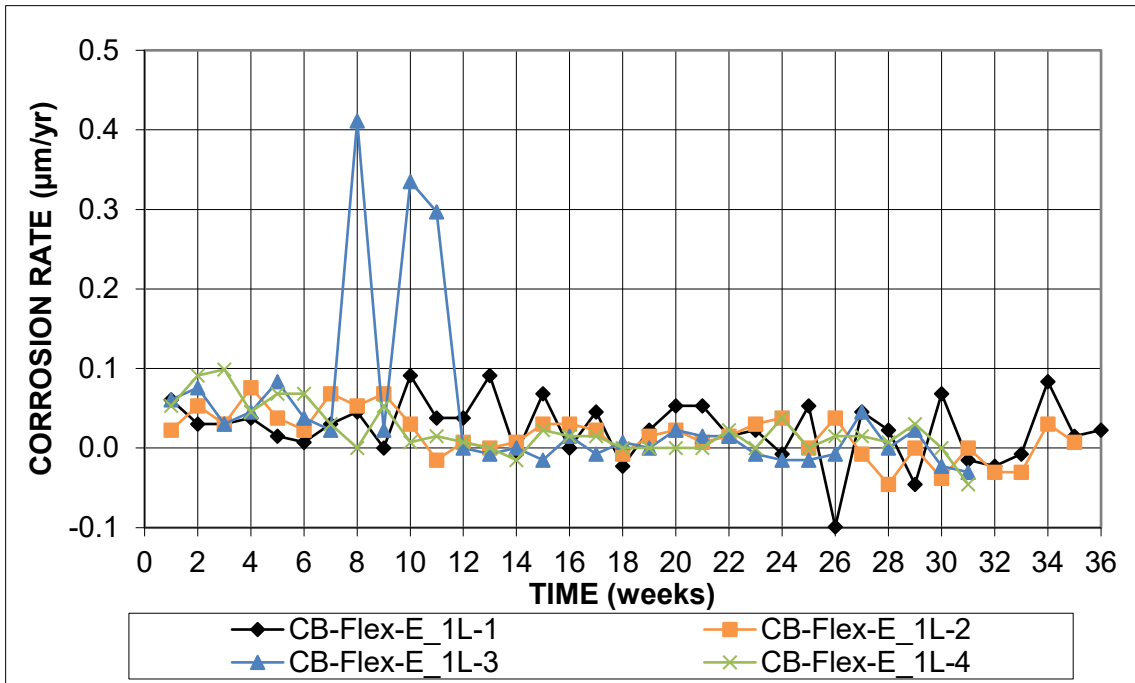


Figure 20: Macrocell corrosion rate versus time for cracked beam specimens with one layer of Flexolith epoxy

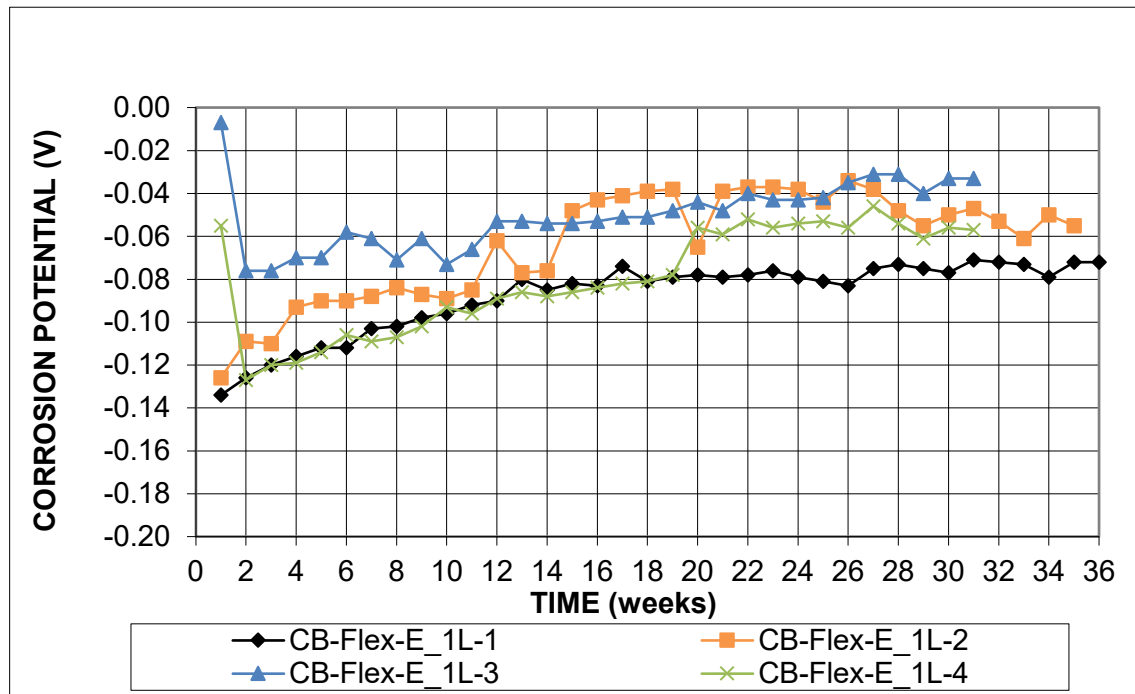


Figure 21: Corrosion potential of top mat of steel versus time for cracked beam specimens with one layer of Flexolith epoxy

Figures 22 and 23, respectively, show the macrocell corrosion rates and corrosion potentials of top mat for individual CB specimens with 1 layer of Flexolith epoxy and 1 layer of

aggregate. The corrosion rate for one specimen in this group, CB-Flex-E_1L_A-1, as shown in Figure 22, started at 18 $\mu\text{m}/\text{yr}$ and the corrosion potential of the top mat started at -0.55 V , as shown in Figure 23, indicating that corrosion was occurring. The corrosion rate then gradually decreased until week 6 and stabilized at around $12.5\ \mu\text{m}/\text{yr}$ from week 6 to 8. The corrosion rate again gradually decreased to $8\ \mu\text{m}/\text{yr}$ at week 12 and stabilized at that value from week 12 to 15 before it again started to gradually decrease until week 24 where it reached $2.93\ \mu\text{m}/\text{yr}$. There was a spike in corrosion rate at week 25 and reached a peak rate of $6.14\ \mu\text{m}/\text{yr}$ at week 26 and stabilized around that value till week 30. After this week, corrosion rate again started to gradually decrease again reaching $3.4\ \mu\text{m}/\text{yr}$ at week 36. The corrosion rate for other specimens in this group reached as high as $0.56\ \mu\text{m}/\text{yr}$ and the corrosion potential of the top mat was never more negative than -0.229 V , indicating that little or no corrosion was occurring.

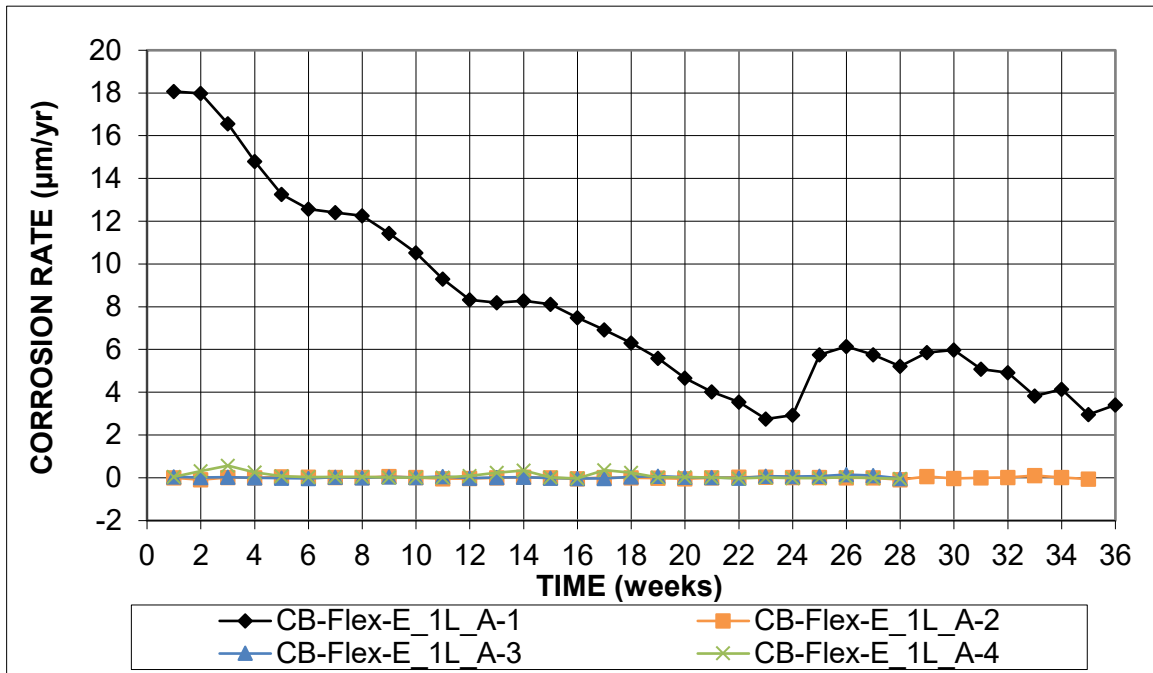


Figure 22: Macrocell corrosion rate versus time for cracked beam specimens with one layer of Flexolith epoxy and aggregate

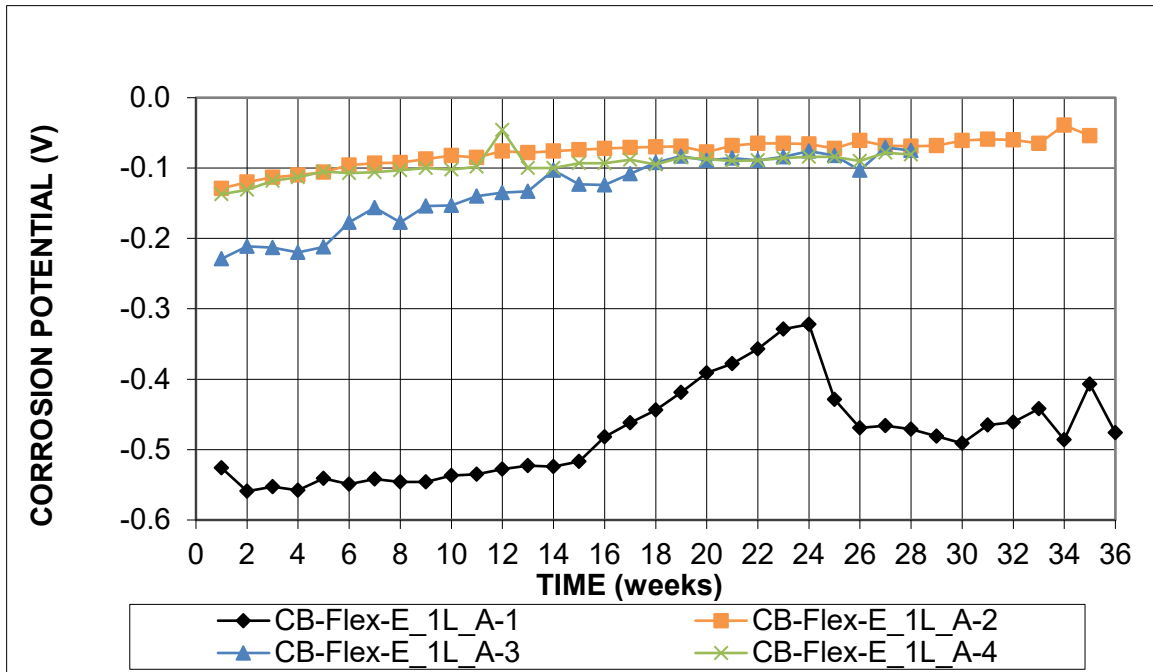


Figure 23: Corrosion potential of top mat of steel versus time for cracked-beam specimens with one layer of Flexolith epoxy and aggregate

Figures 24 and 25, respectively, show the macrocell corrosion rates and corrosion potentials of top mat for individual CB specimens with 2 layers of Flexolith epoxy and 2 layers of aggregate. The corrosion rates for one specimen in this group, CB-Flex-E_2L_A-2, as shown in Figure 24, reached as high as 11.4 $\mu\text{m}/\text{yr}$ and the corrosion potential of the top mat was as low as -0.54 V, as shown in Figure 25, indicating that corrosion was occurring in this specimen. The corrosion rate for the other specimens in this group reached as high as 0.11 $\mu\text{m}/\text{yr}$ and the corrosion potential of the top mat was never more negative than -0.14 V, indicating that no corrosion was occurring.

Figures 26 and 27, respectively, show the macrocell corrosion rates and corrosion potentials of top mat for individual SE specimens with 1 layer of Flexolith epoxy. The corrosion rates for this group of specimens, as shown in Figure 26, reached only as high as 0.25 $\mu\text{m}/\text{yr}$ and the corrosion potential of the top mat was never more negative than -0.13 V, as shown in Figure 27, indicating that no corrosion was occurring.

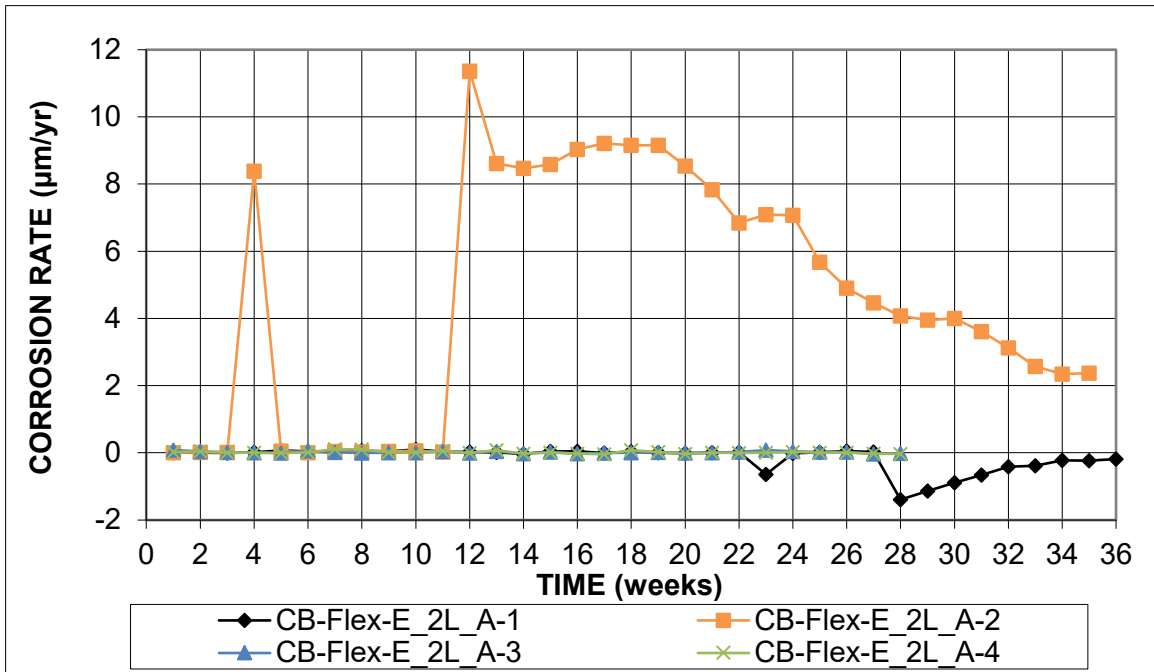


Figure 24: Macrocell corrosion rate versus time for cracked beam specimens with two layers of Flexolith epoxy and aggregate

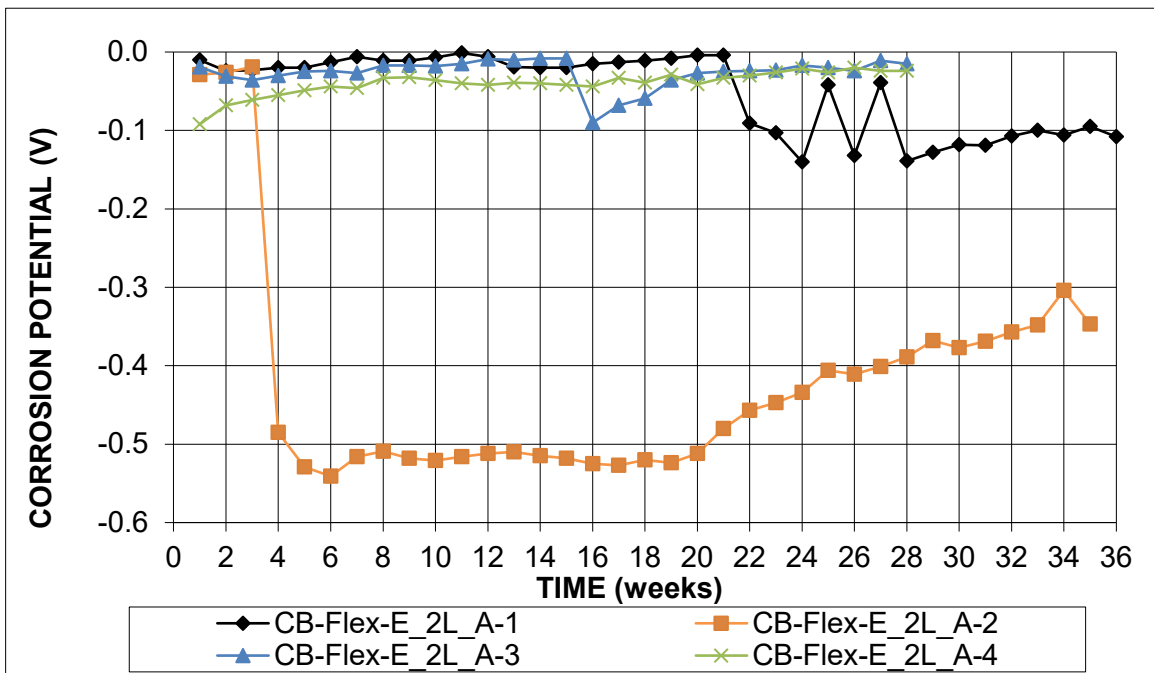


Figure 25: Corrosion potential of top mat of steel versus time for cracked beam specimens with two layers of Flexolith epoxy and aggregate

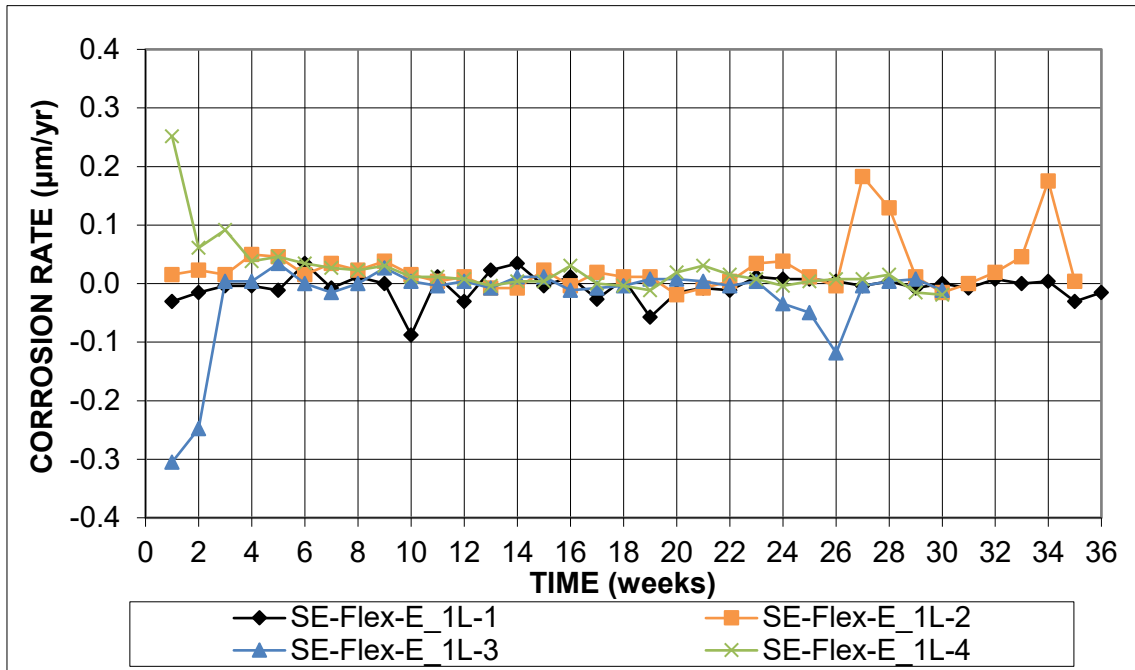


Figure 26: Macrocell corrosion rate versus time for Southern Exposure specimens with one layer of Flexolith epoxy

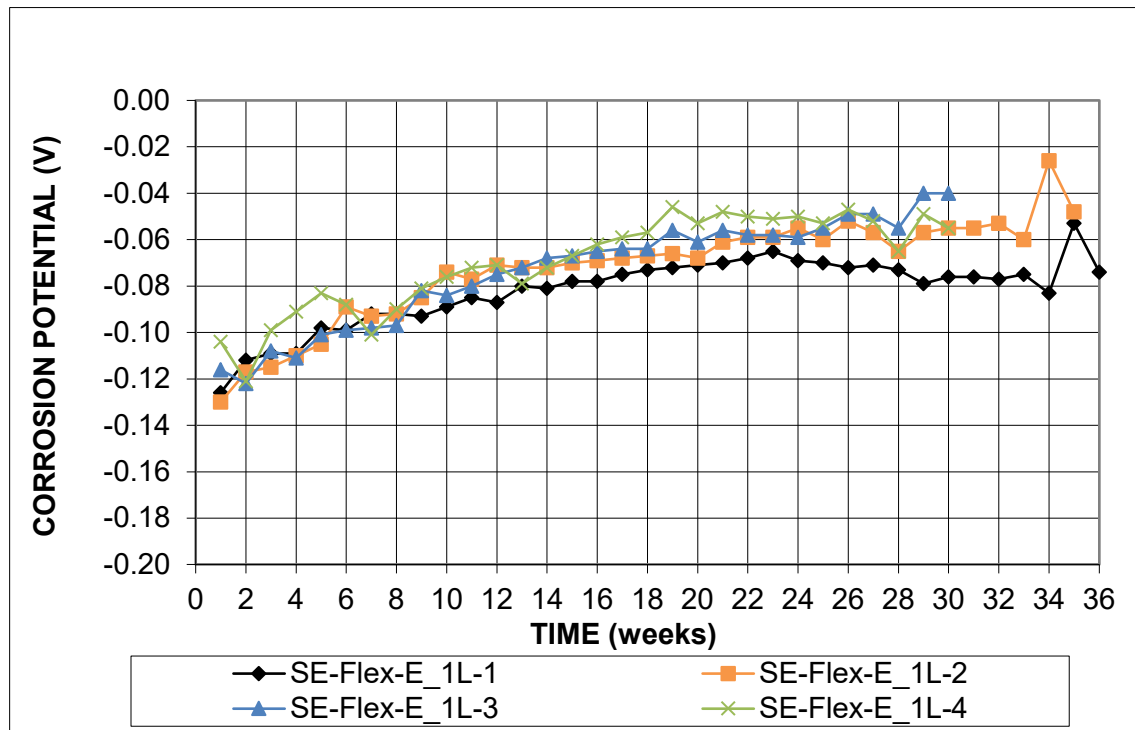


Figure 27: Corrosion potential of top mat of steel versus time for Southern Exposure specimens with one layer of Flexolith epoxy

Figures 28 and 29, respectively, show the macrocell corrosion rates and corrosion potentials of top mat for individual SE specimens with 1 layer of Flexolith epoxy and 1 layer of

aggregate. The corrosion rates for this group of specimens, as shown in Figure 28, reached as high as 0.1 $\mu\text{m}/\text{yr}$ and the corrosion potential of the top mat was never more negative than -0.15 V, as shown in Figure 29, indicating that no corrosion was occurring.

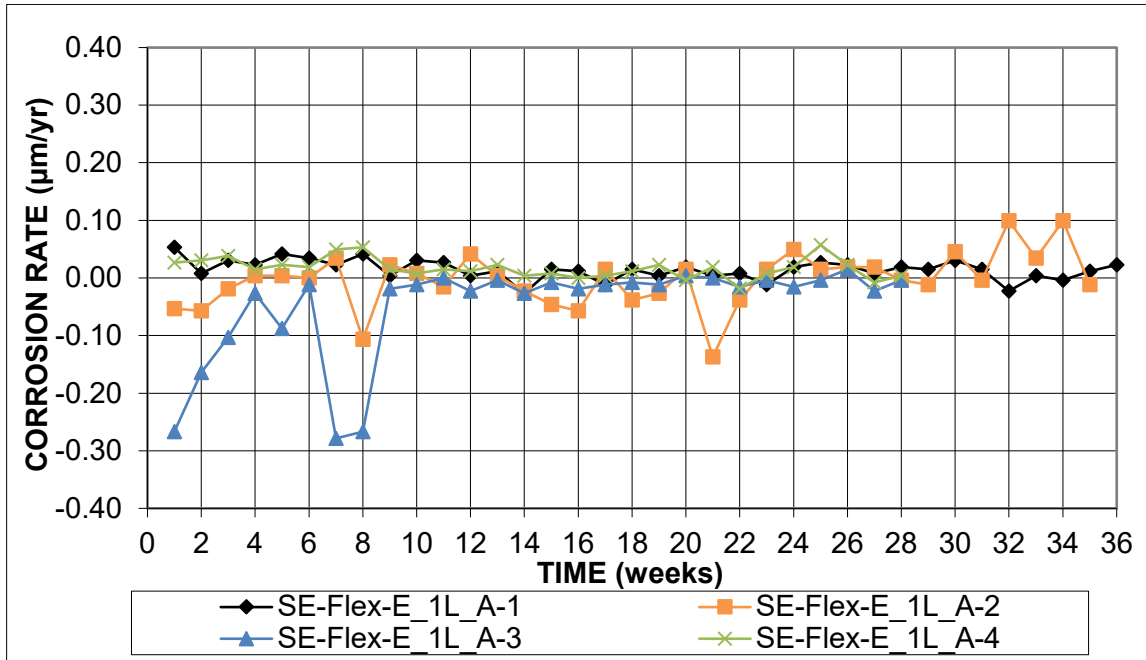


Figure 28: Macrocell corrosion rate versus time for Southern Exposure specimens with one layer of Flexolith epoxy and aggregate

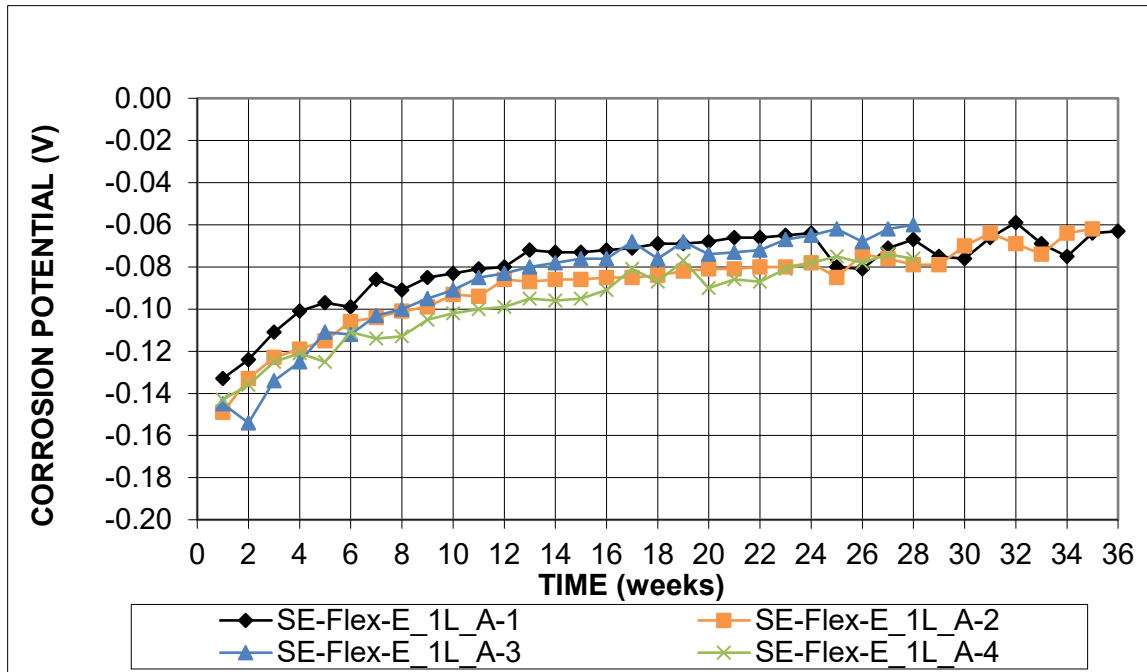


Figure 29: Corrosion potential of top mat of steel versus time for Southern Exposure specimens with one layer of Flexolith epoxy and aggregate

Figures 30 and 31, respectively, show the macrocell corrosion rates and corrosion potentials of top mat for individual SE specimens with 2 layers of Flexolith epoxy and 2 layers of aggregate. The corrosion rate for one specimen in this group, SE-Flex-E_2L_A-3, as shown in Figure 30, reached $0.4 \mu\text{m}/\text{yr}$ at week 3 and dropped to almost $0 \mu\text{m}/\text{yr}$ afterwards, and the corrosion potential of the top mat was never more negative than -0.25 V , as shown in Figure 31. The corrosion rate at week 3 can be associated with the disturbance in the connection and not because of the corrosion activity. The corrosion rate for the other specimens in this group reached as high as $0.08 \mu\text{m}/\text{yr}$, and the corrosion potential of top mat was never more negative than -0.246 V , indicating that no corrosion was occurring. A negative corrosion rate can be observed for SE-Flex-E_2L_A-1. This indicates the difference in oxidation rate between the anode and the cathode bars and does not indicate reduction in corrosion.

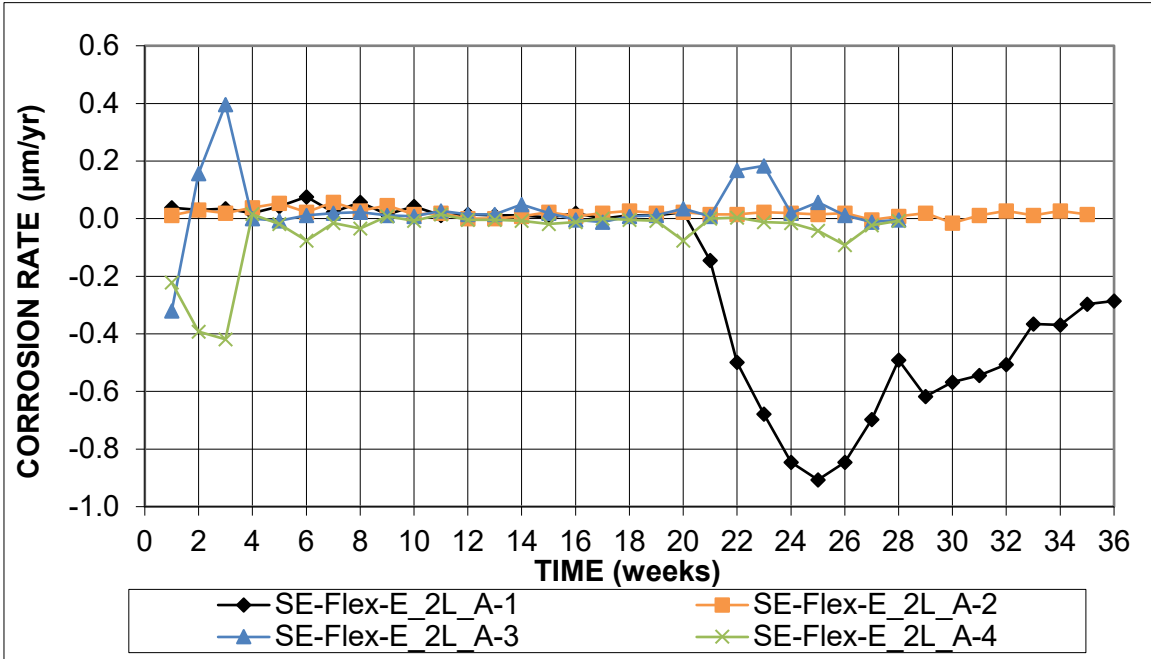


Figure 30: Macrocell corrosion rate versus time for Southern Exposure specimens with two layers of Flexolith epoxy and aggregate

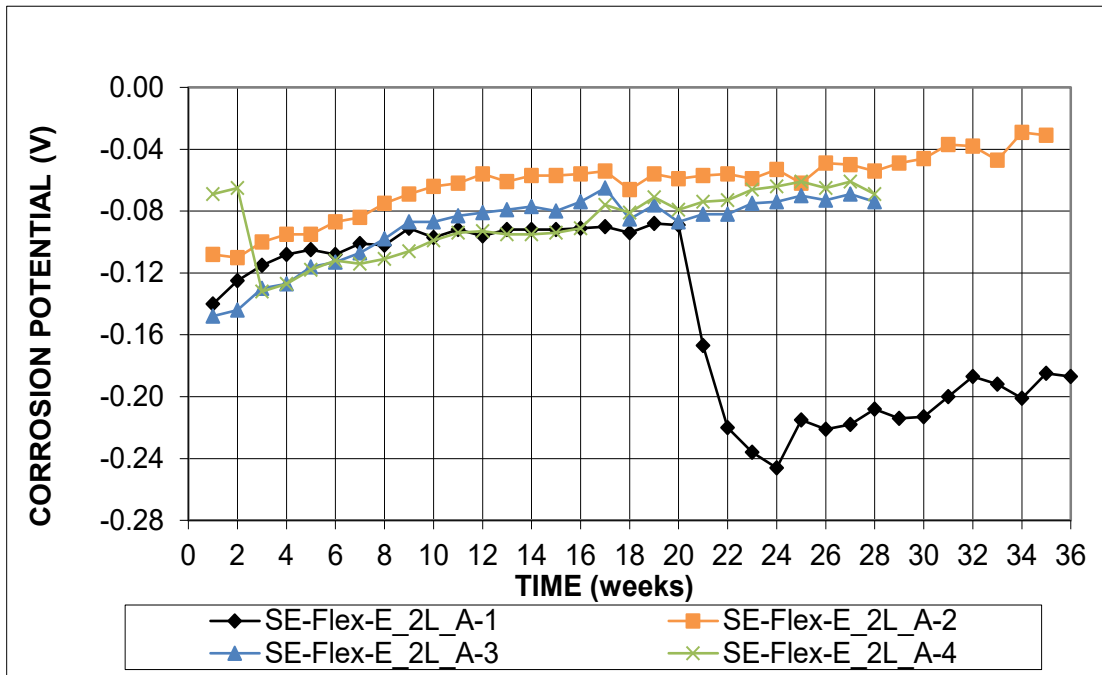


Figure 31: Corrosion potential of top mat of steel versus time for Southern Exposure specimens with two layers of Flexolith epoxy and aggregate

Figure 32 shows the average macrocell corrosion rates for the CB specimens coated with 1 layer of Sikadur epoxy only (CB-Sika-E_1L), 1 layer of Sikadur epoxy and 1 layer of aggregate (CB-Sika-E_1L_A), 2 layers of Sikadur epoxy and 2 layers of aggregate (CB-Sika-E_2L_A), and

the Control CB (CB-Control) specimens. The average corrosion potentials for the top mats of steel are shown in Figure 33. The average corrosion rates and corrosion potentials are based on the average of four individual specimens of each type. The highest average corrosion rate among the specimens with polymer overlay was for CB-Sika-E_2L_A, 1.08 $\mu\text{m}/\text{yr}$, dropping close to zero by week 4, while Control specimens exhibited an average corrosion rate between 11 and 18.35 $\mu\text{m}/\text{yr}$. The average corrosion potential is more positive than -0.2V vs CSE for the specimens with the various layers of polymer and aggregate and close to -0.6V vs CSE for the Control specimens. This shows the corrosion of the cracked beam specimens coated with various layers of Sikadur polymers and aggregate is considerably lower than that of the control specimens. This indicates the application of polymer overlay made with Sikadur polymer is effective in reducing the corrosion of the reinforcing bars in cracked bridge decks.

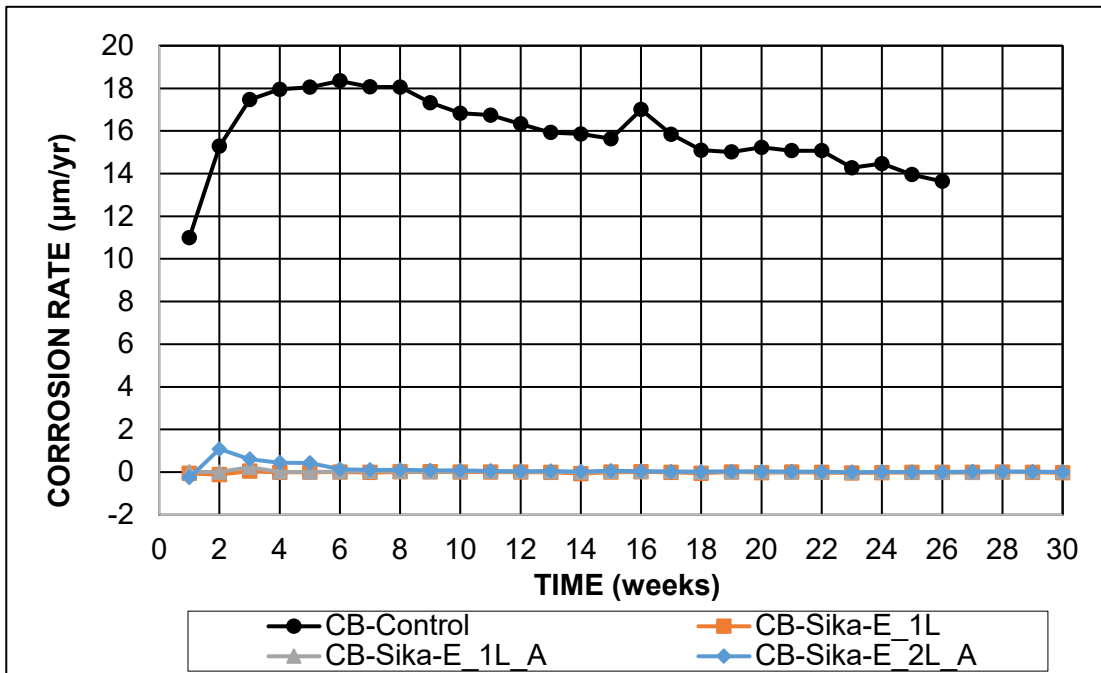


Figure 32: Average macrocell corrosion rate versus time of cracked beam specimens coated with Sikadur along with control specimens

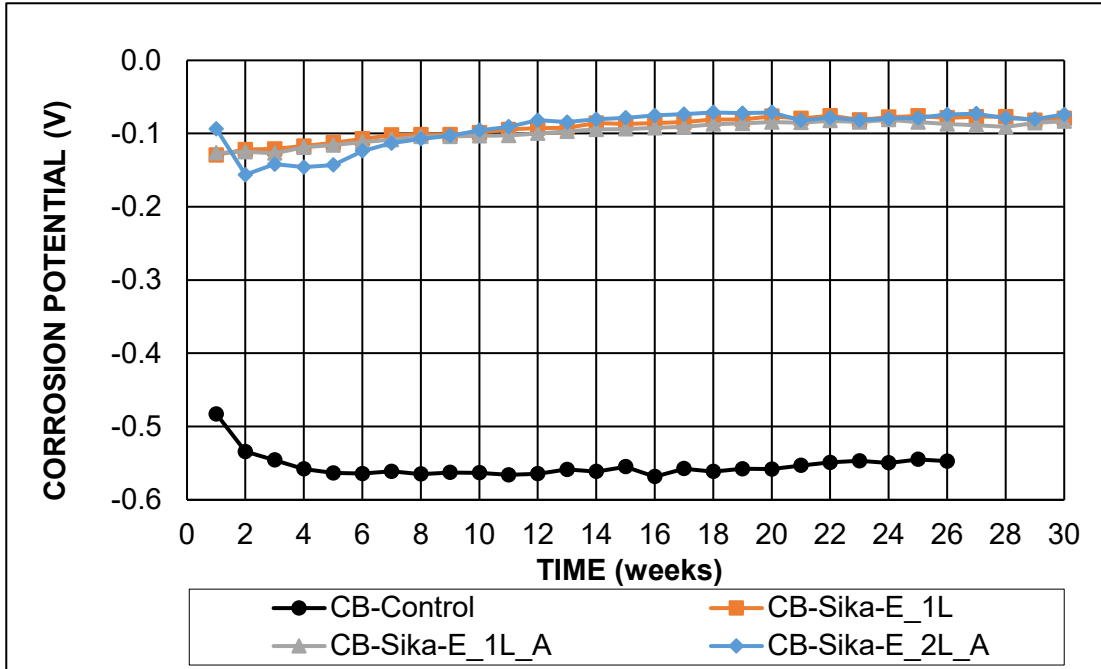


Figure 33: Average corrosion potential of top mat versus time of cracked beam specimens coated with Sikadur along with control specimens

Figure 34 shows the average macrocell corrosion rates for the SE specimens coated with 1 layer of Sikadur epoxy only (SE-Sika-E_1L), 1 layer of Sikadur epoxy and 1 layer of aggregate (SE-Sika-E_1L_A), 2 layers of Sikadur epoxy and 2 layers of aggregate (SE-Sika-E_2L_A), and Control SE (SE-Control) specimens. The average corrosion potentials for the top mats of steel are shown in Figure 35. The average corrosion rates and corrosion potentials are based on the average of four individual specimens of each type. The highest average corrosion rate among the specimens with polymer overlay is for SE-Sika-E_1L, 0.2 $\mu\text{m}/\text{yr}$, while Control specimens exhibit an average corrosion rate as high as 7.76 $\mu\text{m}/\text{yr}$. The average corrosion potential is never more negative than -0.16V vs CSE for the specimens with the various layers of polymer and aggregate but closed to -0.5V vs CSE for the Control specimens. This shows the corrosion of Southern Exposure specimens coated with various layers of Sikadur polymers and aggregate is considerably lower than that of the control specimens again showing that the application of polymer overlay made with Sikadur

polymer is effective in reducing the corrosion of the reinforcing bars in uncracked or new bridge decks.

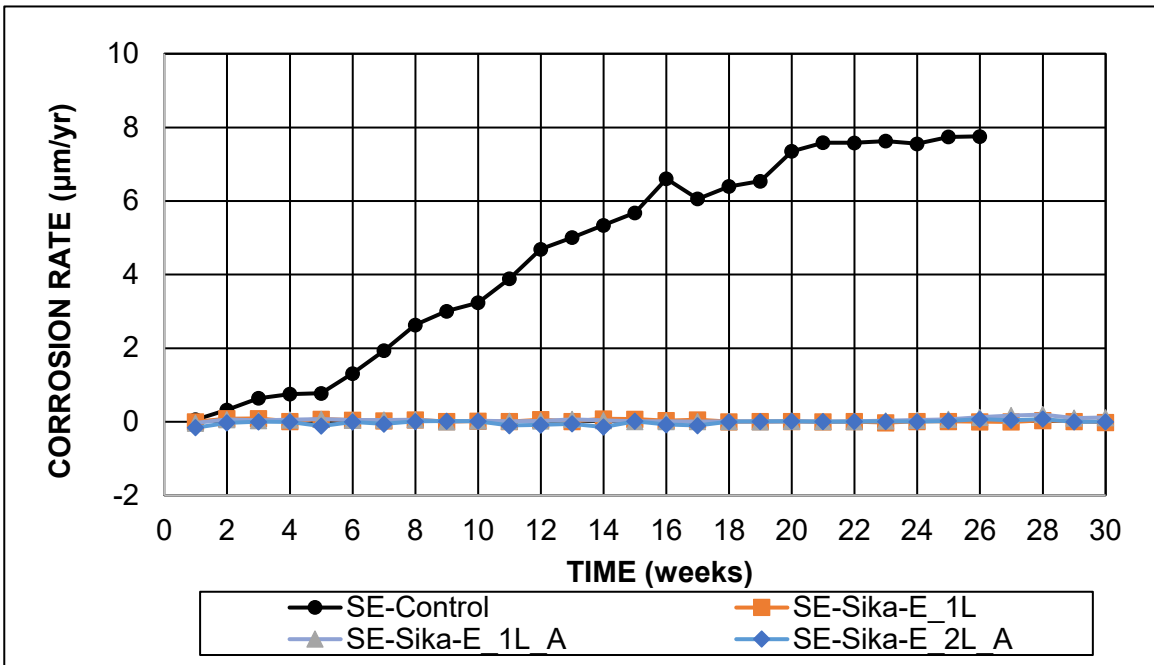


Figure 34: Average macrocell corrosion rate versus time of Southern Exposure specimens coated with Sikadur along with control specimens

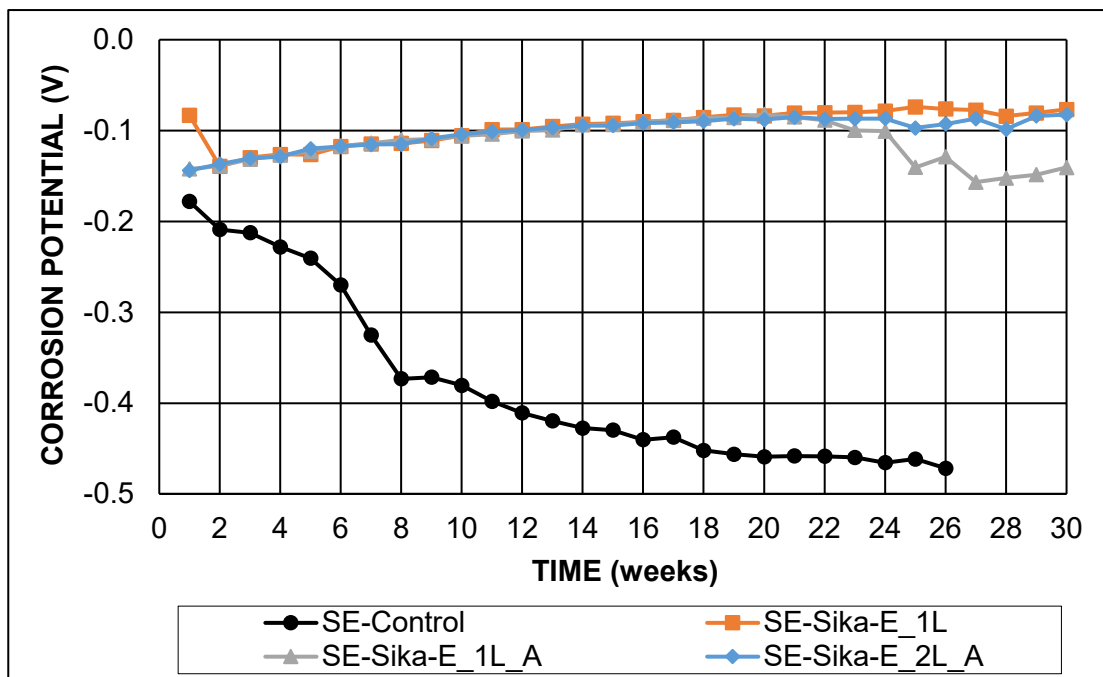


Figure 35: Average corrosion potential of top mat versus time of Southern Exposure specimens coated with Sikadur along with control specimens

Figure 36 shows the average macrocell corrosion rate for the CB specimens coated with 1 layer of Flexolith epoxy only (CB-Flex-E_1L), 1 layer of Flexolith epoxy and 1 layer of aggregate (CB-Flex-E_1L_A), 2 layers of Flexolith epoxy and 2 layers of aggregate (CB-Flex-E_2L_A) and control CB (CB-Control) specimens. Average corrosion potential for the top mats of steel is shown in Figure 37. The average corrosion rates and corrosion potentials are based on the average of four individual specimens of each type. Among the specimens with polymer overlay, the highest average corrosion rate is for CB Flex-E_1L_A, 4.55 $\mu\text{m}/\text{yr}$. The average corrosion potential is below -0.3V vs CSE for the specimens with polymer overlay. The results for the Control specimens are the same as shown in Figures 32 through 35. This shows the corrosion of cracked beam specimens coated with various layers of Flexolith polymers and aggregate is much lower than it is for the control specimens and that the application of polymer overlay made with Flexolith polymer is effective in reducing the corrosion of the reinforcing bars in cracked bridge decks. The highest average corrosion rate for the specimens coated with one layer of Flexolith epoxy is 0.13 $\mu\text{m}/\text{yr}$, which is the lowest among CB specimens with Flexolith polymer overlay. It can be inferred that the use of aggregate may have reduced the effectiveness of epoxy polymer in limiting the penetration of chlorides, which might be because of the improper binding of epoxy polymer with the aggregate particle. The effectiveness of polymer overlays with 1 and 2 layers of polymer and aggregate might be dependent on the effectiveness and carefulness of the application of polymer overlay since highest average corrosion rate with 2 layers of Flexolith polymer and aggregate is less than the highest average corrosion rate of 1 layer of Flexolith polymer and aggregate.

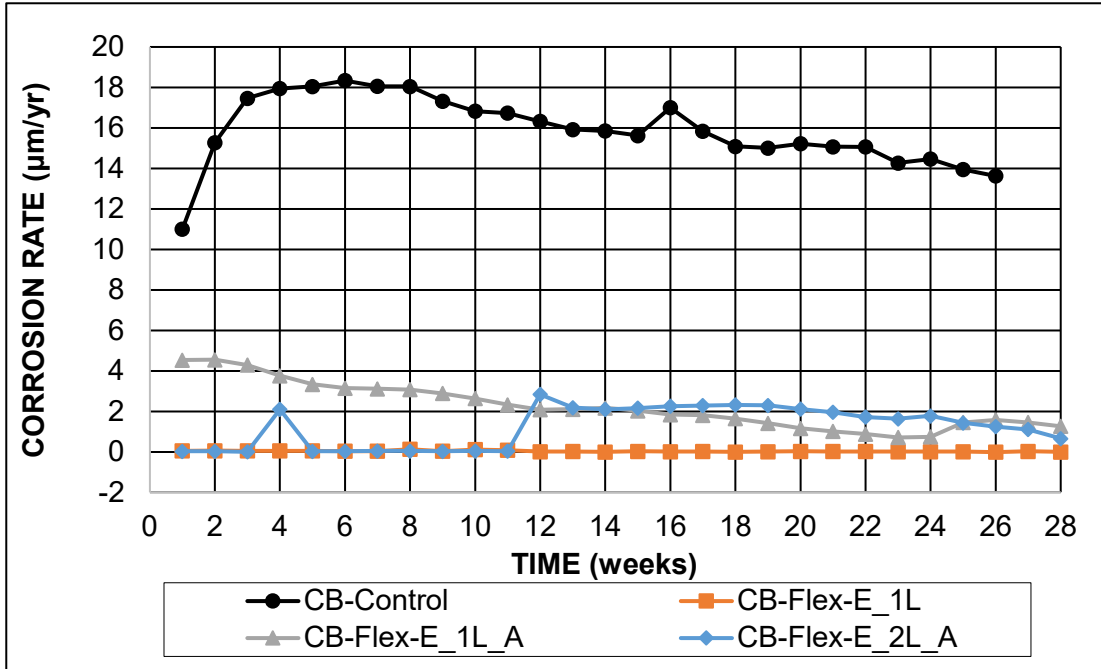


Figure 36: Average macrocell corrosion rate versus time of cracked beam specimens coated with Flexolith along with control specimens

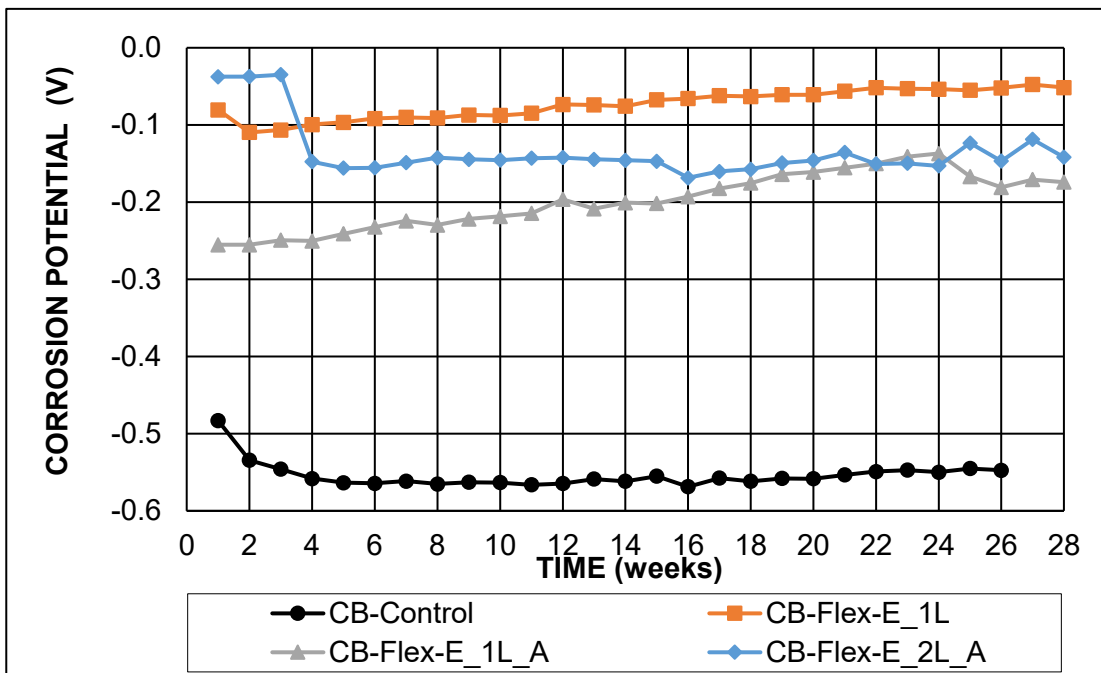


Figure 37: Average macrocell corrosion rate versus time of cracked beam specimens coated with Flexolith along with control specimens

Figure 38 shows the average macrocell corrosion rate for the SE specimens coated with 1 layer of Flexolith epoxy only (SE-Flex-E_1L), 1 layer of Flexolith epoxy and 1 layer of aggregate

(SE-Flex-E_1L_A), 2 layers of Flexolith epoxy and 2 layers of aggregate (SE-Flex-E_2L_A) and the control SE (SE-Control) specimens. Average corrosion potential for the top mats of steel is shown in Figure 39. The average corrosion rates and corrosion potentials are based on the average of four individual specimens of each type. Among the specimens with overlay, the highest average corrosion rate occurs for SE-Flex E_1L, 0.05 $\mu\text{m}/\text{yr}$. The average corrosion potential is below -0.15 V vs CSE for the specimens with polymer overlay. The results for the Control specimens are the same, as shown in Figures 32 through 35. This shows the corrosion of Southern Exposure specimens coated with various layers of Flexolith polymers and aggregate is considerably lower compared to the control specimens. This indicates the application of polymer overlay made with Flexolith polymer is effective in reducing the corrosion of the reinforcing bars in uncracked or new bridge decks.

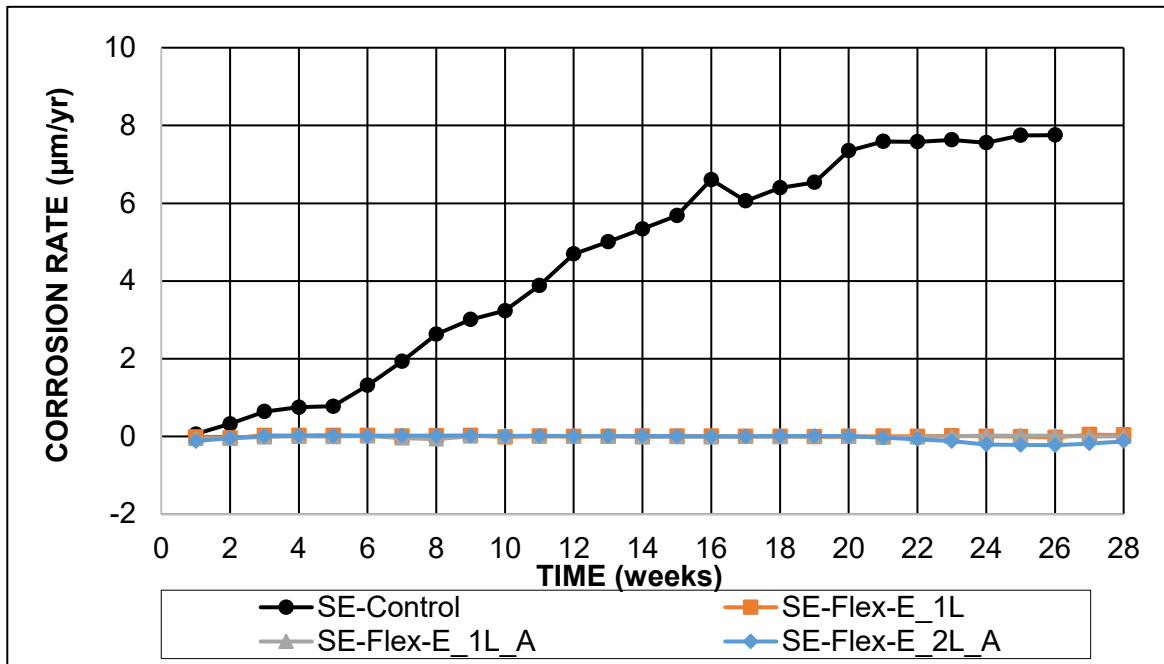


Figure 38: Average macrocell corrosion rate versus time of Southern Exposure specimens coated with Flexolith along with control specimens

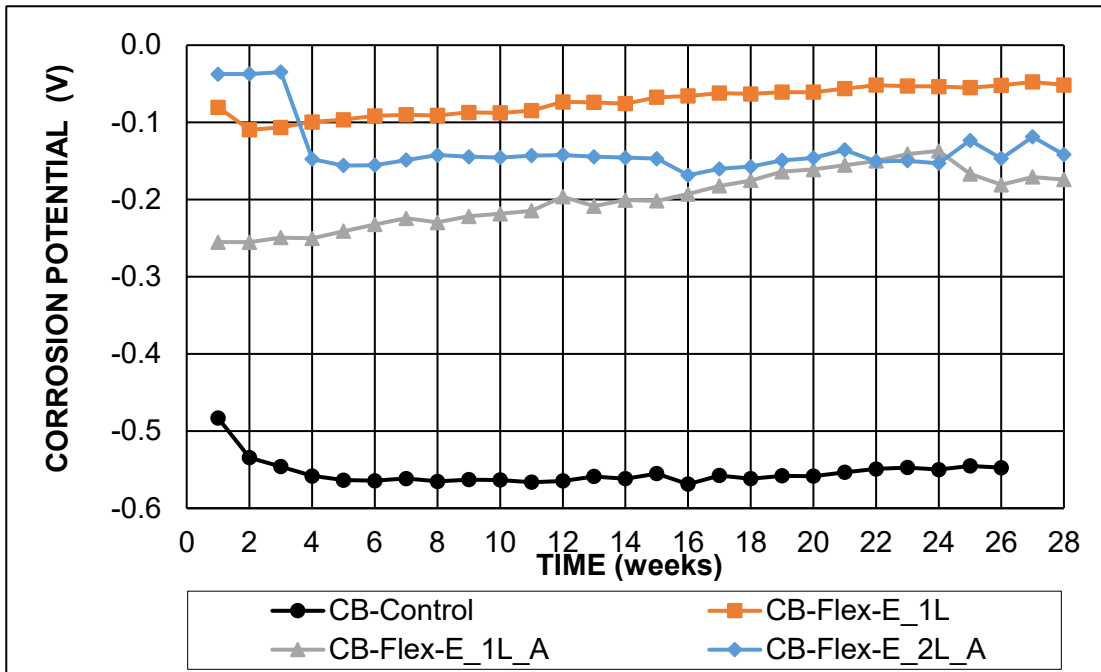


Figure 39: Average corrosion potential of top mat versus time of Southern Exposure specimens coated with Flexolith along with control specimens

While, on average, the results indicate that polymer overlays provide protection to reinforcing steel in bridge decks, the response of some specimens indicate that the system is not perfect, as observed for three specimens in the study. The corrosion rate of specimen CB-Sika-E_2L_A-1, shown in Figure 12, reached a high of 3.6 $\mu\text{m}/\text{yr}$, and the corrosion potential of the top mat was as low as -0.39 V , as shown in Figure 13. The corrosion rate of specimen CB-Flex-E_1L_A-1 reached a high of 19 $\mu\text{m}/\text{yr}$, as shown in Figure 22, and the corrosion potential of the top mat was as low as -0.55 V , as shown in Figure 23. The corrosion rate of specimen CB-Flex-E_2L_A-1 reached a high of 11.4 $\mu\text{m}/\text{yr}$, as shown in Figure 24 and the corrosion potential of the top mat was as low as -0.54 V , as shown in Figure 25. These are the only specimens showing corrosion to date.

Figures 40 through 43 show the results of cracked beam specimens that were exposed to a 15% chloride solution for 8 weeks prior to the application of the polymer overlay with two layers of polymer and aggregate to observe the change in corrosion behavior when a cracked bridge deck

that has been exposed to salt receives a polymer overlay. These specimens are termed “chloride exposed.” Figures 40 and 41, respectively, show the corrosion rate and corrosion potential of cracked beam specimens with 2 layers of Sikadur polymer and aggregate applied at the eighth week. The highest corrosion rate was 19.5 $\mu\text{m}/\text{yr}$ for specimen CB_Sika_CE-4 at week 8; after application of the polymer, the corrosion rate decreased and reached 7.7 $\mu\text{m}/\text{yr}$ at week 24. Similar decreases in corrosion rate were observed for the other specimens in the figure. The corrosion potential for that specimen was -0.58 V vs CSE at week 8 and -0.44 V vs CSE at week 24. Figures 42 and 43, respectively, show the corrosion rate and corrosion potential of cracked beam specimens with 2 layers of Flexolith polymer and aggregate applied at the eighth week. The highest corrosion rate occurred at week 8, 23.12 $\mu\text{m}/\text{yr}$ for specimen CB_Flex_CE-4. After application of the polymer the corrosion rate decreased as it did for the Sika specimens, reaching 7.85 $\mu\text{m}/\text{yr}$ at week 24. Also, as for the Sika specimens, similar decreases in corrosion rate were observed for the other specimens in the figure. The corrosion potential for that specimen was -0.57 V vs CSE at week 8 and -0.42 V vs CSE at week 24. Both the Sika and Flexolith specimens show a decrease in corrosion activity after application of the polymer, even in the presence of chloride-contaminated concrete. This suggests that when an existing bridge deck with cracks that has been exposed to chlorides receives a polymer overlay, the corrosion in reinforcing steel will decrease over time.

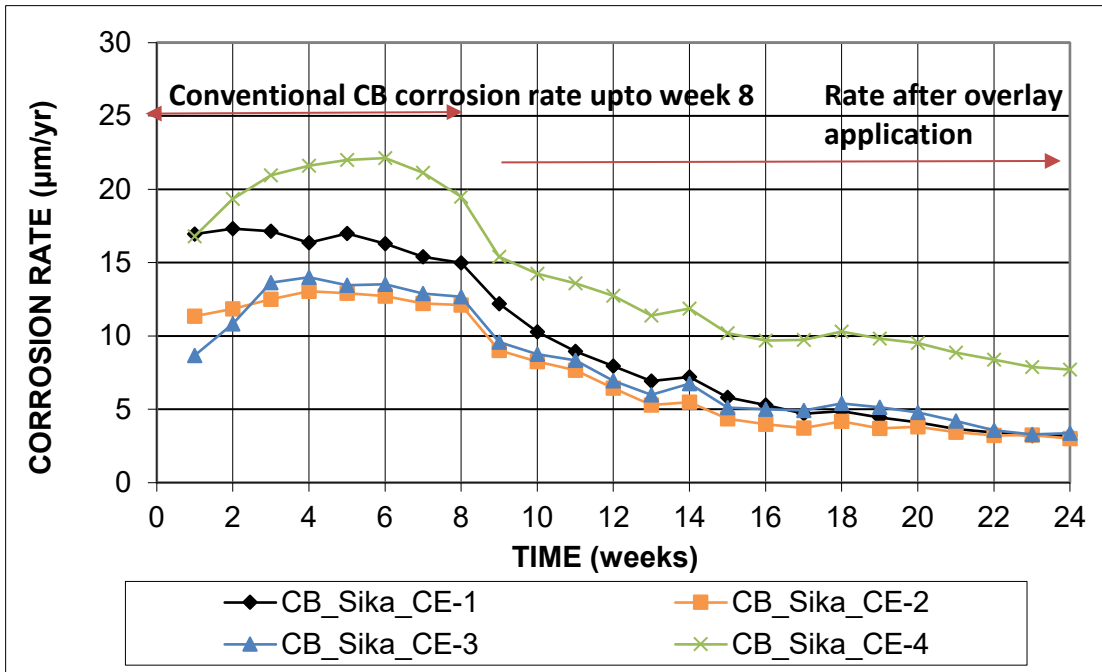


Figure 40: Macrocell corrosion rate versus time for chloride exposed cracked-beam specimens coated with Sikadur epoxy

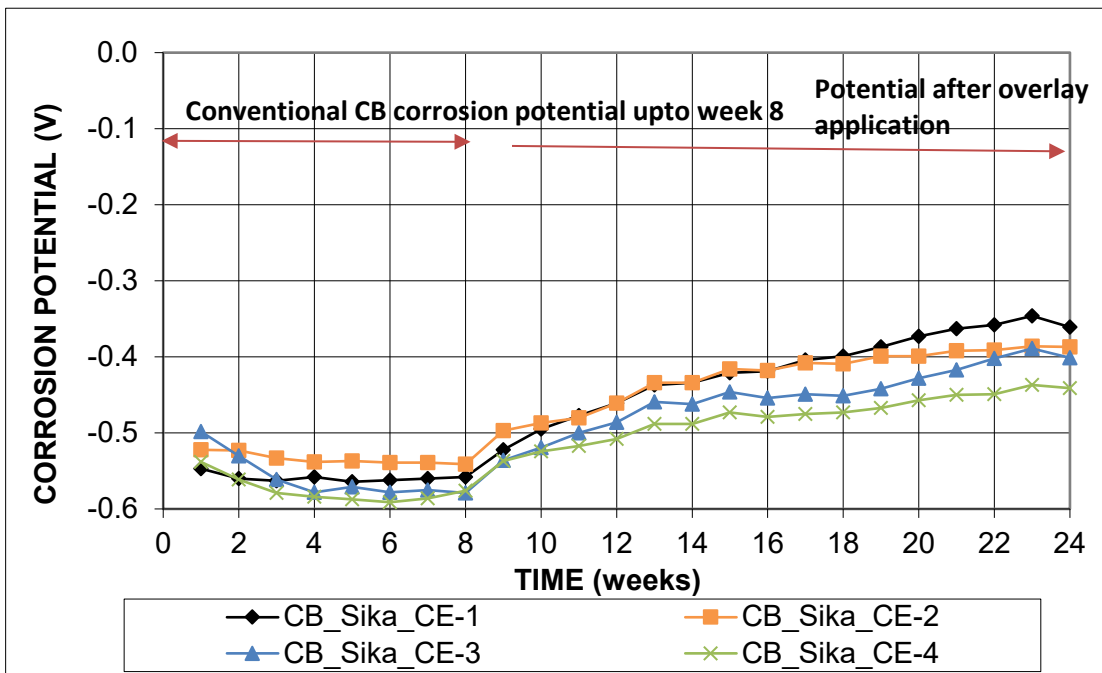


Figure 41: Corrosion potential of top mat of steel versus time for chloride exposed cracked beam specimens coated with two layers of Sikadur epoxy and aggregate

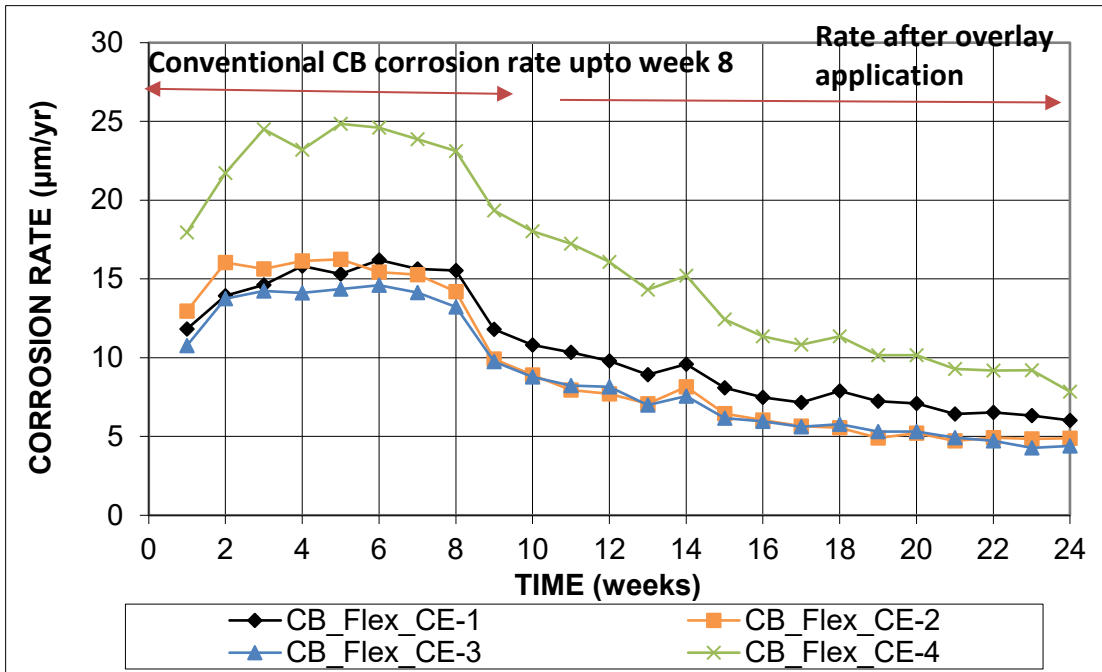


Figure 42: Macrocell corrosion rate versus time for chloride exposed cracked-beam specimens coated with Flexolith epoxy

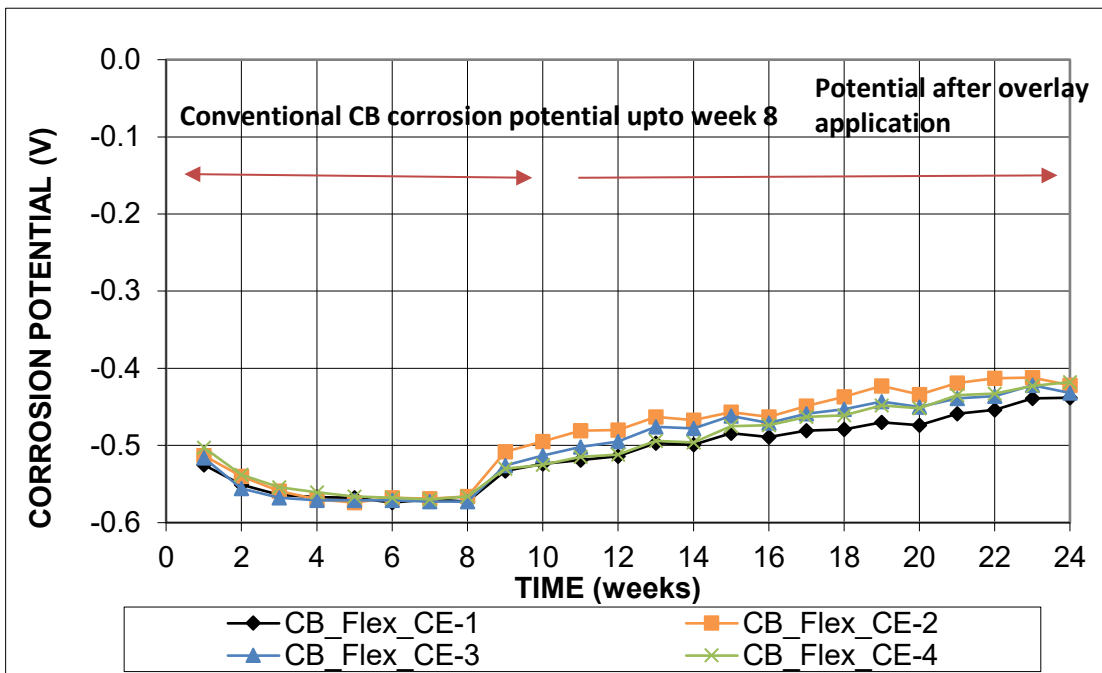


Figure 43: Corrosion potential of top mat of steel versus time for chloride exposed cracked-beam specimens coated with Flexolith epoxy

3.2 CORROSION LOSS

Corrosion loss is calculated by integrating corrosion rate over time. The latest data covering all cracked beam and Southern Exposure specimens coated with Sikadur polymer extends up to 30 weeks, while the data for those coated with Flexolith polymer is available up to 28 weeks. Figures 44 and 45, respectively, show the average corrosion losses as a function of time for the cracked beam and Southern Exposure specimens coated with Sikadur polymer, along with control specimens. The average corrosion loss for the control cracked beam specimens at week 26 is 7.95 μm . The average corrosion loss for the control Southern Exposure specimens at week 26 is 2.27 μm . The average corrosion loss for both the cracked beam and Southern Exposure specimens coated with different layers of Sikadur polymer and aggregate is below 0.1 μm . The average corrosion loss at week 26 for the cracked beam specimens coated with different layers of Flexolith polymer and aggregate: CB-Flex-E_1L, CB-Flex-E_1L_A, CB-Flex-E_2L_A, is 0.02, 1.16, and 0.63 μm , respectively. The average corrosion loss for the Southern Exposure specimens coated with different layers of Flexolith polymer and aggregate is below 0.1 μm .

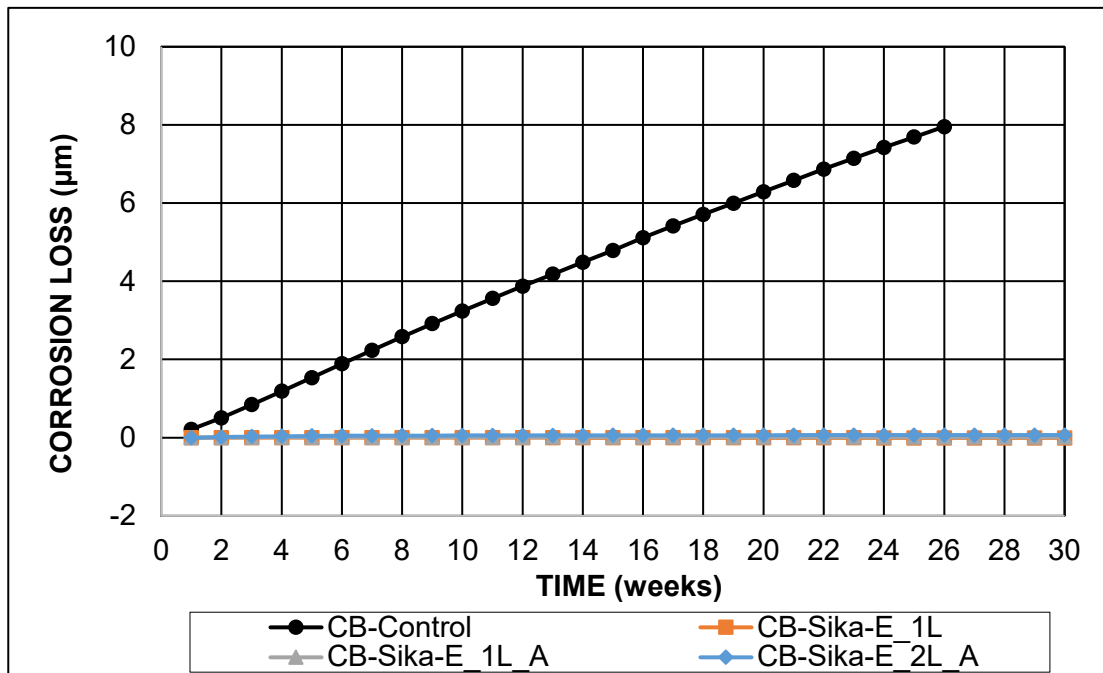


Figure 44: Average corrosion loss (μm) based on total area for cracked beam specimens with Sikadur polymer along with control specimens

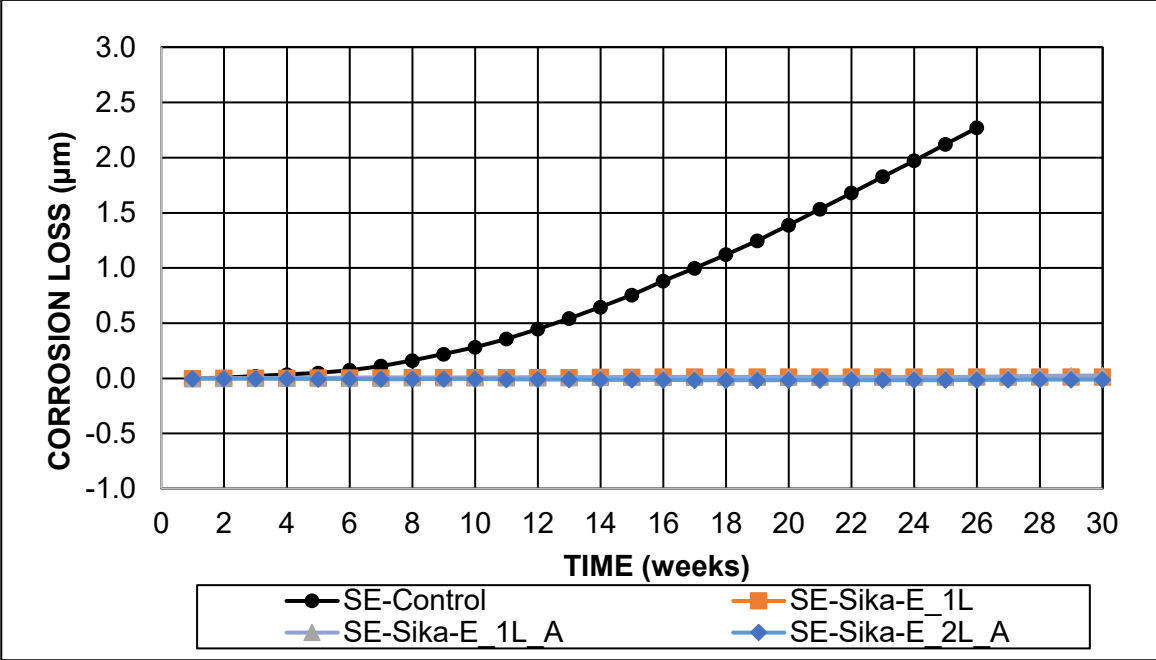


Figure 45: Average corrosion loss (μm) based on total area for Southern Exposure specimens with Sikadur polymer along with control specimens

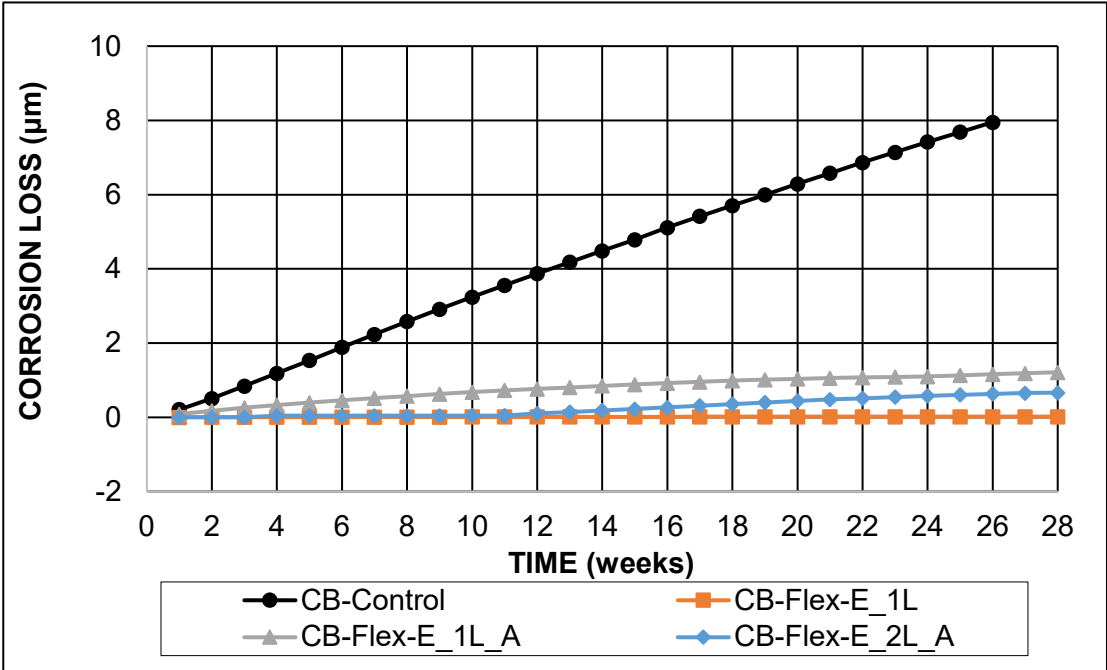


Figure 46: Average corrosion loss (μm) based on total area for cracked beam specimens with Flexolith polymer along with control specimens

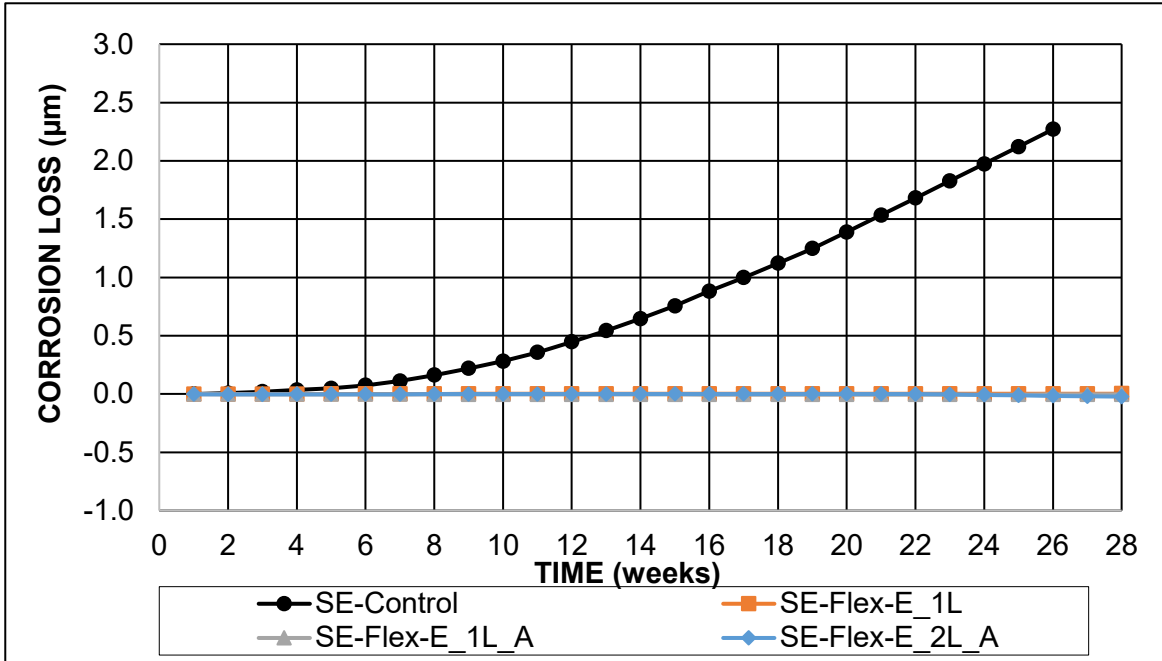


Figure 47: Average corrosion loss (µm) based on total area for Southern Exposure specimens with Flexolith polymer along with control specimens

3.3 LINEAR POLARIZATION RESISTANCE (LPR) RESULTS

For bridge decks and in the corrosion specimens used in this study, microcell corrosion occurs when the anode and cathode are in the same bar. Macrocell corrosion occurs when the top mat of steel is the anode and bottom mat of steel is the cathode. The corrosion rate is determined by measuring by the voltage drop across the 10-ohm resistor, as presented in the previous section. The total corrosion rate is the summation of microcell and macrocell corrosion rates, which can be measured using the linear polarization resistance (LPR) test.

Table 8 shows the average macrocell and total corrosion rates at week 24. The average macrocell and total corrosion rate show very little to no corrosion for both the Southern Exposure and cracked beam specimens coated with polymer overlays. This shows that the system works to prevent chloride penetration to the level of steel. The average total corrosion rate is greater than the average macrocell corrosion rate in most of the cases, except for SE-Conv, CB-Flex-E_1L_A,

and CB-Flex-E_2L_A, with average total and average macrocell corrosion rates, 7.35 and 7.56 $\mu\text{m}/\text{yr}$, 0.57 and 0.75 $\mu\text{m}/\text{yr}$, and 0.04 and 1.78 $\mu\text{m}/\text{yr}$, respectively.

Table 8: Average macrocell and total corrosion rates for Southern Exposure and cracked beam specimens at week 24.

System	Southern Exposure		Cracked Beam	
	Macrocell Rate ($\mu\text{m}/\text{yr}$)	Total Rate ($\mu\text{m}/\text{yr}$)	Macrocell Rate ($\mu\text{m}/\text{yr}$)	Total Rate ($\mu\text{m}/\text{yr}$)
Conv.	7.56	7.35	14.47	21.06
Sika-E_1L	0.01	0.12	-0.03	0.12
Sika-E_1L_A	0.05	0.64	0.00	0.46
Sika-E_2L_A	0.00	0.20	0.01	0.12
Flex-E_1L	0.00	0.17	0.01	0.08
Flex-E_1L_A	0.02	0.37	0.75	0.57
Flex-E_2L_A	-0.21	0.10	1.78	0.04

Table 9 shows the average macrocell and total corrosion rate for the cracked beam specimens coated with Sikadur and Polymer overlays that had been contaminated with chloride for eight weeks by ponding with salt solution. The total corrosion rate in week 8 is 21.28 $\mu\text{m}/\text{yr}$ decreased to 2.79 $\mu\text{m}/\text{yr}$ by week 24 for the specimens coated with the Sikadur polymer overlay. The total corrosion rate in week 8 was 29.7 $\mu\text{m}/\text{yr}$, and it is reduced to 4.13 $\mu\text{m}/\text{yr}$ by week 24 for the specimens coated with the Flexolith polymer overlay. Both systems show significant reductions in both the macrocell and total corrosion rates after the application of polymer overlay, even in the presence of chloride-contaminated concrete. For both overlay polymers, the average total corrosion rate was greater than the average macrocell corrosion rate at week 8, but lower than the average macrocell corrosion rate at week 24.

Table 9: Average macrocell and total corrosion rates for chloride exposed cracked beam specimens at weeks 8 and 24.

System	Week 8		Week 24	
	Macrocell Rate ($\mu\text{m}/\text{yr}$)	Total Rate ($\mu\text{m}/\text{yr}$)	Macrocell Rate ($\mu\text{m}/\text{yr}$)	Total Rate ($\mu\text{m}/\text{yr}$)
CB_Sika_CE	14.82	21.28	4.33	2.79
CB_Flex_CE	16.52	29.70	5.79	4.13

4 SUMMARY AND CONCLUSIONS

Multilayer polymer overlays were evaluated using cracked beam and Southern Exposure specimens to investigate their ability to limit corrosion of reinforcing steel in bridge decks. Corrosion rates, corrosion potentials, and total corrosion rates based on linear polarization resistance results were used for the evaluation. Two polymers, the epoxies Sikadur and Flexolith, were used for preparing the polymer overlays. Test specimens were prepared using three systems: one layer of epoxy polymer, one layer of epoxy polymer and aggregate, and two layers of epoxy polymer and aggregate (matching manufacturers' recommendations). Specimens without polymer overlays were also tested. Some cracked beam specimens were contaminated with chloride and coated with polymer overlay to evaluate the ability of polymer overlays to limit corrosion in chloride-contaminated concrete. The design, fabrication, and testing procedures for post-crack specimens, used to evaluate the ability of the overlays to remain intact when cracks form in the concrete after the overlay has been applied, are described, but no test results are yet available.

The following conclusions can be made based on the test results obtained to date.

1. Specimens without a polymer overlay exhibited the highest corrosion rate.
2. One cracked beam specimen with two layers of Sikadur polymer and aggregate, one cracked beam specimen with one layer of Flexolith polymer and aggregate, and one cracked beam specimen with two layers of Flexolith polymer and aggregate exhibited higher corrosion activity than the other specimens with polymer overlays. Other than these three specimens, little corrosion activity was observed.
3. Overall, multilayer polymer overlays limit corrosion.
4. A measurable reduction in corrosion rate occurred when the chloride-contaminated concrete was coated with a polymer overlay.

REFERENCES

- Broomfield, J.P. (1996). "Corrosion of Steel in Concrete: Understanding, investigation and repair (1st ed.)," CRC Press, London, 264 pp.
- Darwin, D., O'Reilly, M., Somogie, I., Sperry, J., Lafikes, J., Storm, S., Browning, J., "Stainless Steel Reinforcement as a Replacement for Epoxy Coated Steel in Bridge Decks," *SM Report No. 105*, The University of Kansas Center for Research, Inc., Lawrence, Kansas, August 2013, 205 pp.
- Farshadfar, O., O'Reilly, M., Darwin, D., "Performance Evaluation of Corrosion Protection Systems for Reinforced Concrete," *SM Report No. 122*, The University of Kansas Center for Research, Inc., Lawrence, KS, January 2017, 350 pp.
- Gong, L., Darwin, D., Browning, J., and Locke, C.E., "Evaluation of Multiple Corrosion Protection Systems and Stainless Steel Clad Reinforcement for Reinforced Concrete," *SM Report No. 82*, The University of Kansas Center for Research, Inc., Lawrence, Kansas, January 2006, 540 pp.
- Kansas Department of Transportation, "Method for testing polymer overlays for surface preparation and adhesion (Kansas Test Method KT-70)," Topeka, KS, 5 pp.
- Koch, G., Broongers, H., Thompson, N., Virmani, Y., and Payer, J. (2002). "Corrosion Cost and Preventive Strategies in the United States," Report No. FHWA-RD-01-156, FHWA, McLean, VA, 773 pp.
- Krauss, P., Hawkins, K. (2023). "Evaluation of Thin Polymer Overlays for Bridge Decks," FHWA/MT-23-006/9757-705, Helena, MT, Montana Department of Transportation, 172 pp.
- Meggers, D. A. (2016). "Effectiveness of polymer bridge deck overlays in highway noise reduction," Report No. KS-15-11, Kansas Department of Transportation, Bureau of Research, 2 pp.
- O'Reilly, M., Darwin, D., Browning, J., and Locke, C. E. (2011). "Evaluation of Multiple Corrosion Protected Systems for Reinforced Concrete Systems" SM Report No. 100, University of Kansas Center for Research, Inc., Lawrence, Kansas, January 2011, 535 pp.
- Roper, Thomas H. and Henley, Edward H. Jr. (1991). "Thin Overlay SR5 OC Bridge 900/12W, SR5 OC Bridge 900/13W," WA-RD 234.1, Washington State Department of Transportation, Olympia, 58 pp.
- Sprinkel, M. M., Sellars, A. R., & Weyers, R. E. (1993). "Rapid concrete bridge deck protection, repair, and rehabilitation," SHRP-S-344, Strategic Highway Research Program, National Research Council, 116 pp.

APPENDIX A

CORROSION POTENTIAL OF BOTTOM MAT OF STEEL FOR CB, SE, AND CHLORIDE-EXPOSED CB SPECIMENS, AND MACROCELL CORROSION RATE AND CORROSION POTENTIAL OF TOP AND BOTTOM MAT OF STEEL FOR CONTROL SPECIMENS

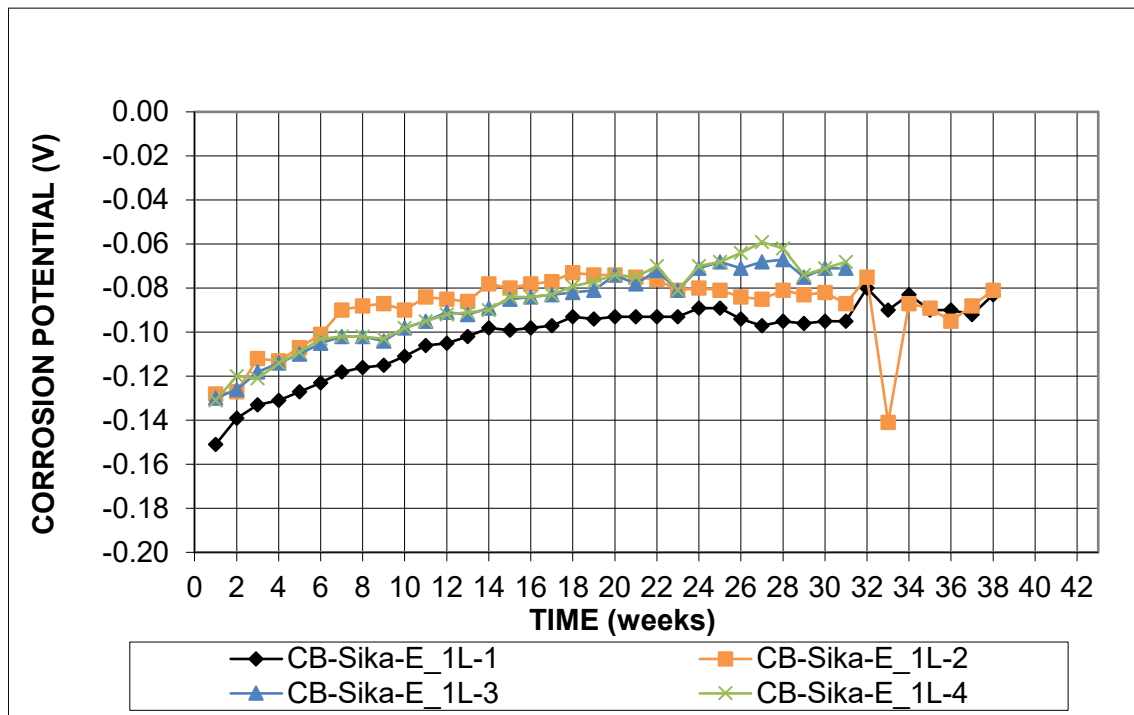


Figure A.48: Corrosion potential of bottom mat of steel versus time for cracked beam specimens with one layer of Sikadur®-22 Lo-Mod epoxy

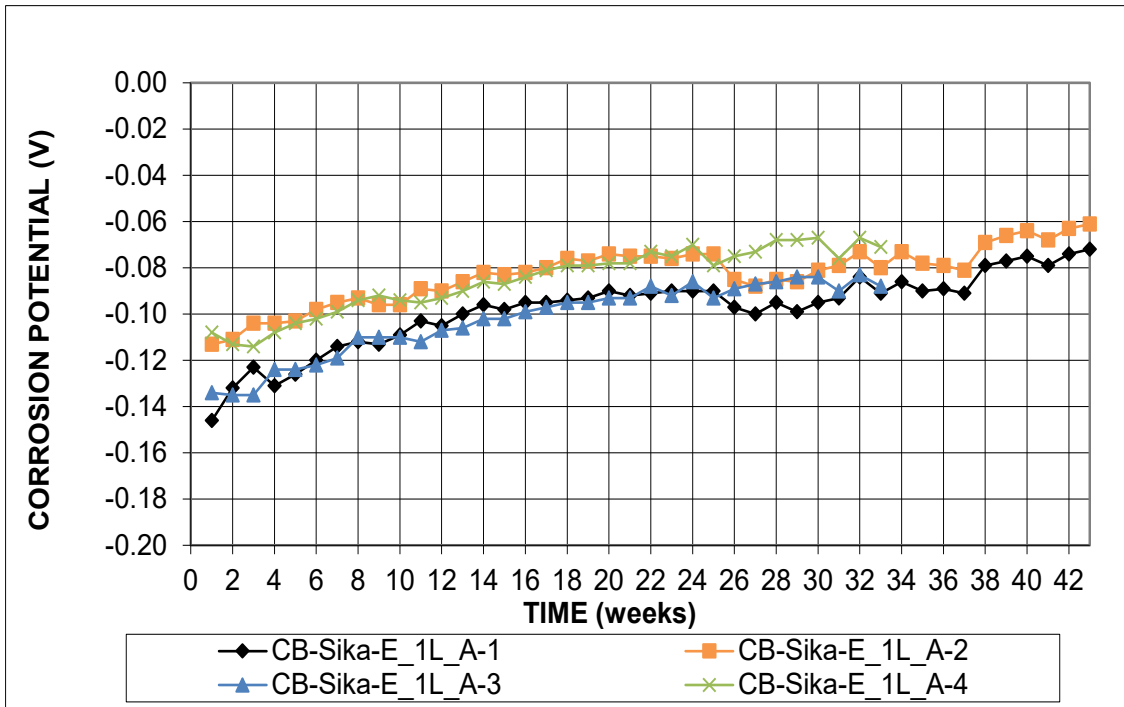


Figure A.49: Corrosion potential of bottom mat of steel versus time for cracked beam specimens with one layer of Sikadur®-22 Lo-Mod epoxy and aggregate

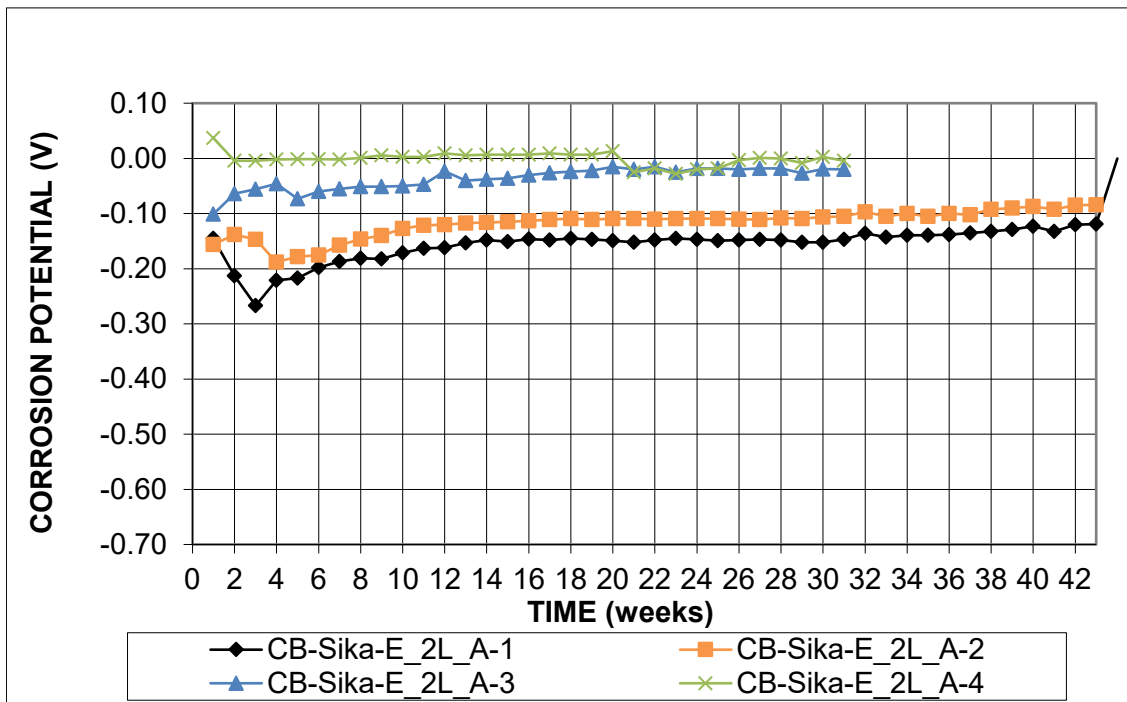


Figure A.50: Corrosion potential of bottom mat of steel versus time for cracked beam specimens with two layers of Sikadur®-22 Lo-Mod epoxy and aggregate

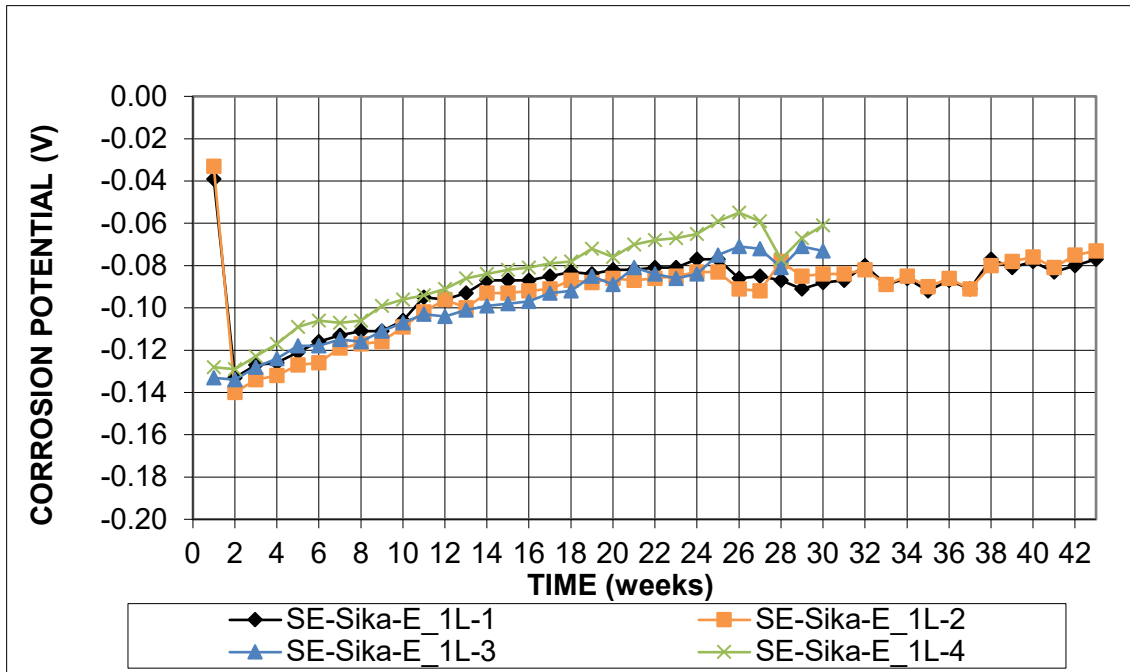


Figure A.51: Corrosion potential of bottom mat of steel versus time for Southern Exposure specimens with one layer of Sikadur®-22 Lo-Mod epoxy

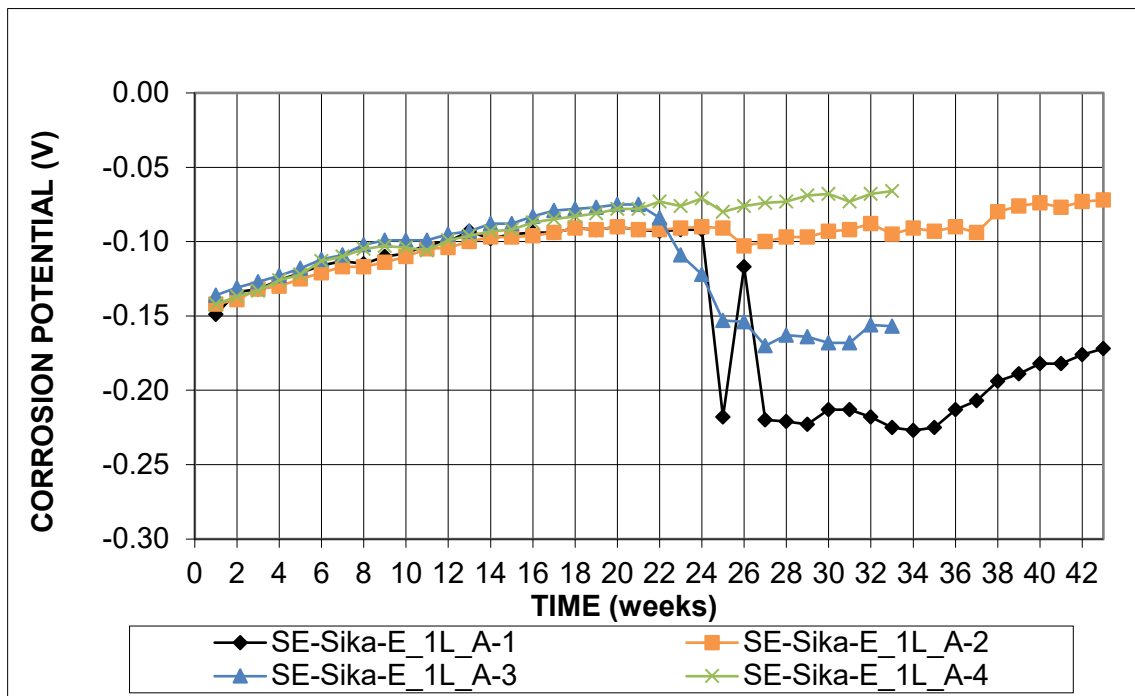


Figure A.52: Corrosion potential of bottom mat of steel versus time for Southern Exposure specimens with one layer of Sikadur®-22 Lo-Mod epoxy and aggregate

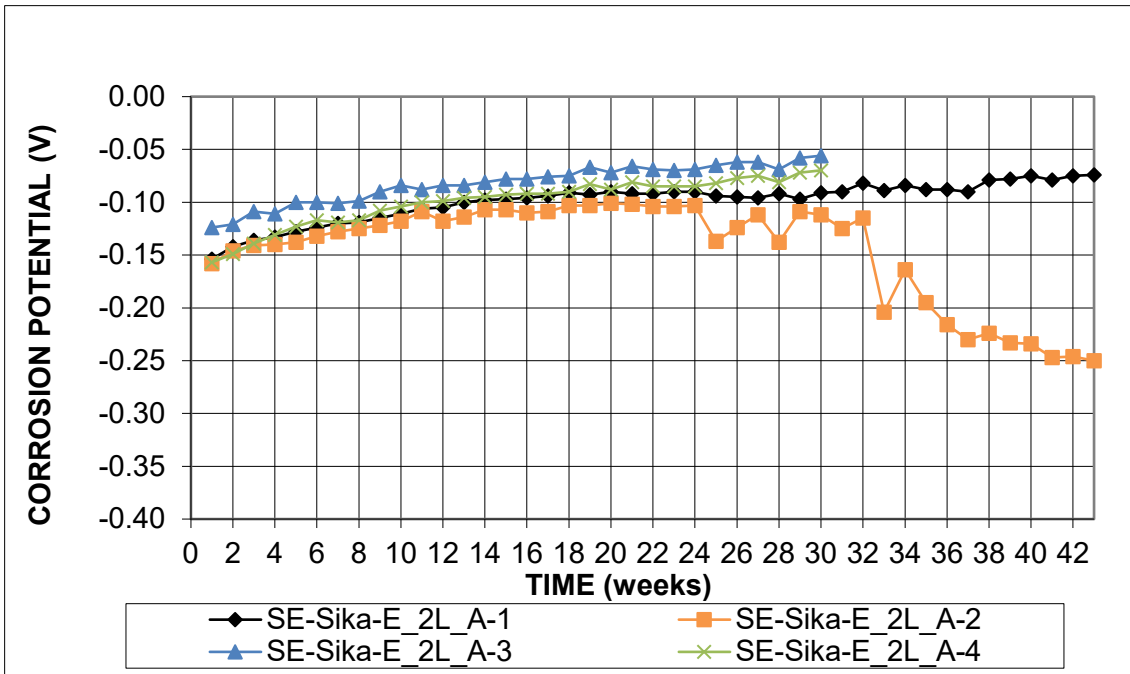


Figure A.53: Corrosion potential of bottom mat of steel versus time for Southern Exposure specimens with two layers of Sikadur®-22 Lo-Mod epoxy and aggregate

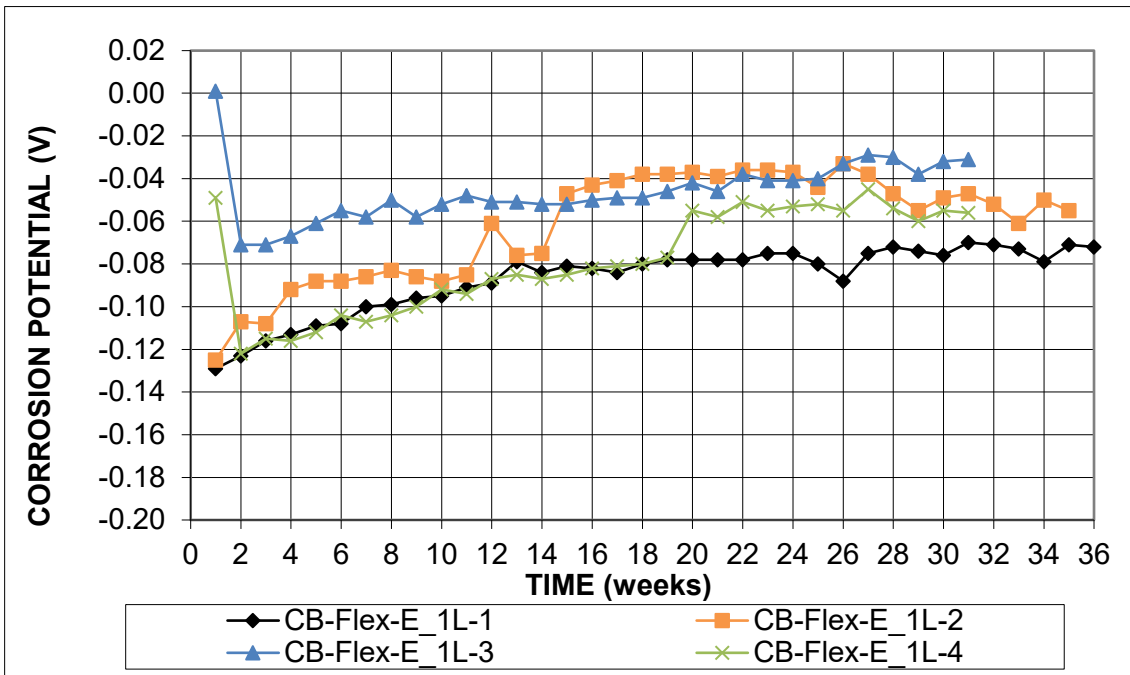


Figure A.54: Corrosion potential of bottom mat of steel versus time for cracked beam specimens with one layer of Flexolith epoxy

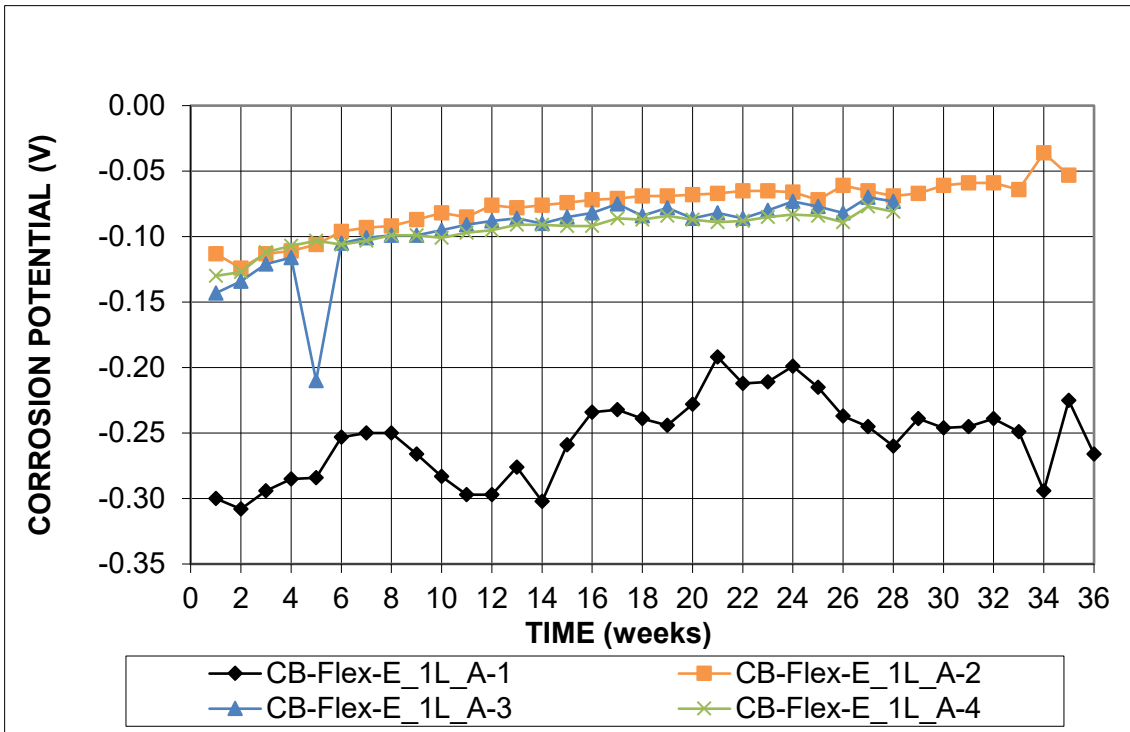


Figure A.55: Corrosion potential of bottom mat of steel versus time for cracked-beam specimens with one layer of Flexolith epoxy and aggregate

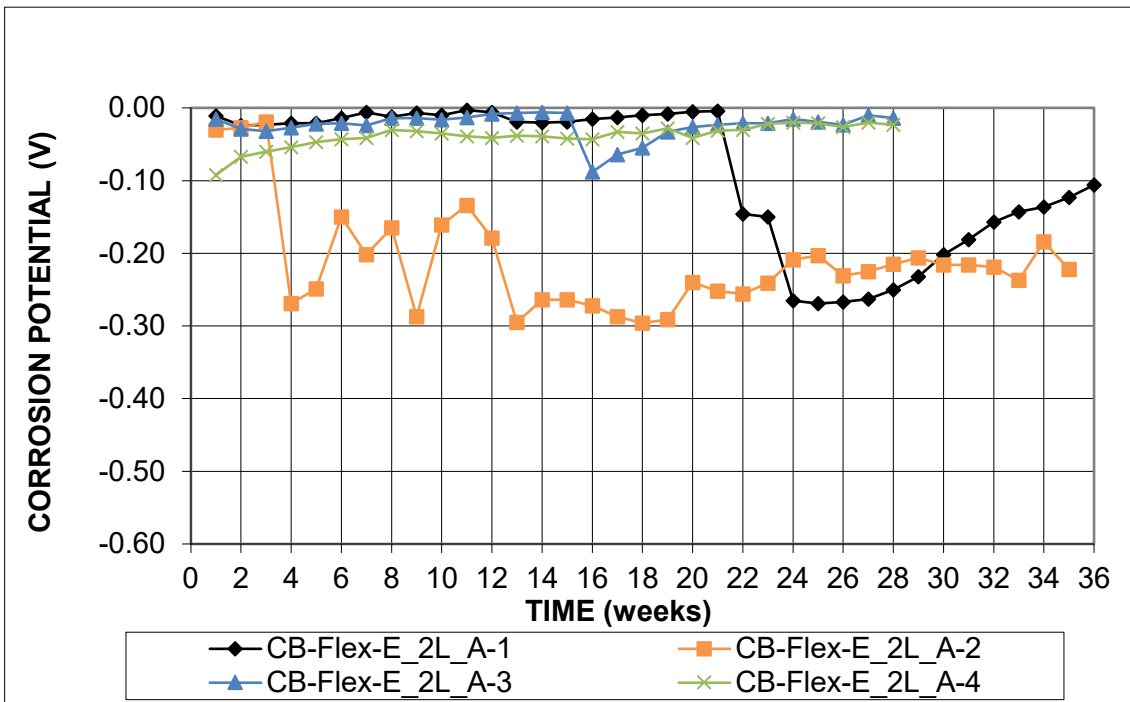


Figure A.56: Corrosion potential of bottom mat of steel versus time for cracked beam specimens with two layers of Flexolith epoxy and aggregate

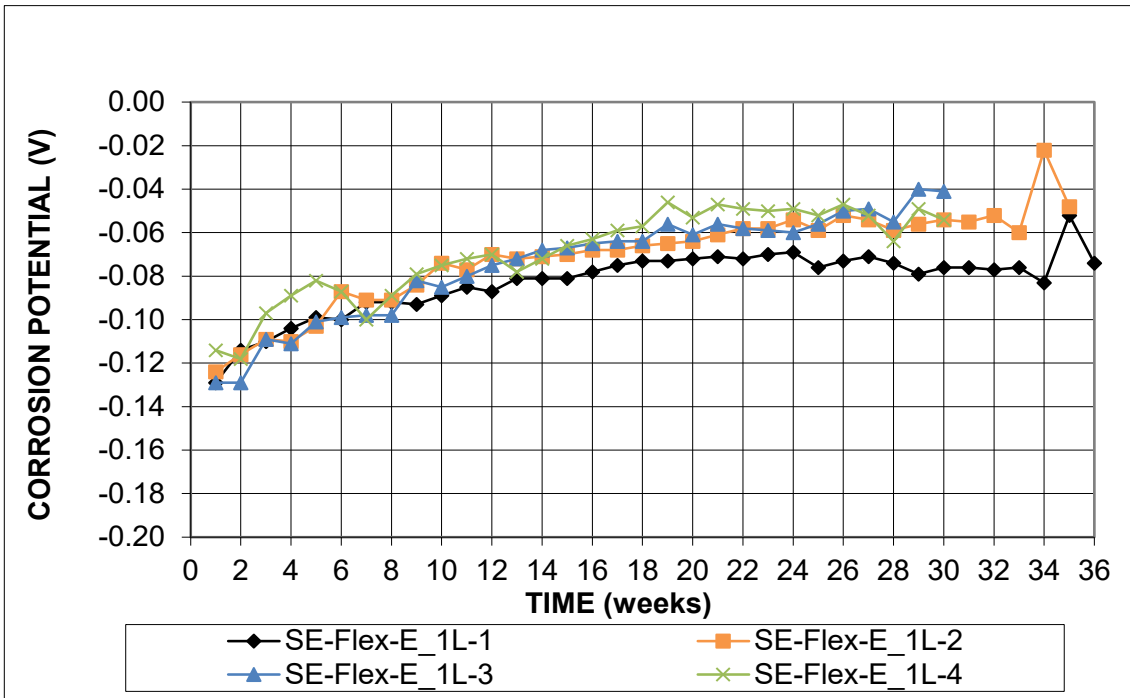


Figure A.57: Corrosion potential of bottom mat of steel versus time for Southern Exposure specimens with one layer of Flexolith epoxy

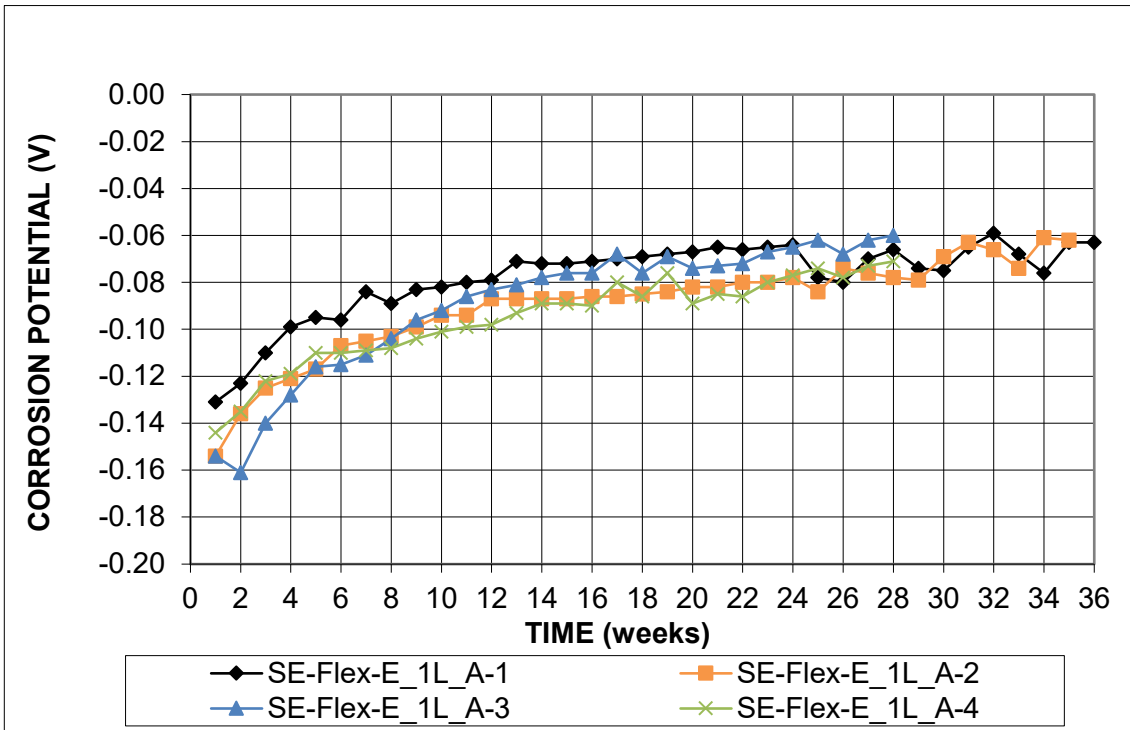


Figure A.58: Corrosion potential of bottom mat of steel versus time for Southern Exposure specimens with one layer of Flexolith epoxy and aggregate

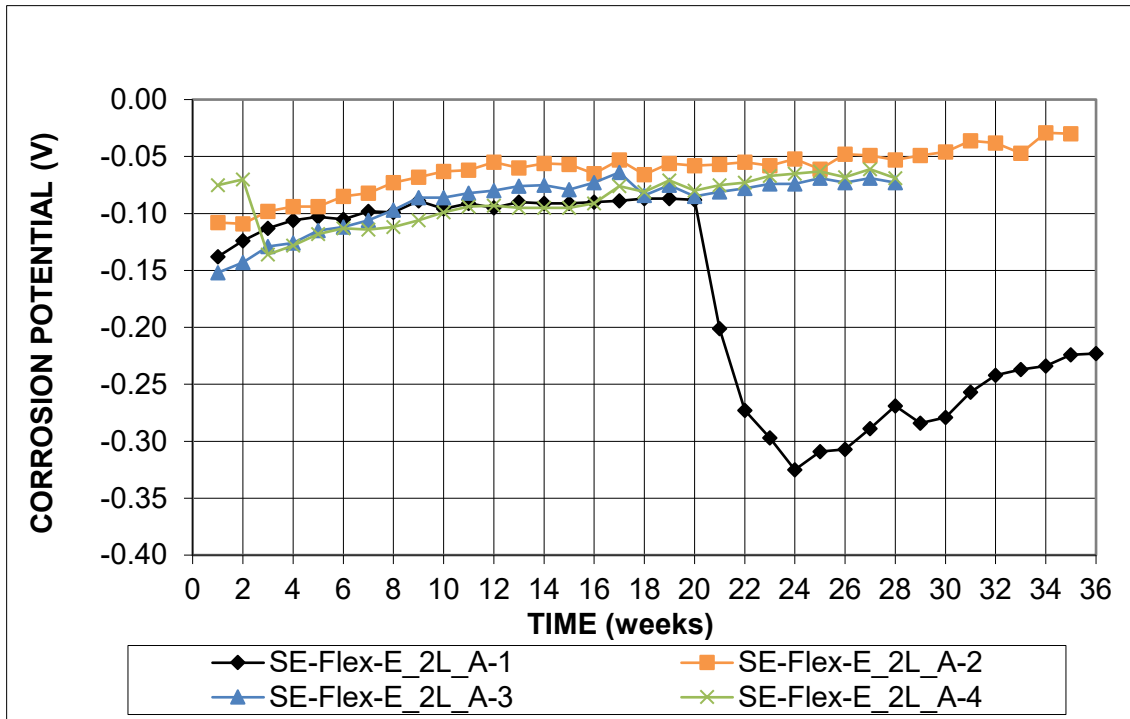


Figure A.59: Corrosion potential of bottom mat of steel versus time for Southern Exposure specimens with two layers of Flexolith epoxy and aggregate

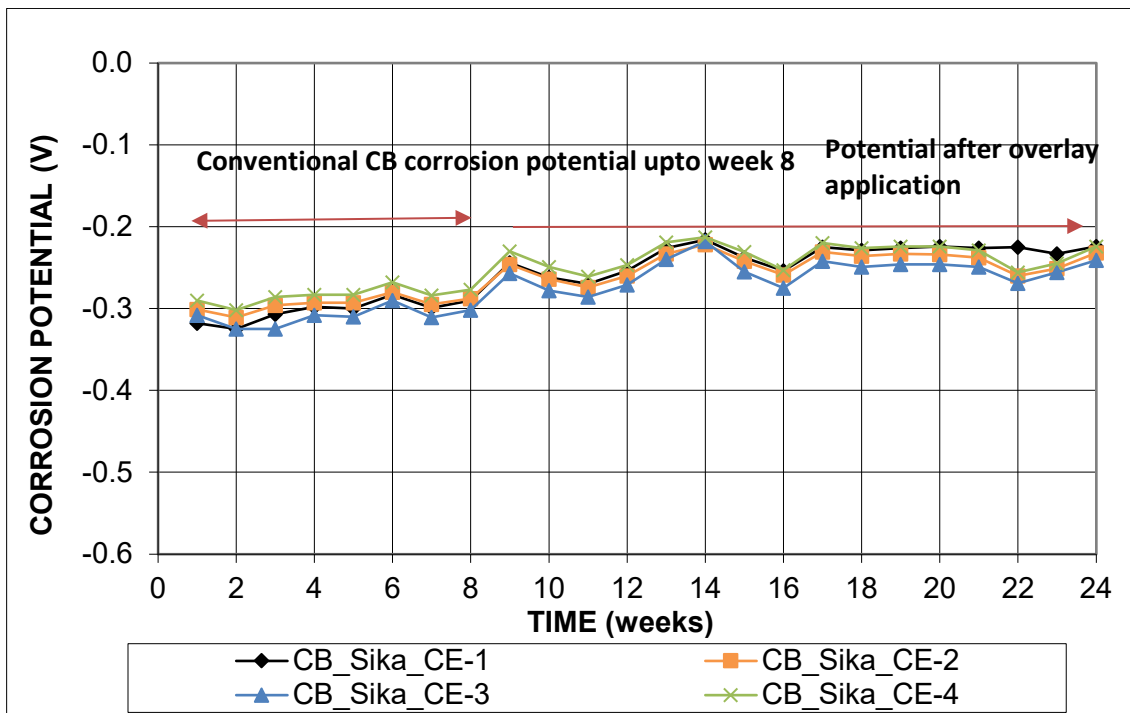


Figure A.60: Corrosion potential of bottom mat of steel versus time for chloride exposed cracked beam specimens coated with two layers of Sikadur epoxy and aggregate

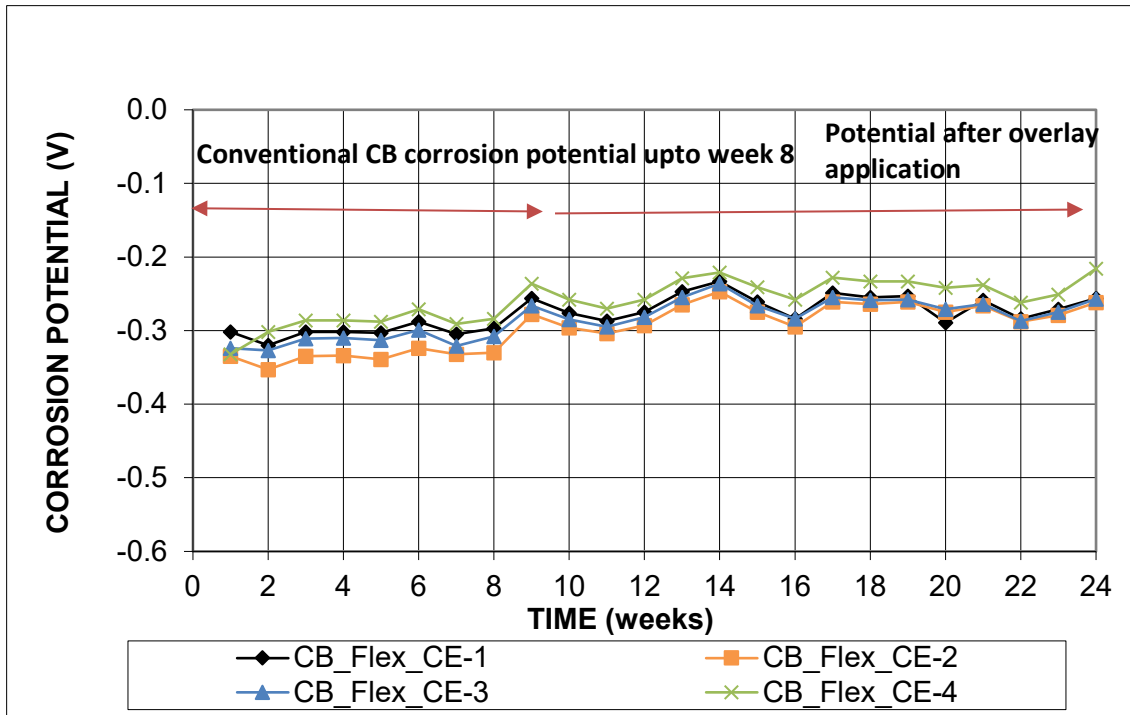


Figure A.61: Corrosion potential of bottom mat of steel versus time for chloride exposed cracked-beam specimens coated with Flexolith epoxy

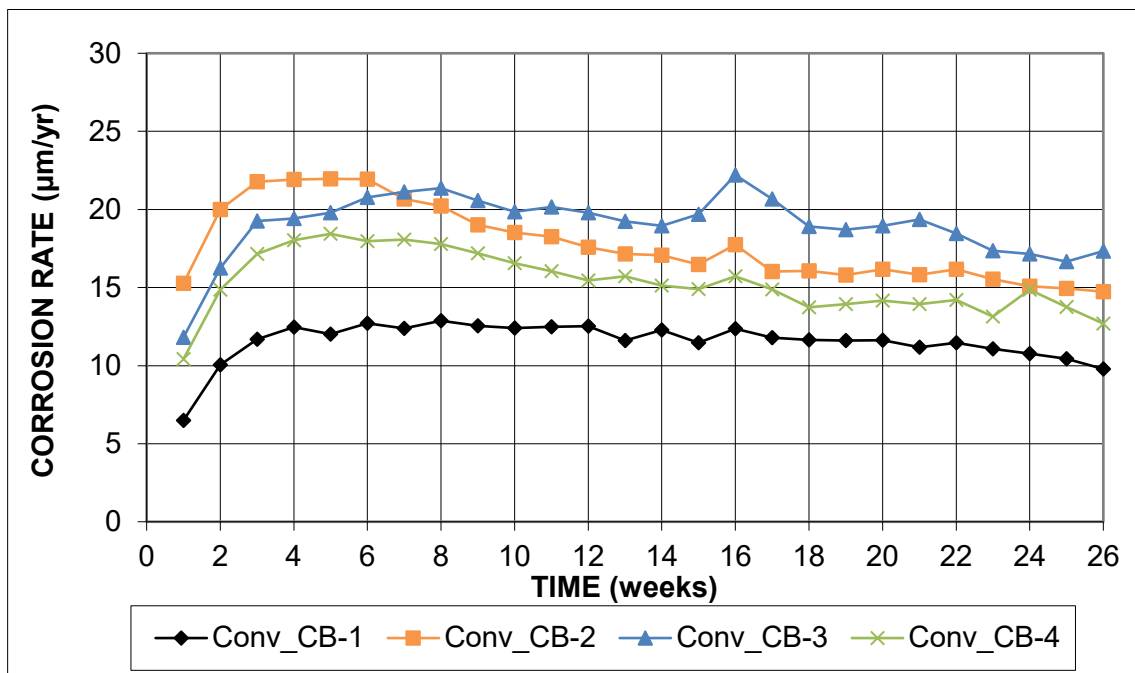


Figure A.62: Macrocell corrosion rate versus time for control cracked beam specimens

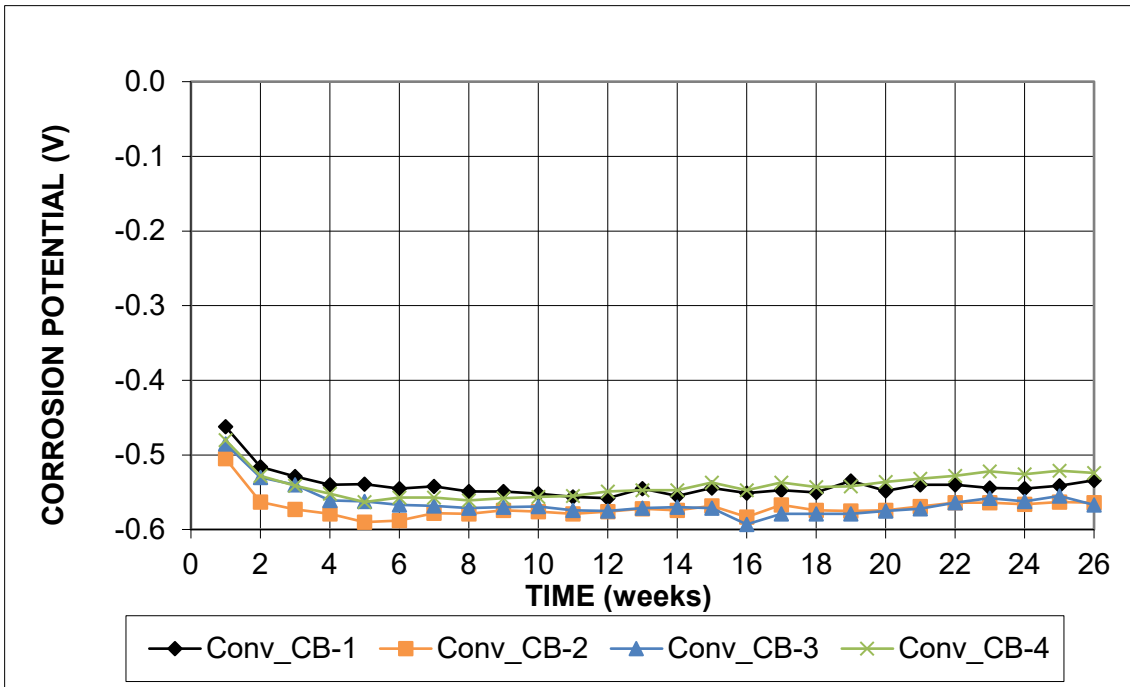


Figure A.63: Corrosion potential for top mat of steel versus time for control cracked beam specimens

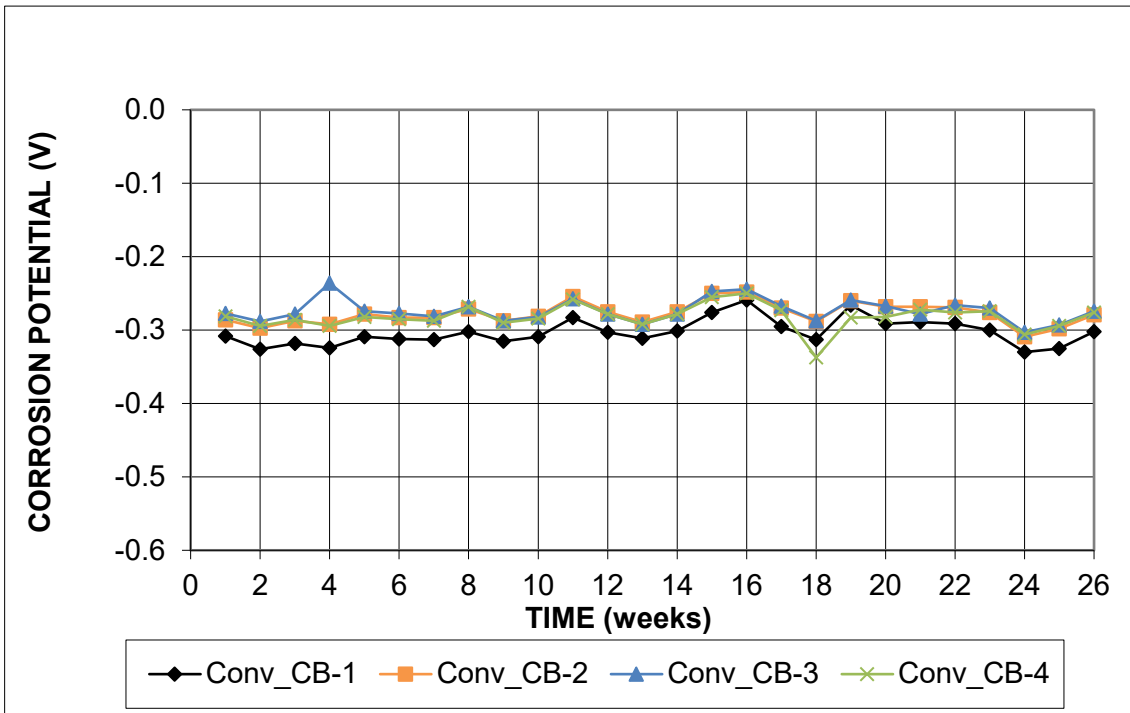


Figure A.64: Corrosion potential for bottom mat of steel versus time for control cracked beam specimens

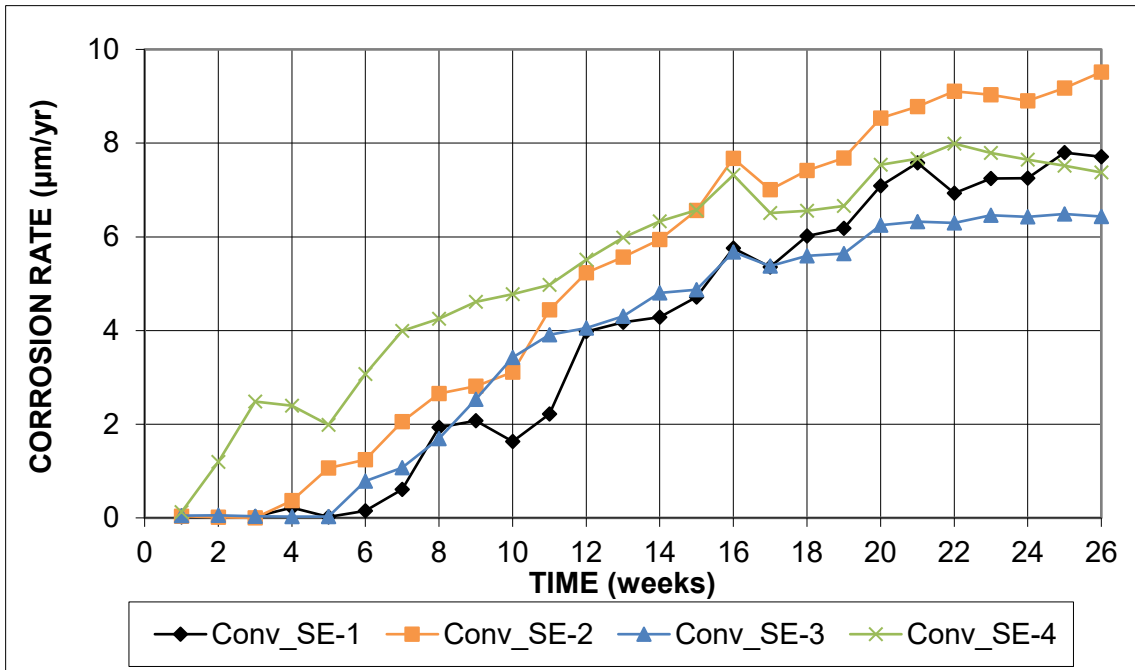


Figure A.65: Macrocell corrosion rate versus time for control Southern Exposure specimens

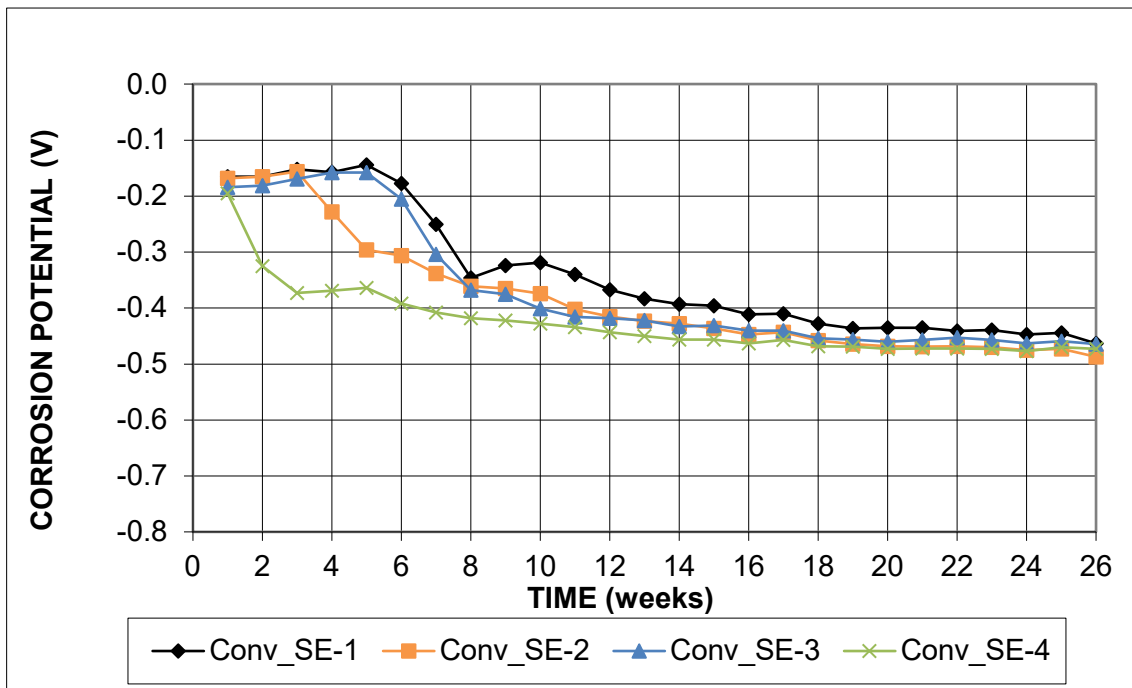


Figure A.66: Corrosion potential for top mat of steel versus time for control Southern Exposure specimens

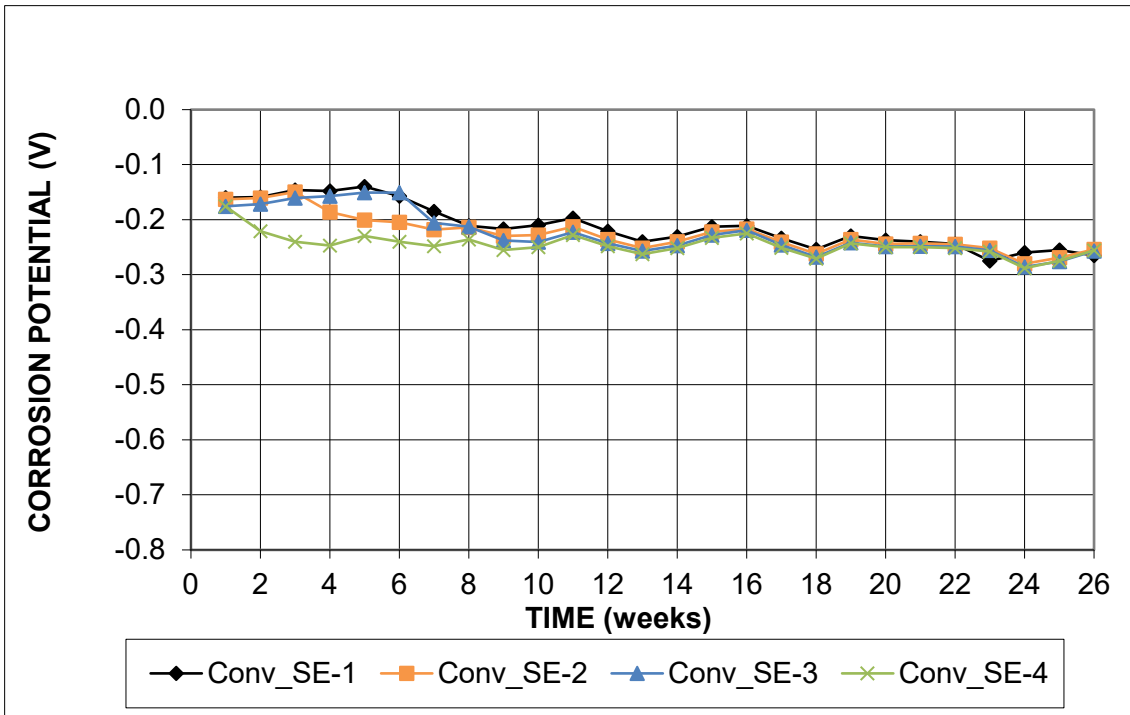


Figure A.67: Corrosion potential for bottom mat of steel versus time for control Southern Exposure specimens

APPENDIX B

CORROSION LOSS FOR INDIVIDUAL CB, SE, CHLORIDE-EXPOSED CB, AND CONTROL SPECIMENS

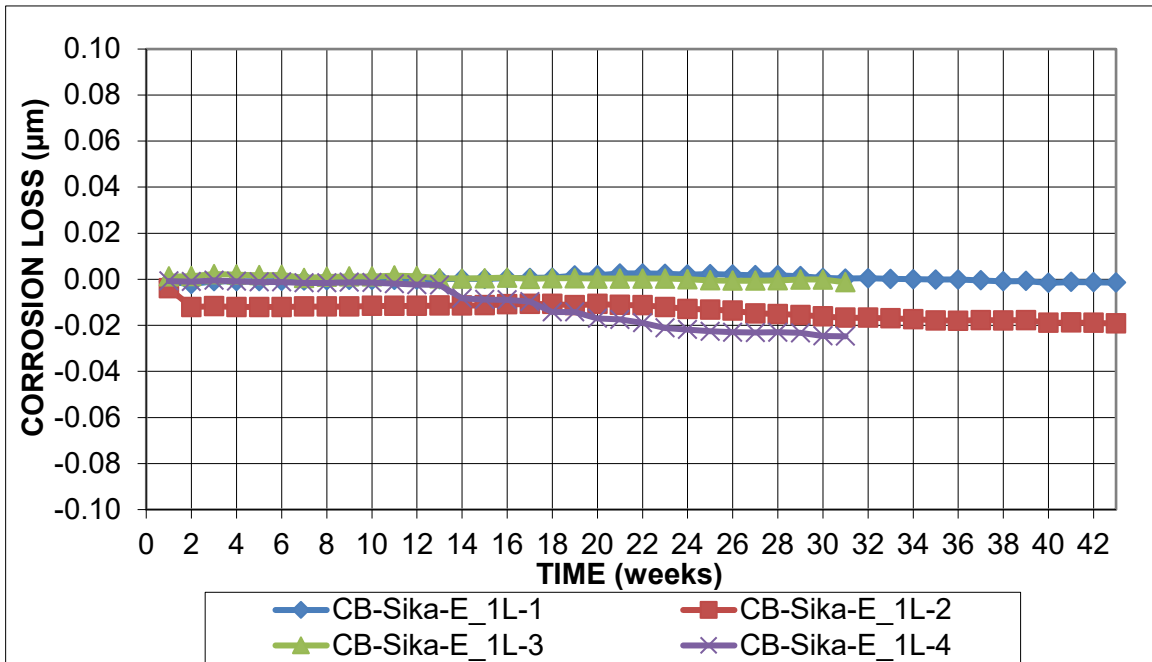


Figure B.68: Corrosion Loss for cracked beam specimens with one layer of Sikadur®-22 Lo-Mod epoxy

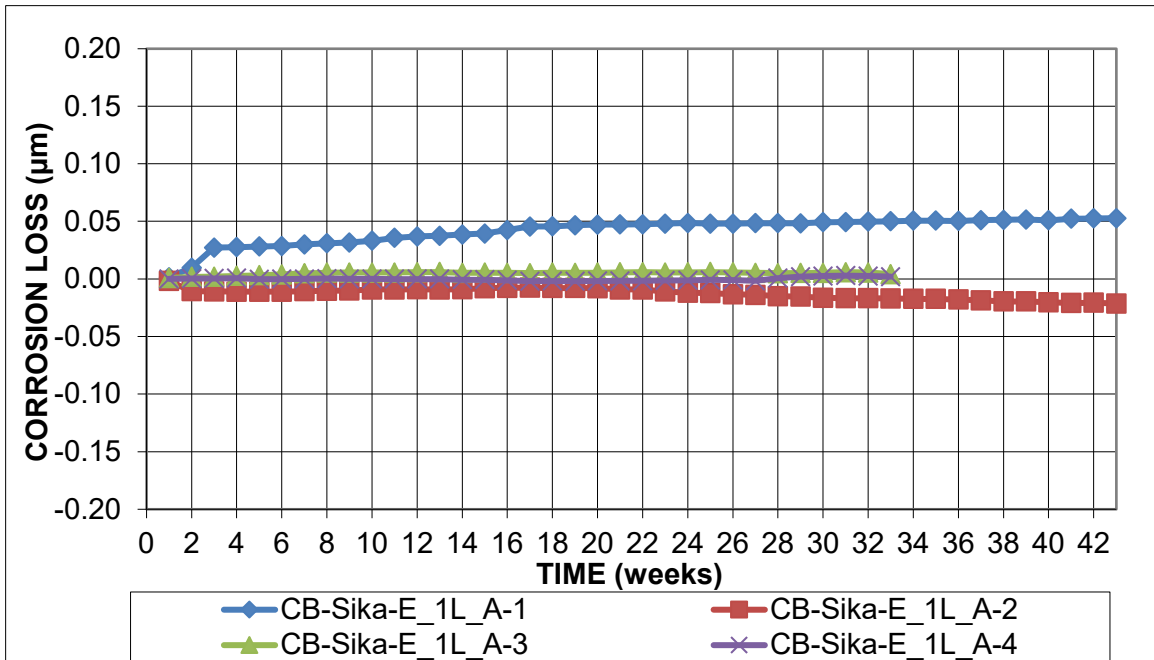


Figure B.69: Corrosion Loss for cracked beam specimens with one layer of Sikadur®-22 Lo-Mod epoxy and aggregate

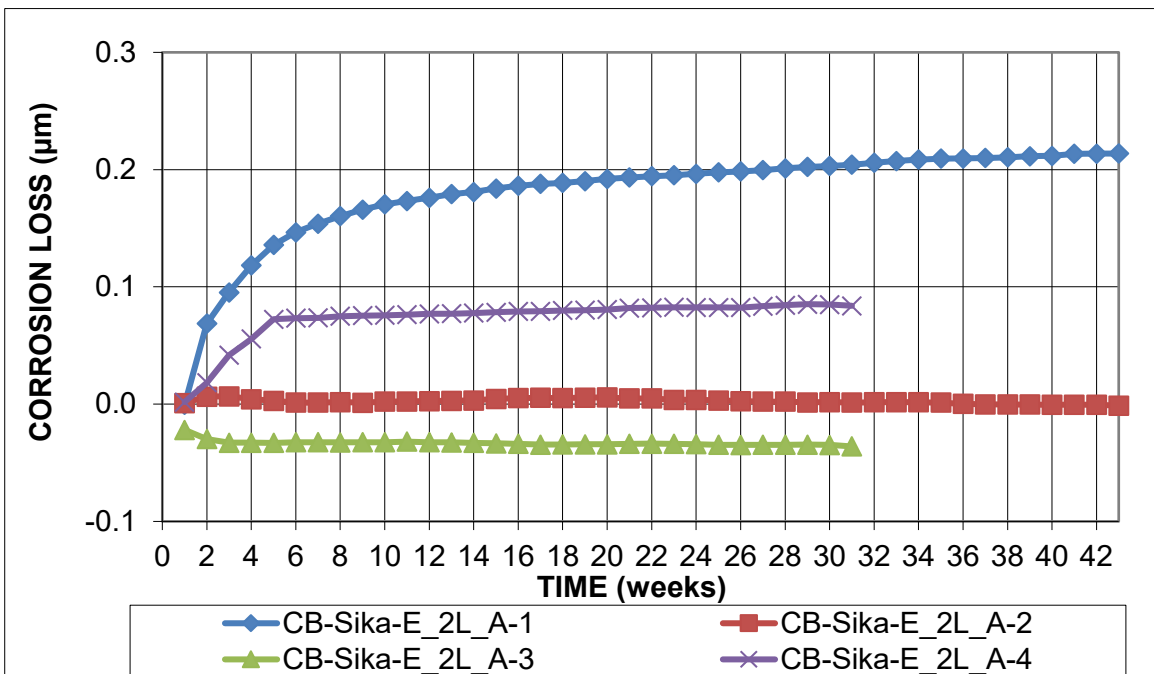


Figure B.70: Corrosion Loss for cracked beam specimens with two layers of Sikadur®-22 Lo-Mod epoxy and aggregate

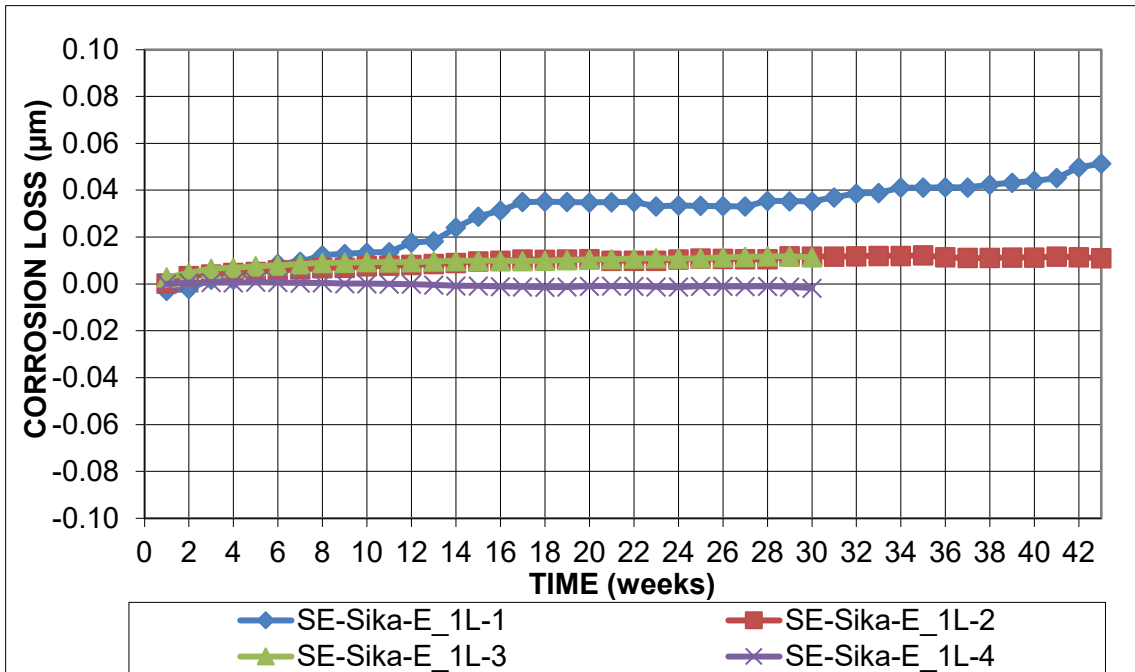


Figure B.71: Corrosion Loss for Southern Exposure specimens with one layer of Sikadur®-22 Lo-Mod epoxy

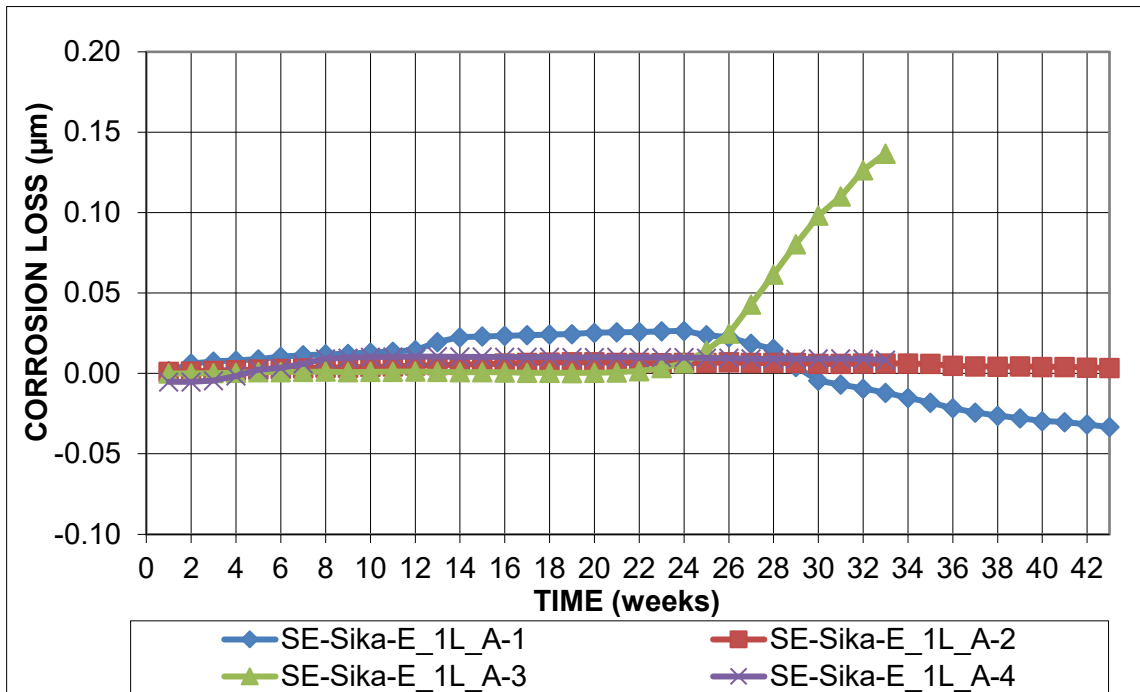


Figure B.72: Corrosion Loss for Southern Exposure specimens with one layer of Sikadur®-22 Lo-Mod epoxy and aggregate

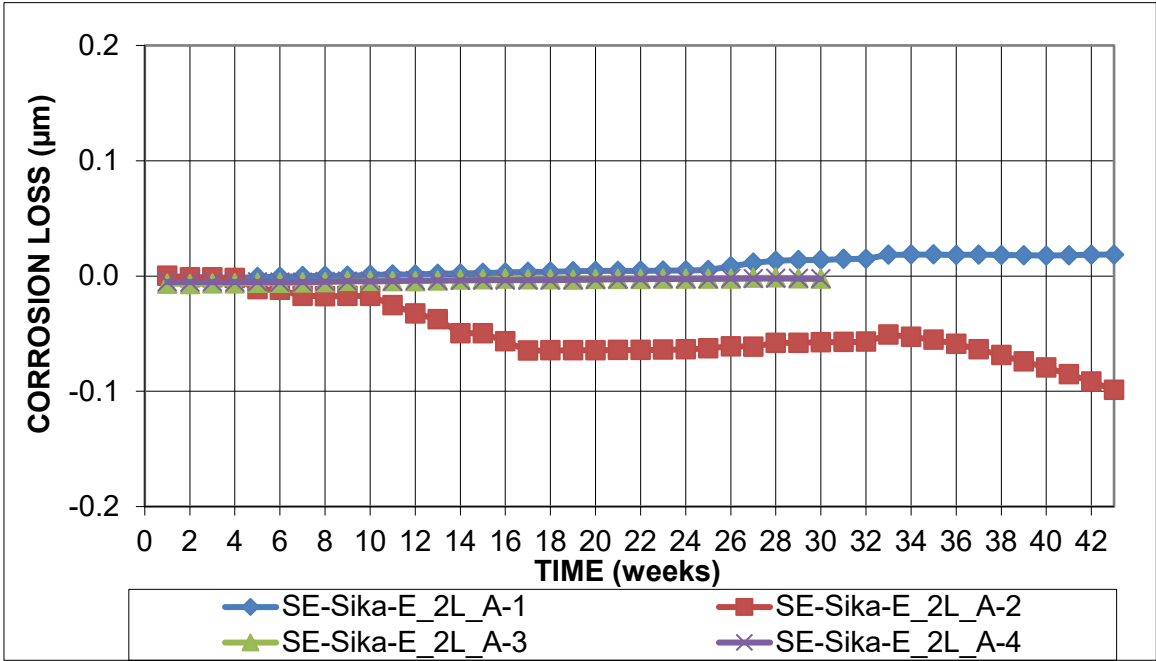


Figure B.73: Corrosion Loss for Southern Exposure specimens with two layers of Sikadur®-22 Lo-Mod epoxy and aggregate

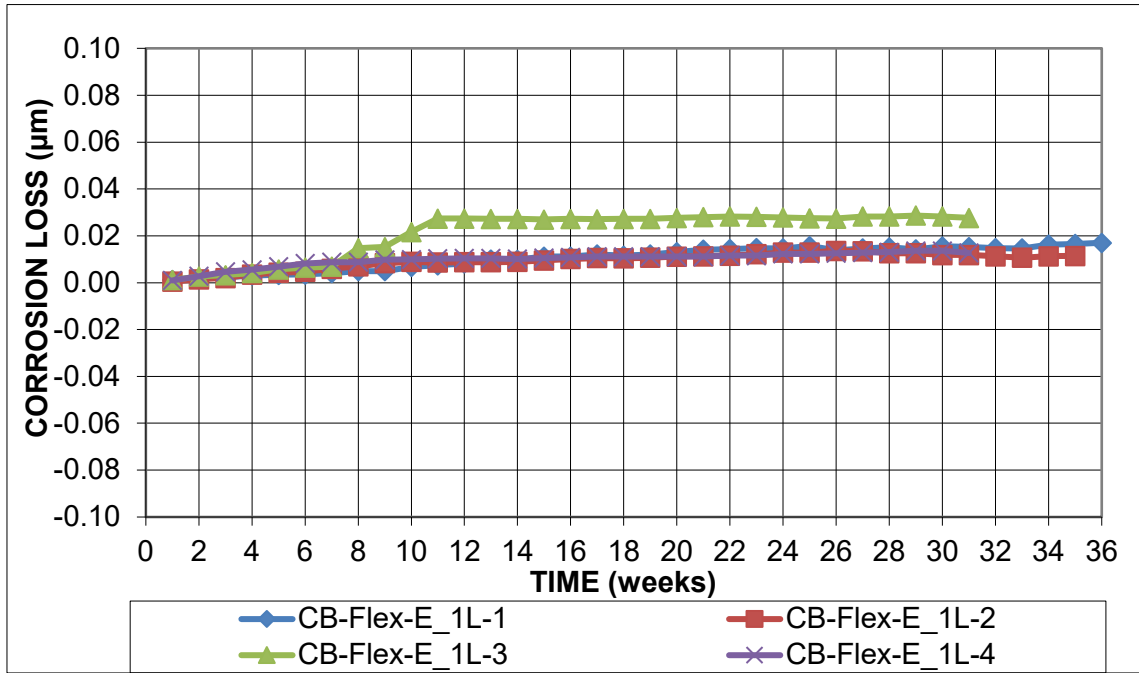


Figure B.74: Corrosion Loss for cracked beam specimens with one layer of Flexolith epoxy

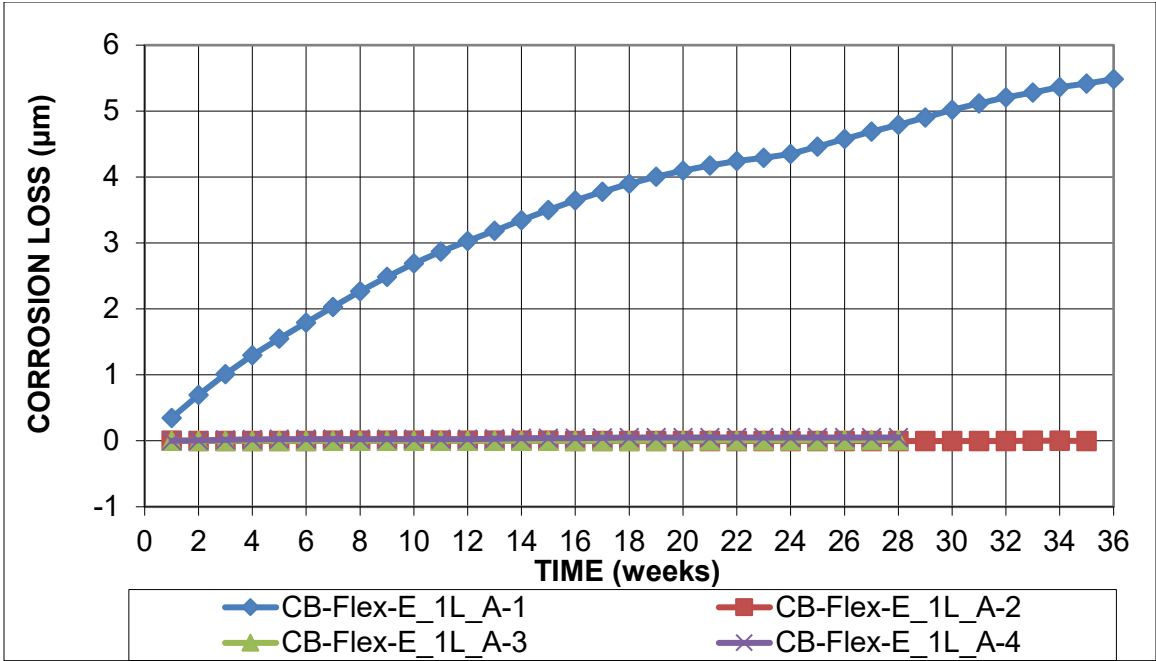


Figure B.75: Corrosion Loss for cracked-beam specimens with one layer of Flexolith epoxy and aggregate

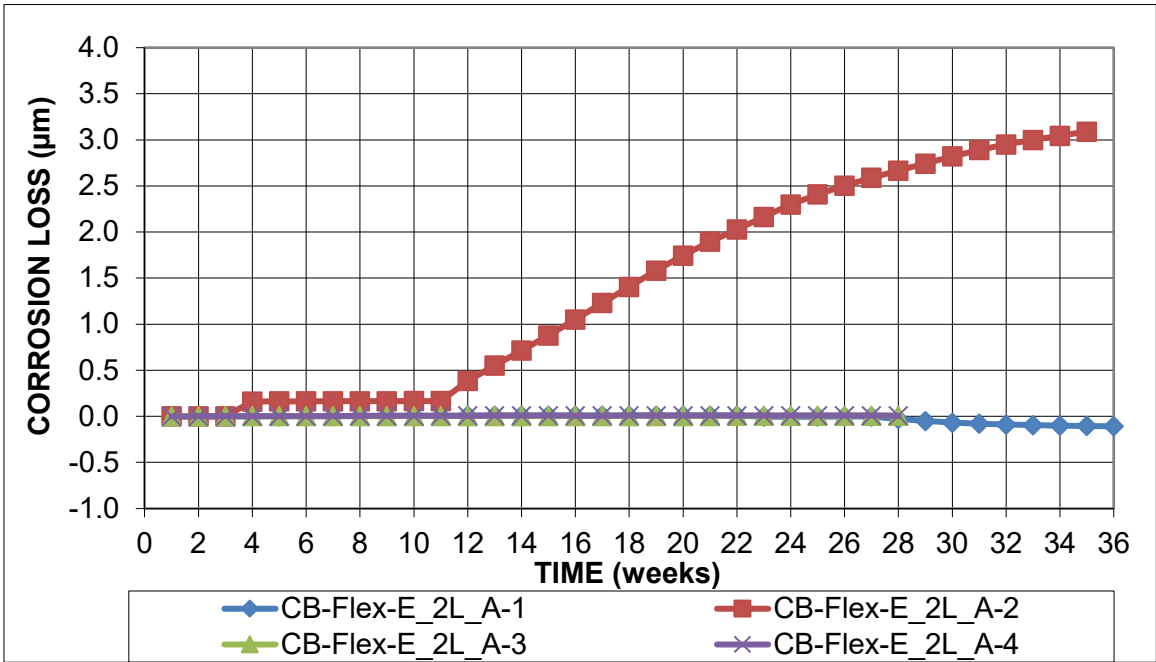


Figure B.76: Corrosion Loss for cracked beam specimens with two layers of Flexolith epoxy and aggregate

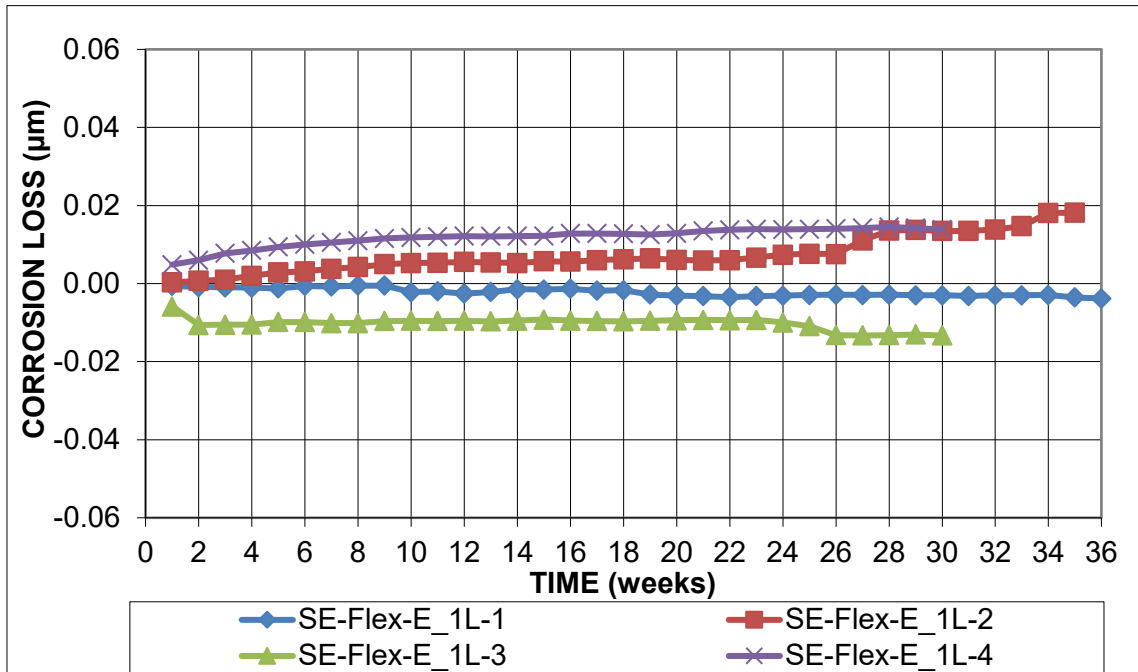


Figure B.77: Corrosion Loss for Southern Exposure specimens with one layer of Flexolith epoxy

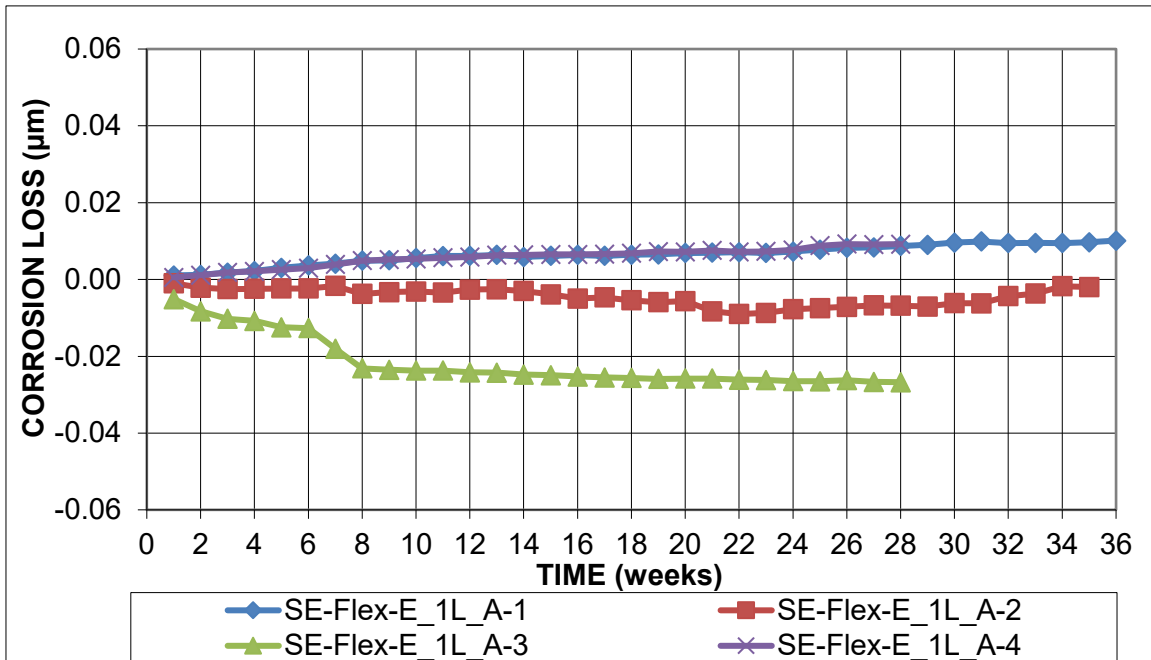


Figure B.78: Corrosion Loss for Southern Exposure specimens with one layer of Flexolith epoxy and aggregate

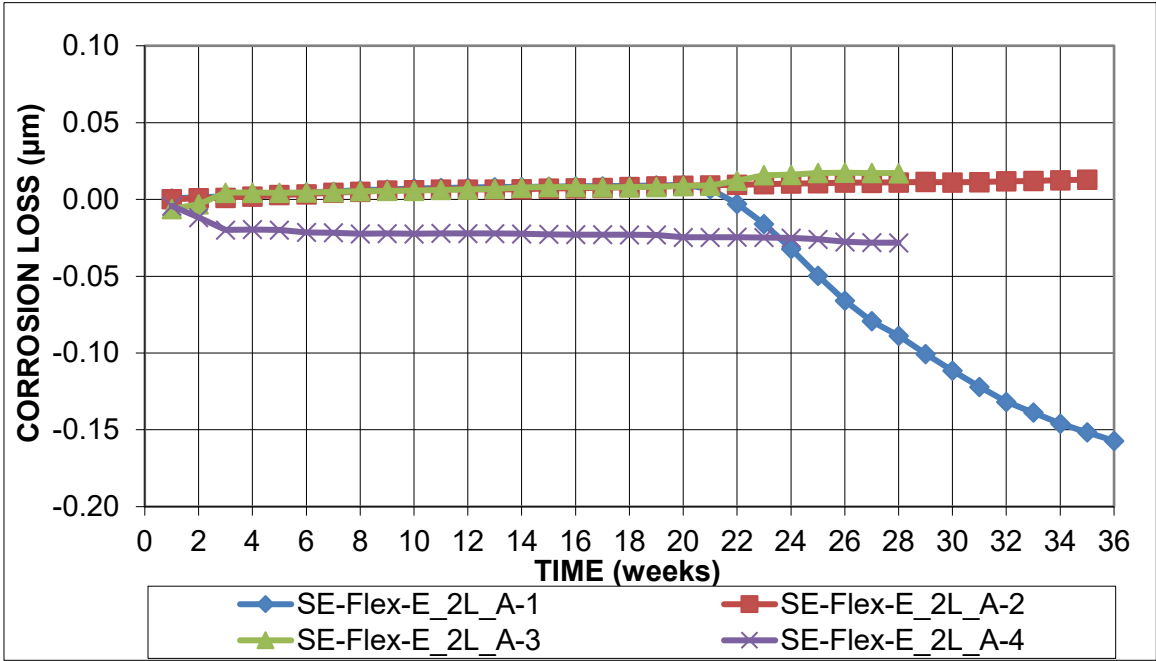


Figure B.79: Corrosion Loss for Southern Exposure specimens with two layers of Flexolith epoxy and aggregate

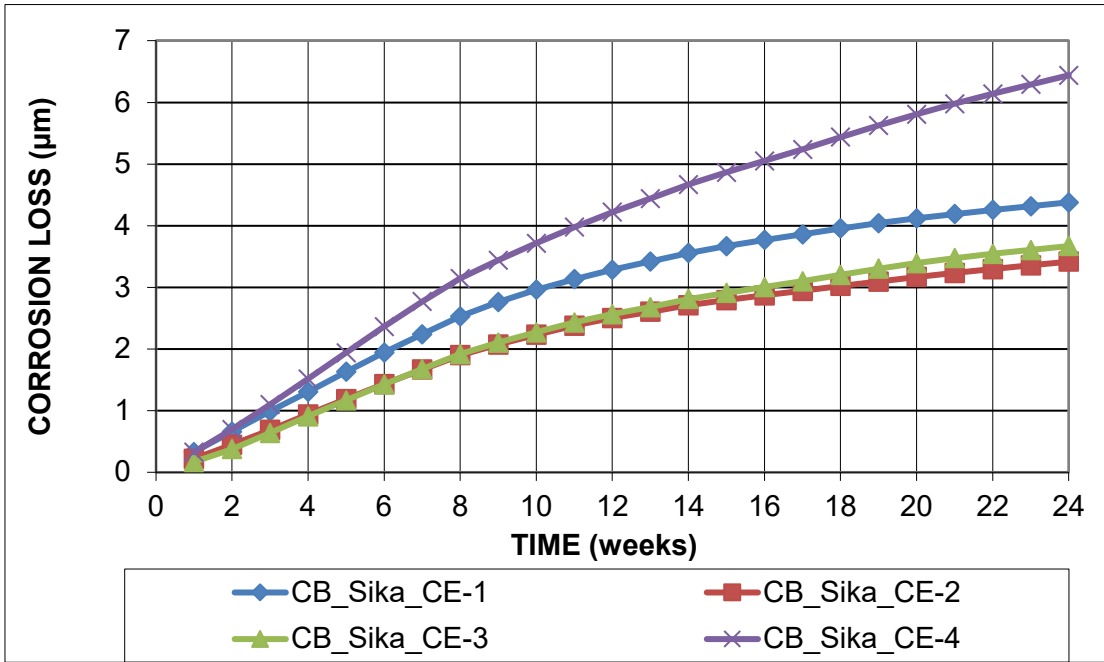


Figure B.80: Corrosion Loss for chloride exposed cracked beam specimens coated with two layers of Sikadur epoxy and aggregate

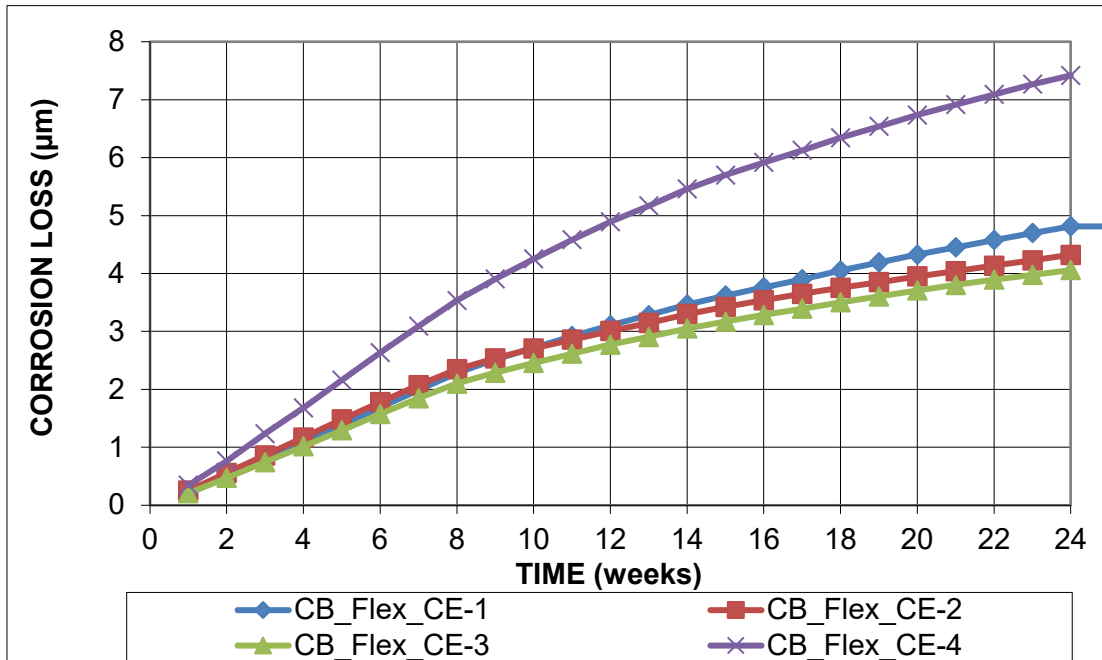


Figure B.81: Corrosion Loss for chloride exposed cracked-beam specimens coated with Flexolith epoxy

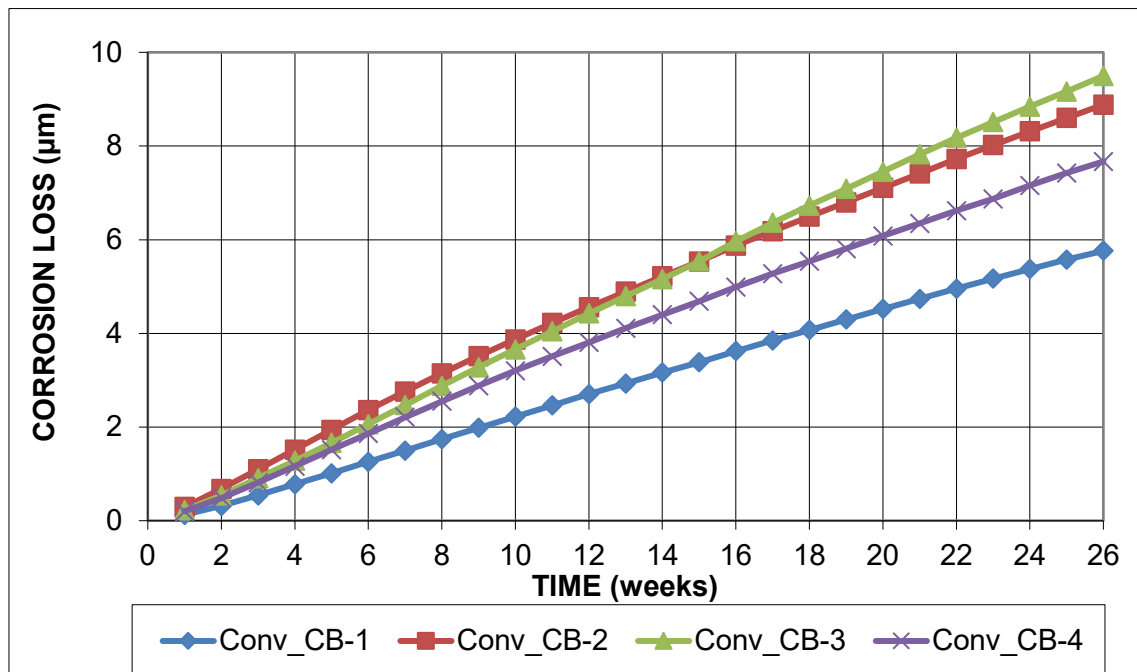


Figure B.82: Corrosion Loss for control cracked beam specimens

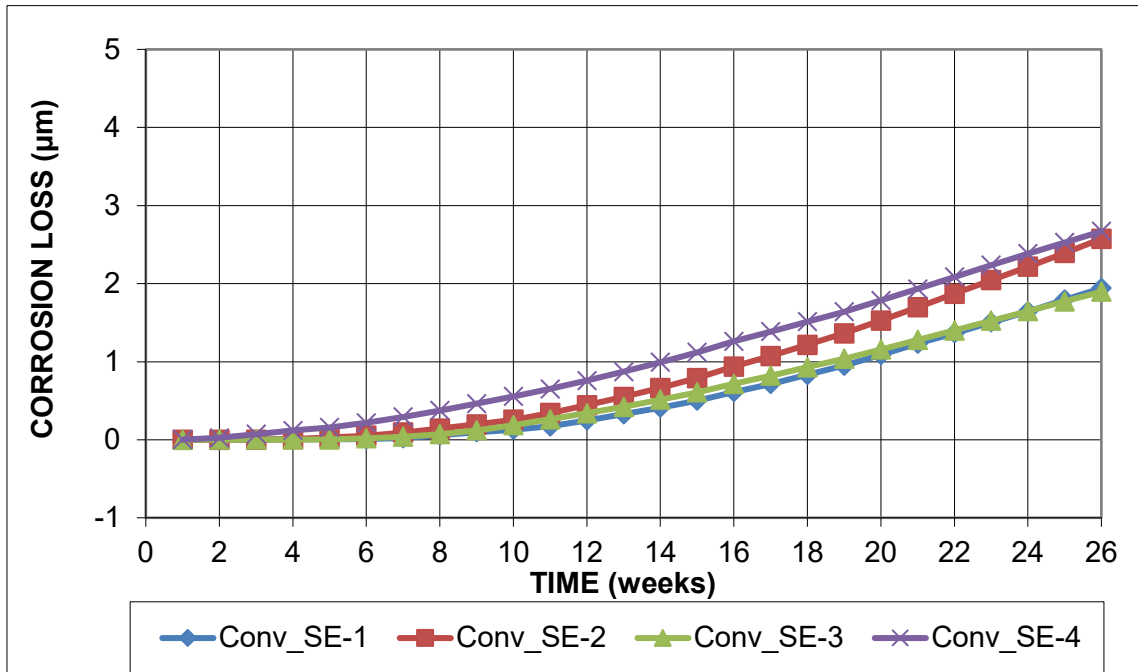


Figure B.83: Corrosion Loss for control Southern Exposure specimens

